LBL-PUB--5346

DE92 017002

Report on
Lawrence Berkeley Laboratory

Exploratory Research and Development Fund

FY 1990

Lawrence Berkeley Laboratory
University of California
Berkeley, California 94720

Prepared for the U.S. Department of Energy under Contract No. DE-AC03-76SF00098

DISTRIBUTION OF THIS DOCUMENT IS UNLIMITED

MASTER

Table of Contents

Introduction vii

Institutional Projects Reports 1

Accelerator and Fusion Research Division 1
Applied Science Division 4
Cell and Molecular Biology Division 7
Chemical Biodynamics Division 18
Chemical Sciences Division 19
Earth Sciences Division 21
Engineering Division 25
Information and Computing Sciences Division 27
Materials Sciences Division 28
Nuclear Science Division 41
Physics Division 42
Research Medicine and Radiation Biophysics Division 49

Innovative Projects 51

Accelerator and Fusion Research Division 51
Applied Science Division 53
Cell and Molecular Biology Division 57
Chemical Biodynamics Division 63
Materials and Chemical Research Division 70
Nuclear Science Division 76
Physics Division 78
Research Medicine and Radiation Biophysics Division 80

Acronyms and Abbreviations 83

Introduction

The *Lawrence Berkeley Laboratory Exploratory R&D Fund FY 1990* report is compiled from annual reports submitted by principal investigators following the close of the fiscal year. This report describes the projects supported and summarizes their accomplishments. It constitutes a part of an Exploratory R&D Fund (ERF) planning and documentation process that includes an annual planning cycle, projection selection, implementation, and review.

The LBL ERF program is a critical tool for directing the Laboratory's forefront scientific research capabilities toward vital, excellent, and emerging scientific challenges. The program provides the resources for LBL scientists to make rapid and significant contributions to critical national science and technology problems. The ERF also advances the Laboratory's core scientific capability and permits exploration of exciting new opportunities. Areas eligible for support include:

- Work in forefront areas of science and technology that enrich Laboratory research and development capability;
- Advanced study of new hypotheses, new experiments, and innovative approaches to develop new concepts or knowledge;
- Experiments directed toward proof of principle for initial hypothesis testing or verification; and
- Conception and preliminary technical analysis to explore possible instrumentation, experimental facilities, or new devices.

The ERF program supports LBL's mission in many ways. First, because ERF funds can be allocated in a relatively short time frame, LBL researchers can support the mission of DOE and serve the needs of the nation by quickly responding to forefront scientific problems. Second, ERF enables the Laboratory to attract and retain highly qualified scientists, and supports their efforts to carry out world-leading research. Finally, the ERF program also supports new projects that involve graduate students and postdoctoral fellows, thus contributing to the education mission of the Laboratory.

LBL has a formal process for allocation of funds for ERF. The process relies on individual scientific investigators and the scientific leadership of the Laboratory to identify opportunities that will contribute to scientific and institutional goals. The process is also designed to maintain compliance with DOE Orders. From year to year, the distribution of funds among the three scientific program areas will change. This flexibility optimizes the Laboratory's ability to respond to opportunities.

Laboratory ERF policy and program decisions are the responsibility of the Laboratory Director. The Director has assigned general programmatic oversight responsibility to the Laboratory Deputy Director. Administration and reporting on the ERF program is supported by the Office for Planning and Development. ERF accounting procedures and financial management are consistent with the Laboratory's accounting principles and stipulations under the contract between the University of California and the Department of Energy, with accounting maintained through the Laboratory's Chief Financial Officer.

In FY 1990, LBL was authorized by the Department of Energy to establish a funding ceiling for the Exploratory R&D Fund of 3% of the Laboratory's FY 1990 operating budget, or $5.4 M. This funding level was provided to develop new scientific ideas and opportunities and allow the new Laboratory Director an opportunity to initiate new directions, even though the FY 1990 ERF review process was completed prior to his appointment in September 1989. However, budget constraints limited available resources, so only $4.2 M was finally allocated.

The Exploratory R&D fund continues to be an important tool for maintaining LBL's forefront scientific capabilities. In FY 1990, scientists submitted more than 115 proposals requesting almost $11.0 M. A total of 51 projects were funded in FY 1990, with awards ranging from $15 to $335 K. Total funding was just less than $4.2 M. These projects are summarized in Tables 1 and 2.

Table 1. FY 1990 Exploratory R&D Fund—Institutional Projects

Division	Investigator	Project Title	($)
Accelerator and Fusion Research Division			
	S. Chattopadhyay R.A. Gough K-J Kim	Investigation of IR and UV FELs at LBL	332,200
	B.M. Kincaid	Investigation of Methods of Producing Variable Synchrotron Radiation	47,700
Applied Science Division			
	J.M. Daisey A.V. Nero M.T. Smith R.C. Spear	Mechanism-Based Rick Assessment for Indoor Air Exposures	50,000
	M.D. Levine	U.S. Energy Model Development	49,500
Cell and Molecular Biology Division			
	M.J. Bissell R.Y. Tsien G. Parry	Molecular Biology Approaches to Studies of Mammary Epithelial Cells in Culture	41,700
	M.J. Bissell M. Stampfer J. Hosoda	Technology Transfer in Biotechnology	125,300
	M. Esposito Aloke Chatterjee Michael Esposito Bea Singer	Mammalian Repair Enzyme(s) Characterization and Identification of Yeast REC Repair Genes	35,000
	J.G. Conboy	Alternative RNA Splicing Mechanisms in Erythroid Differentiation	78,000
	R.M. Glaeser	Cryo-Electron Microscopy	58,700
	P.H. Silverman	Policy Issues in Molecular Biology	55,100
Chemical Biodynamics Division			
	M. Salmeron	Structural Studies of Biomolecules with the Scanning Tunneling and Atomic Force Microscopes	120,700
Chemical Sciences Division			
	Y.T. Lee A.H. Kung	Technical Evaluation of Beamline and Experimental Stations for Chemical Dynamics Applications at the ALS	73,600
Earth Sciences Division			
	D.J. DePaolo B.M. Smith	Advanced Instruments and Techniques for Mass spectrometry Applications in the Geological Sciences	204,100
	P.L. Williams	Fault Assessment and Seismic Risk Estimating	75,000
Engineering Division			
	F.S. Goulding	Search for Dark Matter with Silicon Detectors	60,300

Table 1. Continued.

Division	Investigator	Project Title	($)
Information and Computing Sciences Division			
	D. Hall W. Greiman	Distributed Scientific Data Management in a Heterogeneous Environment	150,800
Materials Sciences Division			
	J. Clarke	Noise in High-T_c Superconductors	46,400
	C.S. Fadley	High Energy Photoelectron Spectroscopy	14,500
	D.E. Morris	Role of Oxygen in High-Temperature Superconductors	134,300
	J.W. Orenstein	Excite and Probe Studies of High-T_c Superconductors in the TH_z Regime	45,400
	P.L. Richards	Antenna-Coupled High T_c Bolometer	54,000
	G.M. Rosenblatt	Raman Studies of Materials and High Temperature Systems	252,800
	C.V. Shank	Femtosecond Dynamics in Condensed Matter	296,500
	D.K. Veirs	Raman Spectroscopy for Advanced Characterization of Materials	57,700
Nuclear Science Division			
	R.G. Stokstad	Exotic Beams at the 88-Inch Cyclotron	80,700
Physics			
	G. Abrams F. Kirsten M. Levi J. Siegrist G. Trilling	Calorimeter Electronics R&D	70,600
	A. Chorin P. Concus	New Postdoctoral Fellowship in Mathematics	25,000
	C. Quigg	SSC Detector Optimization	122,800
	B.M. Novak	New Liquid-Crystalline Polymer Composite Materials through Sol-Gel Processes	30,600
	D.R. Olander	Cluster Formation in the Vapor Produced by Laser Pulsing of the YBCO Superconducting Solid	29,100
Research Medicine and Radiation Biophysics			
	T.L. Hayes P. Echlin E.N. Ashworth	Viability in Synchrotron Microscopy	77,400
TOTAL			*2,895,500*

Table 2. FY 1990 Exploratory R&D Fund—Innovative Science Projects

Division	Investigator	Project Title	($)
Accelerator and Fusion Research Division			
	I. Brown K. Krishnan	Thin Film Diamond Synthesis	84,000
Applied Science Division			
	D.K. Liu	Photochemical Vapor Deposition of Mixed-Metal and Oxide Thin Films	57,000
	R.E. Russo	Optical Fiber Sensors Based on Thermal Lens Spectroscopy	88,000
Cell and Molecular Biology Division			
	E. Rubin	Biological Analysis in Transgenic Mice of Large Defined Segments of the Human Genome Cloned in Yeast Artificial Chromosomes	108,000
	D. Schild	Molecular Analysis of Human Chromosome 21 Region Associated with Down's Syndrome	56,500
	R. Schwarz	Detection of Viral Integration	44,800
	A.N. Tischler	Procarcinogen Activation in Human Mammary Epithelial Cells	66,200
Chemical Biodynamics Division			
	M.P. Klein A. Quintanilha	X-Ray spectroscopy of Sulfur in Biology	63,300
	D.E. Wemmer P.G. Williams Henry Rapoport	Labeling and NMR Study of Nucleic Acids	44,200
Chemical Sciences Division			
	J.M. Prausnitz	Chemistry of Hydrophilic Gels for Separation of Solutes from Dilute Aqueous Solution	57,300
	R.J. Saykally	Laser Produced Microparticle Suspensions	64,700
Earth Sciences Division			
	P. Persoff	Laboratory Demonstration of Aqueous Foam for Mobility Control in Surfactant Washing for Aquifer Remediation	50,800
Materials Sciences Division			
	U. Dahmen K.H. Westmacott	Diamond Hexagonal Silicon	91,900
	T.M. Devine M. Salmeron	Use of Scanning Tunneling Microscopy for In-situ Studies of Metal-Solution Interfaces	48,000
	L.C. De Jonghe J.W. Evans	Synthesis of Composite Ceramics by Microwave-Assisted Chemical Vapor Infiltration	55,000
	G. Somorjai M. Salmeron	Atomic Structure of Catalyst Surfaces under High Pressure Reaction Conditions	88,000
	J.A. Yarmoff	Stimulated Desorption of Halogens from Semiconductor Surfaces	31,100

Table 2. Continued.

Division	Investigator	Project Title	($)
Nuclear Science Division			
	W.D. Myers W.J. Swiatecki	Transition from Order to Chaos in Nuclei	67,100
Physics Division			
	R.A. Muller C.R. Pennypacker	Pulsar Studies	60,000
Research Medicine and Radiation Biophysics Division			
	W.W. Moses	Mechanisms of Heavy Atom Scintillators	60,500
TOTAL			***1,286,400***

Instititutional Project Reports

Accelerator and Fusion Research Division

Investigation of IR and UV FELs at LBL

Principal Investigators: Swapan Chattopadhyay, Richard A. Gough, and Kwang-Je Kim

Funding: $332,200

Project Description

The project involves continuing investigation into the physics and technology of Free Electron Lasers (FELs) for applications in the infrared (IR) and ultraviolet (UV) wavelengths. The IRFEL studies are developmental, aimed at forming concepts and developing techniques that will allow stable and reliable operation of an IRFEL, both spectrally and temporally. These will be crucial features for fruitful scientific experiments in the IR. The goal of IRFEL/UVFEL research and development is to develop concepts, tools and optimization parameters that will allow critical evaluation and assessment of the physics and technology of UVFELs, e.g., storage rings, linacs, undulators, optics, etc.

Accomplishments

New ideas have been explored and basic FEL physics studied. The possibility of attaching a storage cavity to an FEL cavity was examined. A significant enhancement of the FEL field level is possible if the coupling between the storage cavity and the FEL cavity is made uni-directional. This scheme could have an application for infrared FELs. We also have started to study the performance of a Cerenkov FEL as a potential way to provide coherent radiation at longer wavelengths.

In the domain of basic FEL physics, the FEL spectral bandwidth has been one of the most poorly understood subjects so far. Progress was made in this field by deriving explicit expressions for the limiting spectral bandwidths in FEL oscillators. We found that it differs for various accelerator drivers due to different saturation processes. This result could be a decisive factor in arriving at an optimized accelerator system for a short wavelength FEL. This parameter, the limiting spectral bandwidth, was identified as one of the critical parameters that can be used as a tool to discriminate between various technologies and approaches. The thrust of the FEL studies is significantly shifting to short wavelengths now, as the knowledge gained for applications to longer wavelengths such as the infrared has already begun to be incorporated in the design of IRFELs at many laboratories.

In our optical cavity studies, we have been studying a hole-coupled FEL resonator with adjustable apertures as a promising outcoupling scheme for a broadband IRFEL. A versatile numerical code has been developed to calculate the mode profiles, diffraction losses, coupling efficiencies, etc., for a general empty cavity. Initial studies have also been made of the use of intracavity gratings as a method to stabilize the wavelength fluctuations. Extensive computer simulations have established tolerances for energy, charge, and timing fluctuations for stable lasing in the infrared for any general FEL.

Significant progress was made in (i) understanding the energy storage, outcoupling mechanism, and wavelength stabilization of optical cavities for infrared wavelengths; (ii) identifying critical parameters that will allow us to discriminate between various approaches and technologies for short wavelength (UV and beyond) FELs; and (iii) generating new FEL ideas. Future studies will focus on short pulse x-ray generation and the assessment of critical technologies (e.g., superconducting RF) for FEL applications.

Investigation of Methods of Producing Variable Synchrotron Radiation

Principal Investigator: Brian M. Kincaid

Funding: $47,700

Project Description

The production of variable polarization synchrotron radiation using special insertion devices was investigated. This project assessed the capabilities and limitations of different variable polarization techniques and their implications for the design of future synchrotron radiation light sources, as well as form the basis for future insertion devices and beamlines for experiments requiring variable polarization.

Accomplishments

Several insertion device designs producing circular, elliptical, or variable polarization synchrotron radiation have been proposed. With the exception of the K.-J. Kim tandem crossed undulator scheme, these proposed devices all require either the electron beam, the beamline optics, or some mechanical part of the insertion device structure be physically moved in order to change the polarization of the synchrotron radiation beam. For example, in some insertion device schemes, the relative position of two magnetic structures must be changed. In the asymmetric wiggler scheme, the beamline optics must look either above or below the plane of the electron orbit to change the polarization. In other schemes, the electron beam must be moved from one magnetic field region to another to change the helicity of the magnetic field and hence the polarization of the output beam.

All schemes requiring physical movement have serious disadvantages. In experiments using circular polarization, for example, magnetic circular dichroism (MCD) is measured by observing small changes in signal intensity when the polarization of the input beam is changed from right circular to left circular. This change in polarization must be done rapidly, at least at about 10 Hz, for synchronous detection schemes to work properly. Moving large pieces of magnetic hardware at this rate is clearly impractical. Moving the optical components in the beamline is slightly easier, but still a disadvantage. Moving the electron beam is easy to do, but it has its own disadvantages involving interaction with other users of the synchrotron radiation source and moving images on optics and the experiment sample, all leading to undesirable artifacts.

The Kim scheme uses a magnetic modulator between two crossed undulators to provide an adjustable phase shift. This can readily be varied at the required 10 Hz rate, and does not involve any moving parts. Based on these considerations and after a series of discussions and workshops with potential users of such a device, efforts were focused exclusively on the Kim approach.

A series of meetings and workshops with potential users of a variable polarization insertion device beamline were held, including scientists from Florida Atlantic University, the Aladdin Synchrotron Radiation Center, the University of Wisconsin at Madison, Syracuse University, the Advanced Photon Source (APS) at Argonne, and LBL. Estimates of the performance of a Kim crossed undulator insertion device at Aladdin, APS, and ALS were done, and plans were made for a three part project to build such a device and its beamline. In phase one, a prototype insertion device and a simple beamline would be built for use at Aladdin, covering the photon energy range from below 10 eV up to about 40 eV. This will allow overlap with presently used and well-characterized methods of generating circular polarization in the near UV, up to about 10 eV. Depending on the success of phase one, the second part of the project involves building another insertion device and a more advanced beamline at Aladdin, covering up to about 100 eV photon energy. The third phase involves a device and beamline at the ALS, extending the photon energy range up to a few hundred eV, and covering the interesting area of the carbon K-edge at 283 eV.

A proposal for Phase I has been sent to the DOE Advanced Energy Projects office. The insertion device part of the proposal included a conceptual design for a Kim undulator, including an electromagnetic phase shift modulator, whose design was fairly carefully worked out by LBL. Another novel feature of the proposed design is that the tandem undulators are oriented at plus and minus 45 degrees to the horizontal, rather than the normal horizontal and vertical alignment. This allows insertion devices to be tuned to match the polarization response characteristics of the beamline optics, producing precisely controlled output polarization. It also allows more horizontal clearance for the electron beam than the conventional approach.

In preparation for the possible third phase of the work, a special modification to one arc chamber of the ALS vacuum system was made (at no cost). This involved

cutting a larger exit aperture to allow the undulator output more vertical clearance. Such a modification would have been extremely expensive at a later date. In addition, the straight section upstream of the special chamber and the beamline floor area that would be used by a circular polarization beamline have been reserved.

The exploratory R&D work has also stimulated a new interest in using crossed undulators to generate circularly polarized soft x-rays at the ALS. This work neatly complements the ongoing efforts there to use perfect crystal optics to make quarter wave plates for hard x-ray circular polarization beamlines, and has resulted in an ongoing collaboration in this area.

This work has stimulated interest in the use of circular polarization among LBL scientists and has contributed to a proposal to build a bending magnet beamline at the ALS dedicated to circular polarization measurements. It has also kept LBL current with what is going on in this area around the world.

Publications

K.-J. Kim, "The Evolution and Limits of Spectral Bandwidth in Free Electron Lasers," *Proceedings of the Twelfth International Free Electron Laser Conference*, Paris, France, September 17-21, 1990, LBL-29724 Rev.

M. Xie and K.-J. Kim, "Hole Coupling Resonator for Free Electron Lasers," *Proceedings of the Twelfth International Free Electron Laser Conference*, Paris, France, September 17-21, 1990, LBL-29956.

Applied Science Division

Mechanism-Based Risk Assessment for Indoor Air Exposures

Principal Investigator: Joan M. Daisey, Anthony V. Nero, Martyn T. Smith and Robert C. Spear

Funding: $50,000

Project Description

Current methods for determining risks from exposure to toxic chemicals at levels found in indoor air are scientifically flawed and may overestimate or underestimate risk by orders of magnitude. Human health risk assessment would be much improved if mechanism-based models, based on fundamental biology, could be used to extrapolate data from exposures to toxic chemicals at high concentrations or data from laboratory experiments to predict adverse health effects at the low concentrations typically encountered in indoor environments. An interdisciplinary and UC inter-institutional research project has been initiated in FY1990 as a joint project of the the Indoor Environment Program (IEP) at LBL and the Biomedical & Environmental Health Sciences (BEHS) group at UC Berkeley. The long-term goal of the project is to radically change environmental health risk assessment by placing it on a fundamental scientific basis.

The specific objectives of the exploratory research are:

1) To determine the feasibility of mechanism-based risk modeling, based on fundamental principles of biology, as a new approach to risk assessment; and

2) To establish an interdisciplinary and inter-institutional research project in this area with external funding.

The specific approach of this exploratory research is to integrate the UCB/BEHS pharmacokinetic and cancer models and use LBL/IEP indoor exposure data and data from the new human HLA-A mutation assay as model input to predict cancer risk from human exposure to benzene. The model for benzene will be developed as a "proof of principle," and the results will be used to support applications for multiyear research grants. Benzene was selected as the model compound for this work because benzene has emerged as one of the high-risk indoor pollutants from previous work at LBL. The model is being developed and tested using first data from experiments with rats and then with data from human exposure in the workplace. Both exposure and response (cancer) data are available for rats and have been used in the first year of this project. Pharmacokinetic data obtained from the literature is being used as input for the pharmacokinetic part of the model.

In the first year of this research collaboration, a physiologically-based pharmacokinetic (PBPK) model and a simple cancer model have been successfully linked into an integrated model for benzene. A new method, employing global optimization and Monte Carlo simulations, was used to incorporate distributions of input variables rather than a single value for each of the 29 parameters of the coupled PBPK and multistage cancer model. This new approach incorporates biological variability into PBPK modeling and allows a distribution of probabilities to be estimated for low-level exposures. It appears that much more confidence can be placed on extrapolations made with the pharmacokinetic component of the model than with the multistage carcinogenesis component. The estimated distributions of low-exposure risks extend over several orders of magnitude. The results of the modeling demonstrate the limited value of the common animal cancer experiments for quantitative extrapolations to humans and indicate the need for more biological information relevant to the identification of the parameters of the multistage models of carcinogenesis.

The method developed for parametrizing PBPK models makes it possible to obtain much better fits to the data than previously published in the literature for similar models. Figure 1 shows the predicted versus observed data values for our best Monte Carlo run (out of a 1000 runs), Travis et al. simulation model and Medinsky et al. model (the latter two published in *Toxicology and Applied Pharmacology* in 1989 and 1990). The quality of our fit, as measured by the log-likelihood, is better than for the two other models. On the figure, this translates into a better clustering of the black circles along the identity line.

Work is now in progress to incorporate benzene metabolites into the model to modify the pharmacokinetic part of the model for humans and to incorporate a biologically-based cancer model. In the second year of this project, existing data on human benzene

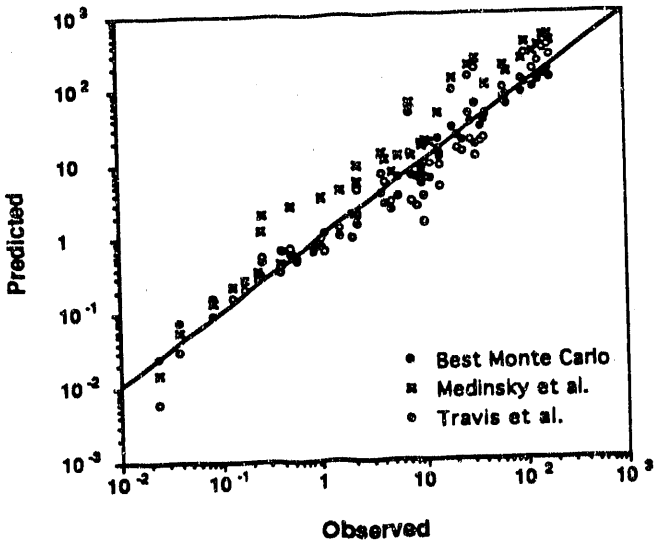

Fig. 1. Predicted versus observed data values for our best Monte Carlo run, Travis et al. simulations and Medinsky et al. simulations. A better fit is indicated by a better clustering of the points along the identity line.

exposure will be collected and integrated. Activities leading to high exposures will be identified and used to model the time variation in exposure needed for the pharmacokinetic modeling. The exposure data will be one type of input for the pharmacokinetic-mechanistic cancer model applied to humans. For the cancer (leukemia) part of the model, a new human, somatic mutation assay, the HLA-A assay, will be applied to provide human input into the model. The HLA-A assay detects a number of important cancer causing lesions and is performed on nucleated white blood cells. The assay can be used for monitoring exposed human populations and can also be used *in vitro* to provide mutational rates, information on mechanisms and spectra of mutations for chemical carcinogens. This assay will also be used to investigate mutation spectra for other important indoor toxic compounds. All of the probes needed for the HLA-A mutation assay have been obtained and work has begun to generate some of the input for the human leukemia model using the assay.

U.S. Energy Model Development

Principal Investigator: Mark D. Levine

Funding: $49,500

Project Description

The major objectives of the project were to begin a process that would: (1) work with Lawrence Livermore National Laboratory (LLNL) to explore different long-term models of U.S. energy supply and demand; (2) select the most appropriate model and enhance it for use in constructing energy scenarios of the United States; and (3) use the model and scenarios to analyze important U.S. energy issues.

Accomplishments

A model, the Generalized Equilibrium Modeling System (GEMS), was identified as the best choice for an improved modeling system in the near term. LLNL purchased a license to this proprietary code, and terms were established so that LBL could also use the code at our site. A division of labor was set up with LLNL. LLNL would take responsibility for getting the GEMS running and would redesign the data structure and update the full data base. LBL would address what, in our view, was the major deficiency of GEMS: the lack of meaningful detail for the end-use structure.

Both groups were able to accomplish their specific objectives. The LLNL team was, with some difficulty, able to get the model running. They developed a new database for the model, produced documentation for the database, and ran the model to generate scenarios. The LBL team learned how to run the GEMS model. We concluded that the industrial end-use structure was particularly weak, and decided to build an entirely new model to forecast U.S. industrial energy demand. The model was intended to be relatively simple, easy to use, and rely on a relatively small number of driving variables to forecast industrial demand. In addition, the project involved LBL

building a reduced-form version of LBL-REM, our detailed residential energy demand forecasting model.

The industrial energy model was completed. The reduced version of LBL-REM not only formed a basis for incorporation of a simplified model into GEMS but also identified some issues with the data structure of LBL-REM, which will require additional research. The work on GEMS indicated that, while the model was theoretically sound and useful for developing U.S. energy scenarios, modern computing techniques could lead to a simpler and more powerful model for creating energy scenarios.

The LBL portion of the work has received funding from DOE to continue to pursue end-use modeling activities. We have received funding from the Office of Planning and Analysis of CE for end-use modeling and related activities, from DOE's Environmental Policy Office to enhance end-use models to analyze policy issues, and from DOE's Office of Building Technologies to enhance end-use models and data. Thus, this project has led to important new work funded by DOE at a higher level and considerably sooner than expected.

Publications

Journals and Proceedings

F. Bois, M. Smith, and R.C. Spear, "Mechanisms of Benzene Carcinogenesis: Application of a Physiological Model of Benzene Pharmacokinetics and Metabolism," *Toxicology Lett.* (in press).

F. Bois and R. Spear, "Analysis of Parametric Uncertainty in Physiological Pharmacokinetic and Multistage Cancer Models," submitted to *Biometrics* (LBL-28631).

F.Y. Bois, T.J. Woodruff and R.C. Spear. "Comparison of Three Physiologically-Based Pharmacokinetic Models of Benzene Disposition," submitted to *Toxicology and Applied Pharmacology* (LBL-29970).

Cell and Molecular Biology Division

Molecular Biology Approaches to Studies of Mammary Epithelial Cells in Culture

Principal Investigators: Mina J. Bissell, Roger Y. Tsien, and Gordon Parry

Funding: $41,700

Project Description

Molecular biology techniques were applied to understanding the mechanism of signal transduction in mammary epithelial cells. The project focused on exploring: (1) the role of intracellular second messengers by using fluorescence radioimaging and confocal microscopy and (2) the role of heparan sulfate proteoglycan (HSPG) structure and function in the mammary gland.

Accomplishments

Application of fluorescence ratio imaging and confocal microscopy to measurement of intracellular second messengers in epithelial cells and tissues. One of the principal investigators (Tsien) in this project became a Howard Hughes investigator at University of California, San Diego. Thus, this part of the project was delayed while efforts were made to regroup and identify another collaborator who could provide instrumentation and expertise to determine Ca^{2+} fluxes. Late in the funding year, a simple model was developed for cell-extracellular matrix (ECM) interactions in which cells on a flat monolayer can be treated with dilute ECM molecules in solution. In addition, a functional cell strain (developed in another project) of CID-9 cells was established. A new collaboration has been initiated with Professor Terry Machen at UC Berkeley, and this study is now ready to proceed.

Molecular Analysis of a Proteoglycan on the Surface of Mammary Cells. Previous work in our laboratory had led to isolation of a cDNA coding for a small HSPG proteoglycan from a mouse mammary gland λ gt11 library.[1] The sequence of this 400 bp cDNA was determined and the peptide sequence predicted. Experiments were then conducted to assess whether this cDNA coded for a novel proteoglycan or whether it was similar to a previously characterized large HSPG. The 400 bp sequence was first compared with the set of sequences in Genbank. No significant homologies to known sequences were found. The size of the mRNA coding for the HSPG in the mammary gland was then determined by Northern blot analysis and compared with the size of the mRNA coding for a previously identified HSPG. Significantly, it was found that the small HSPG was coded for by a mRNA that was 2.6 kb long. The large HSPG is coded for by a mRNA that is 10 kb long. Thus, it is clear that the newly identified small HSPG message is a different gene product from the large HSPG. This conclusion was supported by the finding that even in the EHS tumor, which is a major source of the large HSPG, it was possible to identify a 2.6 kb mRNA using the probe for the small HSPG. It is apparent that two forms of basement membrane HSPGs exist, and they may be simultaneously expressed in the same cells.

Additional experiments were carried out to study the regulation of expression of the 2.6 kb mRNA in culture. Previous work by Streuli and Bissell[2] has shown that mRNA levels for extracellular matrix components are modulated by the cell culture substratum. In this project it was found that this was also the case for the small HSPG mRNA, with maximal expression of the small mRNA being found in cells cultured on plastic substrata and down regulation of mRNA levels in cells cultured on collagen gels.

References

1. J.R. Couchman et al., "Immunological and Molecular Approaches to the Study of Basement Membrane Proteoglycen Diversity," *Biochem. Soc. Trans. 18*, 819 (1990).

2. C. Streuli and M.J. Bissell, "Expression of Extracellular Matrix Components is Regulated by Substratum," J. Cell Biology *110*, No. 4, 1405 (1990).

Technology Transfer in Biotechnology

Principal Investigators: Mina J. Bissell, Martin Stampfer, and Junko Hosoda

Funding: $125,300 (third year of funding)

Project Description

The overall objective of this project is to develop a basic research program to define practical host-vector systems utilizing mammary epithelial cells for synthesis and secretion of exogenously introduced genes. Human and rodent mammary epithelial cells in culture will be analyzed to decipher the processes that control synthesis and secretion of endogenously produced proteins, and this knowledge will be used to explore the possible utility of these systems for synthesis and secretion of the protein products of exogenously introduced genes. Integral to this study is the examination of *cis* and *trans*-acting factors associated with optimal expression and secretion of relevant proteins. It is anticipated that the basic research information obtained will be of value to many aspects of the biotechnology industry.

The accurate synthesis and secretion of biologically valuable protein products by eukaryotic cells requires a series of specific cellular and molecular processes, many of which are poorly characterized. In recent years, it has become apparent that these processes may include extensive post-transcriptional and post-translational modifications. Additionally, the level of gene expression can be controlled by extracellular influences such as cell-cell and cell-matrix interactions, which may modulate the capacity of promoter/enhancer sequences to drive DNA transcription. This project will explore ways to optimize protein secretion using the secretory mammary cell type and studying factors associated with enhanced gene expression and host-vector systems to achieve exogenous gene expression.

The goals of this project were approached from several directions:

1) Determine the most abundant endogenously synthesized and secreted proteins in the human and rodent mammary cell cultures. The promoter and signal sequences of such genes would be promising candidates to use in vectors designed to drive expression of exogenous gene sequences;

2) Determine how variations in the culture conditions might modulate the expression of endogenous secreted proteins, particularly the effects of specific growth factors, and cell-substrate and cell-cell interactions;

3) Optimize conditions for the introduction of foreign genes into the mammary epithelial cells to yield stable expression and secretion;

4) Optimize constructs (promoters, signal sequences) to yield a vector system that will maximize production of a desired protein in a particular culture environment;

5) Examine the expression of the exogenously introduced genes in the mammary cells; and

6) Transfer these technologies to industry.

Accomplishments

Human mammary epithelial cell (HMEC) system. In the past year we have focused on the goal of optimizing vector constructs for transfection of HMEC, and have begun studies on the expression of the exogenously introduced genes. Prior studies had indicated that electroporation provided the most efficient method of transfection. Frequencies of stable transfection, determined by Neo^r, have been ~1.3×10^5 for the immortalized HMEC cell line 184B5 and ~$1\text{-}2 \times 10^5$ for normal HMEC strains. Prior studies also indicated that fibronectin is the most abundantly secreted protein, suggesting that the fibronectin promoter might be useful to drive expression of exogenous genes.

Vector constructs were made using the human CMV (obtained from Monsanto), metallothionein IIA, and fibronectin (obtained from Dr. Suzanne Bourgeouis, Salk Institute) promoters. These promoters have been used to drive transcription of several genes: human c-erbB-2 (obtained from Dennis Slamon, UCLA), lipoprotein-associated coagulation inhibitor (LACI) gene (obtained from Monsanto), NB-1, a newly identified gene from this laboratory, and the bacterial β-galactosidase gene. The vectors containing these gene constructs, along with the selectable neomycin resistance gene, were introduced into the 184B5 via electroporation. These particular genes were chosen for different reasons. The erbB2 gene is of interest for its possible role in human mammary carcinogenesis, and we wished to determine its effect on expression of differentiated properties and malignant potential in the non-malignant 184B5 cells. The LACI gene was chosen, in collaboration with Monsanto, since they have developed efficient assays to measure the secreted LACI protein, and had an interest in determining methods to increase its production in *in vitro* systems. Studies in this laboratory have suggested

that NB-1 may play a key role in carcinogenesis; since it is reduced or absent in transformed HMEC, it was introduced into 184B5 as well as malignantly transformed derivatives of HMEC specimen 184, and the breast tumor cell line MCF-7.

Successful stable transfection of all these genes in the HMEC host cells has been demonstrated. The fibronectin and metallothionein promoter appeared to be the most effective in producing increased levels of mRNA and protein for erbB2 and LACI. The CMV promoter was also effective in the transfection of NB-1 into the malignantly transformed cell lines. Levels of erbB2 could be increased 4-5× when TGFβ was added to cultures transfected with the fibronectin promoter construct. Measurements of LACI secretion (performed by Monsanto) in some transfected 184B5 cells were comparable to those seen by Monsanto using their existing host vector constructs. These levels could be increased by TGFβ exposure of fibronectin promoter constructs, and by heavy metal exposure of the metallothionein promoter constructs. Conditions have been developed that now allow induction of the metallothionein promoter to continue for 1-2 weeks, with maintenance of healthy 184B5 cultures and continued increased levels of LACI production.

Studies are now underway to determine the effect of these transfected genes on the host cells. The studies with erbB2 are continuing in collaboration with Dennis Slamon and Triton (now Berlex Corp.). These cells are being tested for tumorigenicity and used for studies by Triton related to their ongoing research program on erbB2 and antibodies to erbB2. The studies on NB-1 are ongoing in this lab. Tumorigenic HMEC transfected with NB-1 have maintained growth in culture and are now being assayed for their tumorigenic capacity.

These studies have indicated that a host-vector system for high level expression of foreign genes in nonmalignant HMEC can be obtained. This opens up many exciting possibilities in terms of basic research on the effect of exogenous genes in HMEC cultures, as well as potential applications for efficient production of desired protein products in a secretory human cell system.

Murine mammary epithelial cell (MMEC) system. Work with the rodent system last year made significant progress toward achieving all the six goals listed in the project description. After many attempts, it was clear that electroporation in primary cultures was very cumbersome and inefficient. Thus, a considerable amount of time was spent to develop a functional mammary cell strain. This was achieved by taking advantage of existing expertise. Efforts began with cultures of COMMA 1-D cells—a cell strain that is functional in low passage, but loses function and hormone and substrata-responsiveness in later passages. Using expertise developed in culturing primary mammary cells, we selected for the ability of subpopulations of COMMA 1-D cells to form "alveoli" on basement membrane matrices and assayed for milk protein production. After a number of differential trypsinization, a cell strain (CID-9) was developed that is capable of producing high levels of β-casein (> 35% of cells) in response to lactogenic hormones when cultured on a basement membrane matrix.

In collaboration with Monsanto scientists who had isolated the bovine β-casein gene, a number of constructs were engineered, consisting of different lengths of bovine β-casein promoter attached to chloromphenicol-acetyl transferase (CAT) gene. These CID-9 cells could be transfected stably with these constructs whose expression further proved to be hormone and substrata-dependent.

CID-9 cells already fulfill some of our most optimistic predictions; other foreign genes transfected into them can also be processed and secreted. However, the expression is substratum-dependent (as predicted), and therefore it would be desirable to develop permanent cell lines that are both functional and could grow on plastic or in suspension. Monsanto has also expressed an interest in developing new cell strains at LBL using transgenic technology.

Mammalian Repair Enzyme(s) Characterization and Identification of Yeast REC Repair Genes

Principal Investigator: Aloke Chatterjee, Michael Esposito and Bea Singer

Funding: $35,000

Project Description

In the first part of this research effort, the goal has been the identification of mammalian binding proteins involved in repair of carcinogen-caused mismatches. Originally, the standard selected was repair of an O-alkylpyrimidine site specifically incorporated into an oligonucleotide. O^4-methyl T, the first choice, was available in a mismatch with A or G. However, protein binding was very low under the experimental conditions chosen. In contrast, a mismatch of 1, N^6-etheno A (εA) similarly placed in a template, gave a

indicated that this probe would be more useful initially. In further studies, attention will be directed toward both εA and O^4-methyl T protein binding.

This past year, the goal has been to identify a possible first step in repair of defined DNA lesions: the step of recognition, using well-characterized synthetic oligonucleotides as probes. Efforts have particularly concentrated on a previously unknown human DNA-binding protein that recognizes 1, N^6-ethenoadenine (εA) in double-stranded DNA. Ethenoadenine is a product formed *in vivo* in DNA as a result of exposure to vinyl chloride, a well-known human carcinogen. We are tentatively assuming that the DNA-binding protein is associated with repair.

The second part of this research effort involved a study of a yeast DNA strand exchange protein required for general recombination and repair of x-ray damage. Characterization of the properties of yeast mitotic and meiotic recombination by genetic analysis has contributed to the formulation of molecular models describing the DNA-protein interactions that result in gene conversion and crossing over between homologous chromosomes of eukaryotes. Mutations of *REC* genes encoding the recombinases that perform the envisaged recombination reactions are essential to validate mechanistic interpretations of recombination data. The purpose of the research described below is to identify the proteins encoded by yeast *REC* genes identified in this laboratory. The properties of three temperature conditional hyporecombination mutants, *rec1-1*, *rec3-1* and *rec4-1*, that define three novel yeast *REC* genes of *Saccharomyces cerevisiae* are described. Earlier work demonstrated that *REC1*, *REC3* and *REC4* are essential for spontaneous mitotic gene conversion and crossing over, chromosomal stability, meiosis and ascospore formation (sporulation), and, in the instance of *REC1*, repair of potentially lethal x-ray damage. In order to further understand these three *REC* gene functions, control recombination proficient strains and *rec* mutant strains have been characterized for presence of DNA strand exchange activity. The principal result of these experiments is the demonstration that *REC1* encodes a Mr~170,000 DNA strand exchange protein essential for in vivo general recombination and repair of X-ray damage.

Accomplishments

Evidence for a εA-DNA binding factor. Using a DNA electrophoresis bandshift assay and extracts from a human hepatocyte cell line, we first surveyed for the presence of DNA binding factors specific for O^6MeG, O^4MeT and ethenoadenine (εA), since oligonucleotides containing those modified bases at specific sites were available. Of these, the εA-containing oligonucleotide showed a clear and reproducible unique-appearing retarded band (Fig. 1) indicating a DNA binding protein, and attention was focused on this protein. Other modified bases in defined oligonucleotides will be tested when time permits and they are available.

Characterization of the binding reaction. The binding specificity is due to the presence of εA as shown by competition experiments. Competition experiments using excess non-radioactive εA-containing double stranded oligonucleotide prevents appearance of this band, while excess normal A•T-containing oligomer has no effect (see Fig. 1). This binding factor is a protein since the specific radioactive band is not present if the cell extracts are incubated with proteinase K but not by RNase A. Binding requires the presence of a cation, with the highest efficiency in the presence of multivalent cations. Optimal binding is achieved by either 0.2 mM spermine, 0.2 mM spermidine, 2 mM $MgCl_2$ or 150 mM NaCl. This cation requirement may be similar to the presence of histones *in vivo*.

The probe needs to be double stranded, since the protein-binding does occur with εA, a single stranded oligomer. Both a short probe (a 25-mer with εA

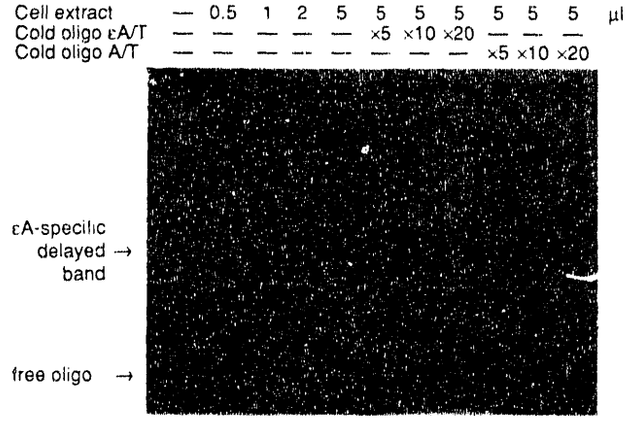

Figure 1. Extracts from HeLa cells were incubated with a ^{32}P-labelled εA-containing oligomer probe, with or without the presence of nonradioactive competitor oligomer. The samples were electrophoresed in a polyacrylamide gel which were then autoradiographed. The amount of extract and amount of unlabeled competitor (relative to probe) is indicated above each lane. The bottom arrow shows the location of unbound DNA probe; the upper arrow shows the εA-specific delayed band. Bands at top are not specific for εA.

adduct six bases from the end) and a longer probe (a 42-mer with the εA close to the middle), are recognized. The base opposite the εA can be T or C (G and A have not been tested). This may be of physiological significance, since *in vitro* DNA polymerase experiments have shown that edATP, a bulky adduct, can pair with both T and C, so both pairs may be present *in vivo* and both are recognized.

Partial purification of the binding protein. Ammonium sulfate precipitation (30 - 50%) and gel filtration on Sephacryl S-200 yield a ten-fold purification. This work is the beginning of a development of methods for a higher level of purification.

Size of the binding protein. A Sephacryl S-200 column calibrated with proteins of known size was used. A partially purified and concentrated sample from human HeLa cells was chromatographed and fractions assayed for the presence of εA DNA binding protein. The peak of binding activity eluted at the position of 35 KDa globular protein.

Presence in different species and human tissues. In addition to two human transformed cell lines (hepatocytes and HeLa cells), the binding factor was also found in human placenta, human liver and rat liver. It was not possible to detect any εA-specific DNA binding factor, however, in wild type *E. coli* and *S. cerevisiae*. While the HeLa cells and human placenta showed one delayed εA-specific band, the hepatocyte cells and livers showed two or three εA-specific bands. Whether the extra band(s) are due to proteolysis during extraction, or are different forms present *in vivo* remains to be determined. The relative amounts of εA binding factor (per mg total protein in raw extracts) were approximately as follows: HeLa 100%, hepatocyte cells 80%, human placenta 20%, human liver 3%, rat liver 2%. These numbers may be subject to change as the extraction procedure is improved. The value for human liver is based only on one experiment.

The apparent low level of the binding protein in rat liver is of interest since the *in vivo* removal of εA-adducts from DNA after vinyl chloride exposure has been studied only in rat liver, and the removal has been found to be absent or extremely slow. The results indicating up to 50 times higher level of the binding protein in human cells (corresponding to 10^4 - 10^5 molecules/cell) may indicate more efficient repair in humans, as compared to rats.

Several yeast DNA strand exchange proteins of mitotic and meiotic cells that may participate in recombination *in vivo* have been described. A Mr~170,000 DNA strand exchange protein of mitotic diploid yeast cells that mediates *in vitro* renaturation of homologous DNA strands, homologous pairing, and DNA strand exchange has been characterized extensively. The Mr~170,000 DNA strand exchange protein catalyzes formation of joint molecules between viral linearized duplex DNA and homologous single-strand DNA in a reaction that is Mg^{2+} dependent and ATP independent, and can be readily detected in partially purified protein extracts prepared by DNA affinity chromatography.

Using partially purified single strand DNA cellulose column fractions, the presence of the Mr~170,000 DNA strand exchange activity was demonstrated in control recombination proficient diploid cells grown at 24 C and 36 C. We then examined *rec/rec* diploids grown at 24 C, the permissive temperature for recombination, and 36 C, the restrictive temperature for recombination, for presence of this DNA strand exchange activity. The column fractions of *rec1-1/rec1-1* cells grown at 24 C exhibited DNA strand exchange activity, however the column fractions of *rec1-1/rec1-1* cells grown at 36 C exhibited no detectable DNA strand exchange activity (Fig. 2). The proteins in these *rec1-1/rec1-1* column fractions were concentrated tenfold by ammonium sulfate precipitation and reassayed. Only a trace of DNA strand exchange activity could be detected.

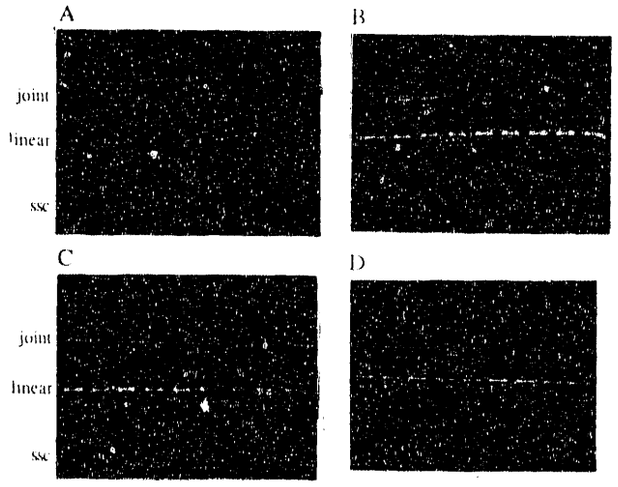

Figure 2. DNA strand exchange activity in protein fractions from single stranded DNA cellulose columns. The positions of the viral ØX174 single-stranded circular DNA (ssc), the double-stranded linear ØX174 DNA (linear), and the joint molecule (joint) are indicated. The NaCl concentration increases from left to right; the peaks of activity elute between 0.2 and 0.3 M NaCl. A. REC1/REC1 cells grown at 24 C. B. REC1/REC 1 cells grown at 36 C. C. rec1-1/ rec1-1 grown at 24 C. D. rec1-1/rec1-1 cells grown at 36 C.

This result demonstrates that the Mr~170,000 DNA strand exchange activity is under control of the *REC1* gene. *rec3-1/rec3-1* and *rec4-1/rec4-1* cells grown at both 24 C and 36 C exhibited DNA strand exchange activity. The activity levels were the same as that observed in the control strain grown at 24 C and 36 C, indicating that *rec3-1* and *rec4-1* mutants possess the DNA strand exchange activity controlled by *REC1*.

The *REC1* and *rec1-1* DNA strand exchange proteins of 24 C grown cells have been purified to 95% homogeneity. Both proteins elute from single strand DNA cellulose columns at 0.25 M NaCl. Subsequent chromatography on Sephacryl S200 gel filtration and PBE-94 columns showed that the peak of the *REC1* DNA strand exchange activity elutes with a Mr ~170,000, as expected, while the peak of the *rec1-1* DNA strand exchange activity elutes with a Mr ~43,000. Denaturing polyacrylamide gel electrophoresis showed that both proteins are single polypeptide chains (Fig. 3). The Mr~43,000 DNA strand exchange protein purified from the *rec1-1* strain does not cross react with three monoclonal antibodies to the REC1 protein. The Mr~43,000 DNA strand exchange protein may be either a truncated version of the REC1 protein or a different DNA strand exchange protein made by *rec1-1* cells. Nonetheless, the Mr~170,000 DNA strand transfer protein is required for normal levels of recombination and repair of x-ray damage in vivo.

The *REC1*, *REC3* and *REC4* genes are being cloned and sequenced to provide further information regarding the proteins encoded by these *REC* genes and the viability of *rec* deletion mutants.

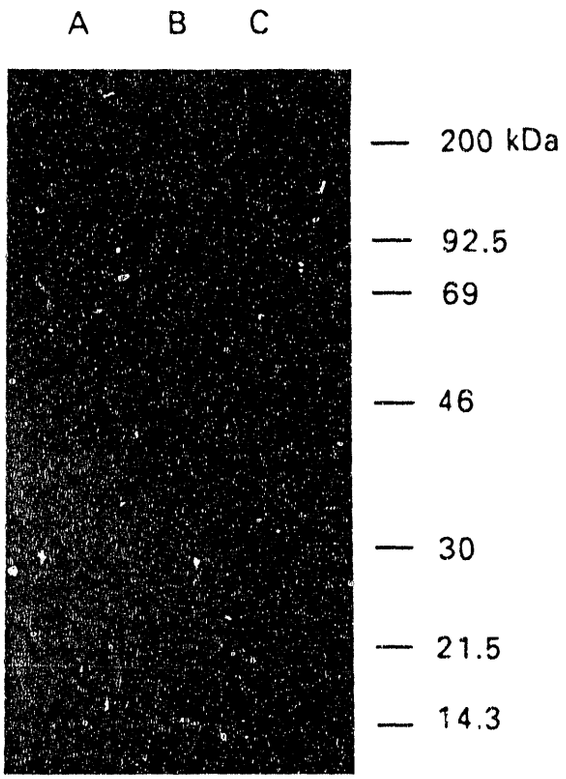

Figure 3. Purification of REC1 and rec1-1 strand exchange proteins. After purification on PBE-94 columns, strand exchange proteins were subjected to 10-17.5%/5-20% acrylamide/sucrose double gradient SDS-polyacrylamide gel electrophoresis. Lane A REC 1 strand exchange protein; Mr~170,000. Lane B rec1-1 strand exchange protein; Mr~43,000. Lane C Molecular weight calibration proteins (Rainbow molecular weight markers, Amersham, IL.). The molecular masses, in kilodaltons, of the calibration proteins are listed down the right side of the figure.

Alternative RNA Splicing Mechanisms in Erythroid Differentiation

Principal Investigator: John G. Conboy

Funding: $78,000

Project Description

The principal long range goal of this project is to study the mechanism of alternative RNA splicing in the differentiation of erythroid cells during erythropoiesis. The project focused on the protein 4.1 gene, a complex locus organized into introns, constitutively expressed exons, and alternatively expressed exons. At the level of nuclear RNA processing, the exons are joined together in specific combinations to form mRNAs that encode distinct protein 4.1 isoforms in erythroid and nonerythroid cells. Whereas our previous studies concentrated on defining the structure of these protein 4.1 isoforms, this project has a quite different aim: to study nuclear RNA processing factors that regulate tissue-specific splicing events. In order to study the RNA:protein interactions that regulate alternative splicing at intron/exon boundaries, the following specific aims will be addressed: (1) construction of protein 4.1 minigenes containing cloned 4.1 genomic DNA sequences in regions of critical splicing choices; (2) reconstitution of alternative splicing of minigene substrates using *in vivo* and *in vitro* splicing systems; (3) identification of regulatory nucleotide sequences in the pre-mRNA splicing substrate, by deletion/mutation of sequences flanking splice junctions in the transcribed minigene; and (4) identification and molecular cloning of *trans*-acting RNA binding proteins that regulate alternative splicing. Because tissue-

specific splicing also occurs in other structural proteins such as tropomyosin, these results may have broader implications not only with respect to control of the differentiated erythroid phenotype, but also in our understanding of differentiation of other cell types.

Accomplishments

Although these aims were very ambitious for a one year period, sufficient progress was made with preliminary work to successfully obtain a five year NIH grant to study the same splicing questions (with virtually the same specific aims, see below). Chiefly, two regions of the 4.1 gene in which regulated splicing events occur have been defined. One is in the 5' region and involves alternative splicing of two exons containing two different AUG translation initiation sites that in turn encode 4.1 isoforms of two different molecular weight classes possessing different amino termini. This portion of the 4.1 gene has been successfully cloned, and it was determined that splicing of the "upstream" AUG is governed by alternate usage of two splice acceptor sites located just 17 base pairs apart. Figure 1 shows the genomic sequence in this region. The labels indicate the two splice acceptor sites, the consensus acceptor sequences, and two heptanucleotide repeats that are candidates for binding by *trans*-acting splicing factors. Also, in collaboration with Drs. Mohan Narla and Joel Chasis in the hematopoiesis group, we have shown at the protein level that two hematopoietic tissues—T-lymphocytes and reticulocytes—express very different ratios of the high and low molecular weight isoforms initiated at the two alternative AUGs. This region is likely regulated by *trans*-acting factors that bind differentially to these splice acceptor sites. This cloned minigene will be employed as a substrate with which to explore the aims concerning *cis* sequences and *trans* factors which regulate splicing.

The second alternatively spliced region with interesting regulation is the so-called spectrin-actin binding domain, which exists in four varieties by virtue of alternative splicing of two exons in this region. Most interestingly, the splicing of one exon ("21", encoding a peptide of 21 amino acids) is switched on during erythroid maturation in both humans and mice. This splicing switch can be reproduced *in vitro* using cultured mouse erythroleukemia (MEL) cells; before differentiation MEL cells do not splice the "21" exon into 4.1 mRNA, whereas after chemically-induced differentiation the exon is spliced in. Efforts are currently under way to try to isolate genomic clones for this region. Unfortunately, the 4.1 gene is very large (>100 kb) and all of the clones obtained thus far from lambda and cosmid vectors do not contain this region. We are now screening a human genomic library constructed in a YAC (yeast artificial chromosome library), one repository of which resides in the Human Genome Center here at LBL.

As an outgrowth of this research, several new directions have been identified.

Helicase studies. In recent years it has become abundantly clear that many aspects of RNA function, including RNA splicing, are regulated by secondary structure, i.e., formation of double-stranded regions and stem-loop structures by base pairing between homologous sequences within a single long RNA polymer. The equilibrium between an extended single stranded conformation versus a more ordered double-stranded conformation is apparently regulated in

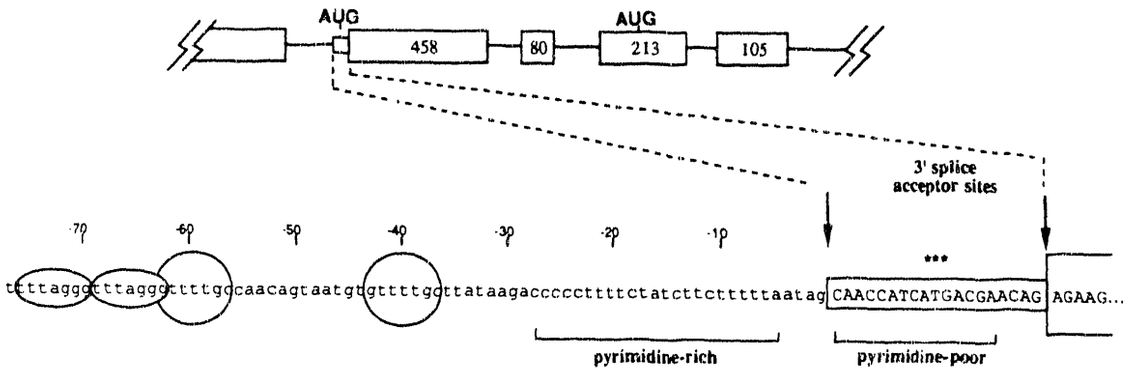

Fig. 1. Nucleotide sequence analysis of alternative 3' splice acceptor sites in genomic DNA. Upper panel indicates the deduced intron/exon structure of a 5' portion of the protein 4.1 gene containing the two translation initiation sites in two different exons. In lower panel, position of the putative upstream AUG is marked by the asterisks, and the splice acceptor sites are indicated by arrows. Circled regions show two repeated heptamers in the intron sequences.

many cases by a key class of enzymes known as "helicases" (the name derives from their ability to unwind a double-stranded RNA helix). At least ten members of this helicase family have been identified recently in yeast, including several that are constituents of the snRNPs (small ribonucleoprotein particles) that are integral components of the constitutive RNA splicing apparatus, the spliceosome. In addition, the MSS116 gene has been implicated in alternative splicing of the cytochrome b and cytochrome c oxidase subunit I mRNAs in yeast mitochondria.

We have become interested in characterizing helicases expressed in MEL cells during erythroid maturation, as these changes in expression or activation of these enzymes could potentially regulate the changes in protein 4.1 RNA splicing that occur during differentiation. As a first step toward this goal, partial cDNAs encoding 6-8 different putative helicases have been cloned from uninduced MEL cells. To accomplish this, two sets of degenerate oligonucleotides (16-256 members in each class) homologous to three regions that are highly conserved within all members of the helicase family were designed (see Fig. 2). These oligonucleotides were used as primers to clone helicase-related sequences using reverse transcriptase/polymerase chain reaction techniques. One of our newly isolated helicase cDNAs is very highly homologous to the human "p68" protein, a nuclear helicase believed to function in RNA processing, and thus appears to encode the mouse counterpart (which had not previously been cloned). The other putative helicase cDNAs appear to represent new members of the helicase family, as they are not highly homologous to previously reported sequences. In order to obtain full length cDNAs for these helicases, we are now in the process of screening an excellent expression library constructed from MEL cells with the partial cDNAs cloned by PCR.

Alternative splicing of erythroid ALAS (aminolevulinic acid synthase) RNA. As one of the major goals of this project is assessment of the role of alternative splicing

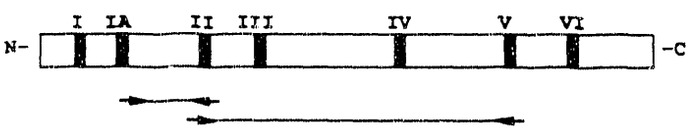

Fig. 2. RT/PCR cloning strategy for erythroid RNA helicases. This diagram shows a model of a typical RNA helicase protein; motifs I-VI represent sequences that are highly conserved among all members of the helicase protein family. Arrows below indicate the position of oligonucleotide primers used to amplify helicase mRNA sequences from MEL cells by RT/PCR techniques.

in erythroid differentiation, we are interested in identifying additional alternatively spliced genes that may prove useful substrates in later mechanistic studies. In collaboration with Dr. Sylvia Bottomley at the Veterans Administration Medical Center in Oklahoma City, we have recently detected a novel alternatively spliced RNA encoding a structural isoform of erythroid ALAS. In all erythroid cells tested, this gene appears to be spliced in two forms by alternative splicing of exon 4.

Cryo-Electron Microscopy

Principal Investigator: Robert M. Glaeser

Funding: $58,700

Project Description

New techniques in the use of frozen-hydrated biological specimens in high resolution electron microscopy were utilized to gain information about cell structure at the level of macromolecules and macromolecular assemblies. This research focused on the structure of and interaction between cell membrane and cytoskeleton.

Accomplishments

Low temperature electron microscopy (cryo-EM) of cell membranes was used to obtain high resolution images of a specialized region of the cell-surface membrane known as the gap junction. This specialized region, ranging in size up to 1 μm^2 in area, contains many copies of a single type of membrane protein that forms a small aqueous channel ~15 Å in diameter at its narrowest point. These channels serve the biological function of providing a pathway for the diffusion of ions and small organic molecules between adjacent cells. Dr. Santosh Sikerwar prepared small quantities of these gap junction membranes, isolated from lobster hepatopancreas. With the help of Dr. Ken Downing, images of glucose-embedded specimens were recorded at -120 C. After computer processing, these images yielded substantially higher structural resolution than has ever been obtained previously on the gap junction.

A laser light-trap was used as an optical tweezers to measure the force exerted by ATPase molecules, which are responsible for moving vesicles and small particles along the microtubules of a cell called *Reticulomyxa*. This work was done by Dr. Manfred Schliwa in collaboration with Dr. Arthur Askin. The laser light-trap work was intended to be used in conjunction with

rapid cryo-fixation methods and cryo-EM to provide a structural characterization of the ATPase. Continuation in this direction will not be possible, however, as Dr. Schliwa has accepted a professorship in Munich.

Dr. Ken Downing has succeeded in getting long monolayer crystals of tubulin, up to 0.5 µm wide. These are still too small for electron diffraction, so further work will have to continue in the area of crystallization before the cryo-EM phase with this specimen can begin.

Policy Issues in Molecular Biology

Principal Investigator: Paul H. Silverman

Funding: $55,100

Project Description

Molecular biology in general (i.e., genetic engineering) and the Human Genome Project in particular, face a range of public policy and awareness issues that have the potential for adversely affecting the research programs. The root causes for these concerns have been ascribed to various societal factors, including widespread scientific illiteracy. The scientists themselves contribute to the problem of misperception by the way in which they communicate, raising public expectations unrealistically or exaggerating risks or benefits.

This project is aimed initially at identifying and analyzing the various social, ethical, and legal issues raised by the Human Genome Project. The next phase is to develop strategies to resolve the concerns. This may be accomplished by establishing a strong, science-based group in association with relevant social scientists and persons in the humanities who can deal effectively with the social, ethical, and legal issues identified in this preliminary survey.

Accomplishments

The project began with a series of round table discussions and individual interviews with selected molecular biologist, scientists, sociologists, humanists, and members of the legal profession. Additional consultations and active participation in a number of national and international conferences which featured the Human Genome Project were pursued, e.g., "The impact of new technologies on Civil Liberties," sponsored by the University of Delaware, the Widener University School of Law, and the American Civil Liberties Union; "Public Policy Conference: Biotechnology, future directions, future Policies," sponsored by the College of William & Mary; "Biotechnology: Public perceptions and public policies," sponsored by IBEX '90.

The current growing popular literature was surveyed and the alarmist tone of journalist articles and books led to the development of a series of workshops on molecular biology and the Human Genome Project for the UCB School of Journalism organized by Professor Tim Ferris and sponsored by the UC Biotechnology Education and Research Program. There is clearly a great need to be met in the area of public communications.

The following list of social, legal, and ethical concerns have emerged from the survey described above. The genetic information currently being generated and anticipated to be developed by the Human Genome Project may alter the way medicine is practiced, insurance and health care is provided, and information is shared. There is a strong core of concerned and capable individuals in LBL and in the nearby community who are anxious and available to focus on these issues. The National Institutes of Health Center for Human Genome Research, operated by the Center for the Study of Law, Science, and Technology of Arizona State University, is currently examining the legal aspects of the Human Genome Project. LBL can provide expertise in a number of areas listed below.

HUMAN GENOME PROJECT
SOCIAL, LEGAL, AND ETHICAL CONCERNS

Privacy, Confidentiality and Access
- Ownership and control
- Consent to disclosure
- Computer storage and access

Fairness
- Insurance
- Employment
- Criminal justice system
- Military
- Adoptions

Genetic Counseling
- Prenatal testing and reproductive issues
- Pre-symptomatic testing
- Carrier status testing
- Testing for untreatable disorders
- Polygenic disorders

Impact on Individual
- Stigmatization
- Labeling and stereotyping
- Self-esteem
- Education

Impact on Medical Practice
- Human DNA probes — specificity
- Preventative medicine
- Transplant compatibility
- Professional standards and education
- Physician standards and education
- Physician-patient relationship

Impact on Community
- Testing
- Screening
- Eugenics
- Public health
- Behavioral genetics
- Education/communication

Legal Implications
- Property rights and commercialization
- Patents, copyrights and licenses
- Public interest interventions
- Public interest DNA typing
- Research rights

Philosophical Questions
- Personal identity
- Personal responsibility (nature vs. nurture)
- Sacredness of DNA
- Reductionism and holism

Publications

Journals and Proceedings

A. Askin, K. Schutze, J.M. Dziedzic, U. Euteneuer, and M. Schliwa, "Force Generation of Organelle Transport Measured *in vivo* by an Infrared Laser Trap," *Nature 348*, 346 (1990).

S. Sikerwar, K.H. Downing, and R.M. Glaeser, "Three-Dimensional Structure of an Invertebrate Intercellular Communicating Junction," submitted to *J. Struct. Biol.*

J.G. Conboy, J. Chan, J. Chasis, Y.W. Kan, and N. Mohandas, "Tissue- and Development-Specific Alternative RNA Splicing Regulates Expression of Multiple Isoforms of Erythroid Membrane Protein 4.1," *J. Biol. Chem.*, in press (1991).

M.S. Esposito and J.T. Brown, "Conditional Hyporecombination Mutants of Three *REC* Genes of *Saccharomyces cerevisiae*," *Current Genetics 17*, 7 (1990).

H.W. Moise, N. Rudin, J.T. Brown, G. Thomson, and M.S. Esposito, "The REC1 DNA Strand Transfer Protein of *Saccharomyces cerevisiae*," *Yeast 6*, s89 (1990). (Abstracts of the 15th Int. Conf. on Yeast Genetics and Molecular Biology, The Hague, The Netherlands).

N. Rudin, H.W. Moise, J.T. Brown, and M.S. Esposito, "The *REC3* Gene of *Saccharomyces cerevisiae*: Molecular Cloning, Disruption and DNA Sequencing." (Abstracts of Genetics Soc. of America Meeting, San Francisco) (1990).

C. Schmidhauser, G.F. Casperson, C.A. Myers, and M.J. Bissell, "Extracellular Matrix and Hormones Regulate β-casein Gene 5′ Sequences," in *The Therapeutic Implications of the Molecular Biology of Breast Cancer, Proceedings of the Second Pezcoller Foundation Symposium*, M. Lippman and H. Mihich, eds., Centro Italiano Congressi, Rome, Italy (1990).

C. Schmidhauser, G.F. Casperson, C.A. Myers, and M.J. Bissell, "Extracellular Matrix (ECM) and Hormones Regulate β-casein Gene 5' Sequences," The American Society for Cell Biology 30th Annual Meeting, Abstract #2144 (1990).

C. Schmidhauser, G.F. Casperson, C.A. Myers, and M.J. Bissell, "Extracellular Matrix and Hormones Transcriptionally Regulate Bovine β-casein 5' Sequences in Stably Transfected Mouse Mammary Cells," *Proc. Acad. Natl. Sci., 87*, 9118 (1990).

Presentations and Seminars

J. Conboy, J. Chasis, Y.W. Kan, and N. Mohandas, "Developmental Changes in Skeletal Protein 4.1 Pre-mRNA Splicing During Erythroid Differentiation," poster presented at the 1990 RNA Processing meeting at Cold Spring Harbor (1990).

J. Conboy, T.C. Cox, M.J. Bawden, B.K. May, and S.S. Bottomley, "Two Transcripts of Human Erythroid 5-aminolevulinate Synthase due to Alternative Splicing: Rapid Detection by Enzymatic Amplification of Reticulocyte mRNA," oral presentation at the 1990 annual meeting of the American Society of Hematology (1990).

S. Blam, "Growth Factor Control and Introduction of Exogenous Genes into Human Mammary Epithelial Cells in Culture," Triton, August 1990.

M.J. Bissell, "Basement Membrane is Necessary for Mammary Cell Organization and Gene Expression," UCLA Colloquium on Molecular, Biochemical and Cellular Biology of Human Breast Cancer, February 1990.

M.J. Bissell, "The Role of Extracellular Matrix on Mammary-Specific Gene Expression," The Therapeutic Implications of the Molecular Biology of Breast Cancer, Second Pezcoller Foundation Symposium, Rovereto, Italy, June 1990.

C. Schmidhauser, "Function of Extracellular Matrix in Differentiation and Development," Mini-Symposia at the American Society for Cell Biology 30th Annual Meeting, December 1990.

Chemical Biodynamics Division

Structural Studies of Biomolecules with the Scanning Tunneling and Atomic Force Microscopes

Principal Investigator: Miquel Salmeron

Funding: $120,700 (second year of funding)

Project Description

This project is the continuation of initial efforts to apply the Scanning Tunneling Microscope (STM) to image biological molecules, including DNA, RNA, etc. The project includes an instrument development component in order to adapt the STM to the operation conditions required by the biological material. In the previous year, efforts to obtain good images of DNA were only partially successful. The forces exerted by the tip on the material being imaged causes displacement and results in poor reproducibility. Therefore, efforts were devoted to change the conditions of operation to minimize these forces. An Atomic Force Microscope (AFM) was developed to measure the forces exerted and to simultaneously measure the current. In this manner the right conditions to image biological material can be determined.

Accomplishments

The STM was modified in collaboration with the Engineering Division and the Human Genome Center. It is now able to operate at 1,000 times lower currents than previously. In this manner the tip is maintained at a higher elevation over the surface. This modification has proven to be a success.

Layers of RNA on silicon wafer surfaces have been imaged. It has also been possible to image DNA on the same substrate and illustrate how the higher currents used in the past causes the tip to be close enough to the surface to often displace the adsorbed biomolecules. Images were also obtained of layers of self-assembled crystals of PDA on graphite. In spite of the larger thickness of these layers (roughly twice that of DNA and RNA), they can still be imaged. One disadvantage of operating at the lower currents is that atomic resolution is lost, although the overall shape of molecular objects is still visible (typically 10 Å or more).

The relationship between forces and currents as the tip is brought close to the surface was determined by using model molecules of known length and chemical bonding to the substrate (alkylsilanes on silicon and alkylthiols on gold). It was demonstrated that for these molecules, currents of up to 10 picoamperes are attained just before repulsive contact with the layer of alkylsilane at bias voltages of more than 6 volts, with the tip positive. These experiments are crucial to understanding the conditions required for imaging. They were performed with the AFM developed as part of this project.

Another AFM began operation recently. It is a substantially improved design, using microfabricated cantilevers on a Si chip. It is very compact and results in a much improved stability. It has been used to image bacteriophage T4 virus in its native form. Previously the virus, with a size in the range of 1,000 Å, could only be imaged in vacuum with the scanning electron microscope after metal shadowing. With this AFM, the virus is imaged naked in air. Experiments are presently continuing to image the virus in a water cell.

Publications

Journals and Proceedings

T.E. Wilson, M.N. Murray, D.F. Ogletree, M.D. Bednarski, C.R. Cantor, and M. Salmeron, "Scanning Tunneling Microscopy at High Gap Resistances and on Chemically Modified Silicon Surfaces," *J. Vac. Sci. and Technol.*, in press.

D. F. Ogletree, C. Ocal, H.-C. Wang, and W. Kolbe, "Tip-Surface Forces during Imaging by Scanning Tunneling Microscopy," *J. Vac. Sci. and Technol.*, in press.

Presentations and Seminars

M.N. Murray, W. Kolbe, G. Neubauer, D.F. Ogletree, C.R. Cantor, and M. Salmeron, "Imaging of Biomolecules with the STM and AFM," abstract submitted to the Human Genome Workshop, Santa Fe, New Mexico, Feb. 1991.

W. Kolbe, D.F. Ogletree, and M. Salmeron, "Atomic Force Microscopy Studies of Uncoated T4 Bacteriophage on Si Substrates," abstract submitted to the Human Genome Workshop, Santa Fe, New Mexico, Feb. 1991.

Chemical Sciences Division

Technical Evaluation of Beamline and Experimental Stations for Chemical Dynamics Applications at the ALS

Principal Investigators: Yuan T. Lee and Andrew H. Kung

Funding: $73,600

Project Description

This project is a preliminary technical analysis and assessment of various options for synchrotron UV beamline designs and associated experimental station designs in order to conduct high quality chemical physics experiments at synchrotron radiation sources. The goal is to evaluate specific technological options for a high-resolution, high-throughput synchrotron beamline in the region of 5–30 eV that are most suitable for research in chemical dynamics and combustion chemistry. Another goal is to evaluate new types of molecular beam and surface science experimental stations suitable for operation with such beamlines.

The approach involves identification of technological options by holding technical workshop discussions, computer analysis and modeling of specific designs, and fabrication of experimental facilities that will lead to the testing of more mature ideas at the National Synchrotron Light Source of the Brookhaven National Laboratory. Beamline technological areas that form the focus of the study are the choice of monochromator and grating design to achieve wavelength resolution of better than one part in 50,000, undulator design, mirror design, and gas filter design to achieve spectral purity of one part in 10^5, efficient beamline branching, and effective handling of corrosive and/or toxic gas in synchrotron source settings.

Accomplishments

Choice of undulator for 5–30 eV photon range. The ALS parameters (electron energy = 1.5 GeV, electron current = 400 mA) are optimized for operating in the x-ray to the soft x-ray region. It will also provide unprecedented performance in the 5–30 eV region in resolution and brightness with the proper choice of undulator parameters. To arrive at this choice, a number of technological tradeoffs needs to be considered. The factors to be considered are narrow emission bandwidth, acceptable magnetic field strength, and high spectral brightness. The performance characteristics of three undulators with a period of 8 cm, 10 cm, and 12 cm respectively are calculated for 7 eV operation. The results are tabulated in Table 1. From these results, an undulator with a 10-cm period is recommended as the best choice for the 5–30 eV photon range.

Beamline high-order suppression. An essential feature of a superior synchrotron UV beamline for chemical applications is very high spectral purity. In a user workshop held in April 1990, it was determined that a background radiation of less than one part in 50,000 is necessary. For the 10-cm undulator, the origin of background radiation is dominated by higher-order emission from the undulator. Suppression of this emission requires a combination of critical technologies. A new, differentially-pumped molecular-beamless gas-filtering system (Fig. 1) has been proposed, which can serve as the primary high-order suppressor for UV synchrotron beamlines. The features of this design include three stages of differential pumping, use of sperm-whale nozzles and molecular beam chokes to destroy molecular beam action along the optical beam axis, and modest requirements on pumping speed. Estimates show that this filter will result in suppression of high-order radiation from 10 eV to > 1 keV of over five orders of magnitude in undulator beamlines. The suppression could be

Table 1. UX Undulators Performance[a]

	U8	U10	U12
λ_u(cm)	8	10	12
$N_{M\alpha\xi}$	56	45	
$\Delta\lambda\lambda$(%)	1.8	2.2	2.6
$K_{n=1}$01500 Å)	7.9	7.1	6.4
$I_{n=1}$0.1% BW[b]	3.1×10^{15}	2.5×10^{15}	2.1×10^{15}
$I_{n=1}$(natural BW)	5.6×10^{16}	5.5×10^{16}	5.5×10^{15}

[a]E = 1.5 GeV, I (ring) = 400 mA.
[b]Photons/sec in central cone.

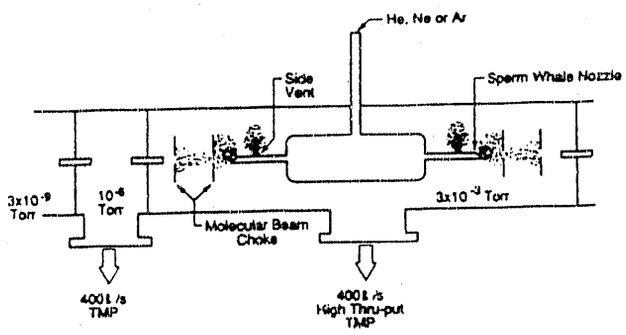

Fig. 1. Molecular beamless gas filter.

further enhanced by modified design tolerances for undulator magnets and use of non-grazing and near-normal incidence optics.

Toxic and corrosive chemicals. Two of the major concerns in storage ring synchrotron operation are the ring contamination masses of 40 amu or higher, which could destroy electron residence time, and the corrosion of expensive optics by chemicals used in end-station experiments. The gas filter described above will be used on-axis to the beamline and uses inert gases. When properly designed, it can be an effective means for isolating chemicals between the beamline optics and the end-stations. This effectiveness will be quantified when the filter is tested in a beamline setting in this coming year.

Beamline experimental stations for chemical dynamics research. A workshop was held in April 1990 to identify and provide preliminary design of end-stations for a UV undulator beamline. Six scientific working groups proposed at least nine different stations for studies ranging from crossed-molecular beam photofragmentation to cluster spectroscopy and dynamics to surface kinetics and dynamics. The groups also emphasized the need for developing high-speed detection and data acquisition to fully utilize modern synchrotrons.

Publications

Other Publications

"Combustion Dynamics Facility Scientific Program Summary," LBL PUB-5284 (1990).

"Combustion Dynamics Facility," April 1990 Workshop Working Group Reports, LBL-29800 (April 1990).

Earth Sciences Division

Advanced Instruments and Techniques for Mass Spectrometry Applications in the Geological Sciences

Principal Investigators: Donald J. DePaolo and Brian M. Smith

Funding: $204,100 (third year of funding)

Project Description

Efforts continued to determine technological improvements needed to enhance the applicability and utility of mass spectrometric techniques in the geologic sciences.

Accomplishments

A further stage of development was completed on the microsampling device, which is being used to obtain up to ~50 mm spatial resolution on solid materials for high precision isotopic characterization. The optics were improved by installation of a new mirror assembly, and the documentation segment was completed with the installation of a video cassette recorder on the video camera. The microsampling capability, in consort with the clean chemistry laboratory, provides "microprobe"-like capabilities for high precision isotopic analysis. This capability is not possible with *in situ* measurement techniques like SIMS. We will continue to advance this approach with design and construction of prototype automated chemical separation modules funded by the BES/Geosciences program.

A large effort was also devoted to completion of the instrumentation for stable isotope measurements. A vacuum line designed to convert oxygen from silicates into CO_2 using BrF_5 was designed and constructed. This system has high-throughput capability (24 sample reaction vessels) and a low-volume, low-blank design. It is a model system from the standpoint of operational efficiency and safety.

Enhancement of the stable isotope analysis capability was begun with purchase of an automated $CaCO_3$ reaction system and construction of a vacuum line for conversion of water oxygen to CO_2. These systems provide the capability for stable isotopic analysis of virtually any geological materials.

Areas of emphasis have developed over the three-year period toward hydrology (both high- and low-temperature fluid systems), climate change records in the recent geologic past, certain types of magmatic processes related to energy and waste management issues, crustal structure, and sedimentary basin evolution.

The approach used in research combines sensitive measurements of natural materials—at scales ranging from sub-millimeter intragrain effects to >100 km field scale effects—and mathematical models to build an understanding of geological processes. This is a compromise between purely theoretical approaches, which are problematic because of the complexity of geologic processes, and pure empiricism which, although it still pervades geology to a substantial degree, does not lead to predictive capabilities. Our particular contribution is to characterize natural materials with novel techniques (isotopic ratio measurements) that are sensitive indicators of both process and time scale.

Fault Assessment and Seismic Risk Estimating

Principal Investigator: Patrick L. Williams

Funding: $75,000

Project Description

This research program investigates the earthquake recurrence behavior of two segments of the Hayward fault. Studies under this project are designed to recover temporal evidence of past seismogenic movement of the Hayward fault.

The Hayward fault produced two large earthquakes in the 19th century and thus is a key focus of concern with respect to the imminence of future damaging earthquakes. No opportunity for direct measurement of the frequency of Hayward fault ruptures had been recovered prior to this study. Furthermore, the fault's slip rate and segmentation remain relatively poorly known. Inferences of the fault's recurrence behavior [Working Group, 1990] required assumptions to be made about segmentation, frictional properties, slip rate, and characteristic seismogenic displacement. Uncertain knowledge of these parameters argues that

any current estimates of recurrence behavior be regarded with caution. Research outlined here recovers direct geological measurements of past recurrence behavior. These measurements have great promise for critical testing of a number of assumptions made in current analyses of Hayward fault rupture hazard.

Accomplishments

Substantial evidence of the timing of Hayward fault slip over the past ~ 1,000 years in excavations at the "Tule Pond" in Fremont (Figure 1). While this record requires corroboration and development, it represents the only known data on the timing of the Hayward rupture prior to about AD 1800. At the Tule Pond site lacustrine and alluvial deposits record vertical separations consistent with the identification of this site as a fault-bounded depression (Figure 2).

During 1990 two trenches were excavated across the fault at the northern end of Tule Pond (Figure 2). These trenches revealed evidence for several Hayward fault ruptures. Figures 3 and 4 illustrate how the detailed layering of the Tule Pond deposits allows recovery of the timing of the southern Hayward fault's recent displacement.

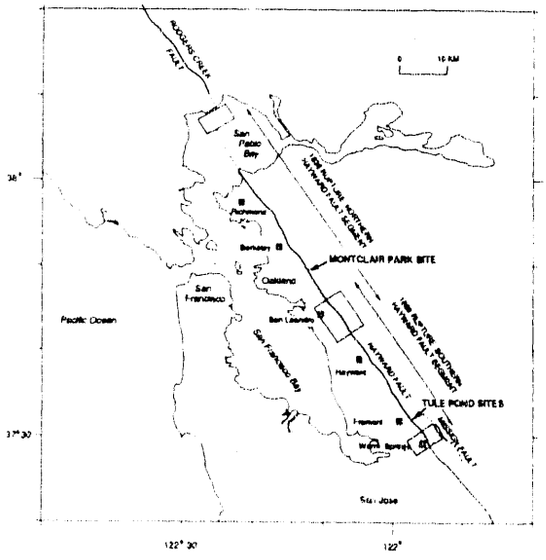

Fig. 1. Map of the Hayward fault showing segment boundaries (shaded) and position of Tule Pond and Montclair Park sites. Modified from Working Group [1990].

Recurrent motion of the Hayward fault is recorded by offset, tilt, and liquifaction of late Holocene pond and fluvial deposits. A minimum of four and up to seven episodes of major fault slippage during the past 1200 years are recorded at Tule Pond. Significant gaps were also identified in the sedimentary record, thus some late Holocene ruptures are almost certainly not recorded at this site. Two ruptures within the past ≤450 years (events R, U) are suggested by 19° and 8° tilts of successive, originally flat-lying pond strata that onlap a buried fault scarp. A maximum southern Hayward fault recurrence time of 320 years is inferred from the ≤450-year-age of the the package of successively tilted strata and subtraction of the 133-year age of historical rupture of the southern Hayward fault. Corroboration and development of these interpretations requires description of additional backhoe exposures and more precise radiocarbon analyses. The record so far recovered can also be improved by exposing the fault where it has a different relationship to a young cross-cutting channel. This channel is beneficial in that it records fault slip after circa 300 years BP, but detrimental in that it cuts away information on earlier displacement.

Additional trench exposures are needed to confirm several ruptures, and additional more precise radiocarbon analyses are required to improve the resolution of rupture ages. The evidence supports a 320-year maximum recurrence interval.

Publications

Journals and Proceedings

P.L. Williams, P. Holland, M. Wopat, F. Yeates, "Preliminary evidence of Hayward fault Paleoseismicity," *EOS Trans. AGU* 71, 1560 (1990).

Williams, P.L, "Evidence of Late Holocene Ruptures, Southern Hayward Fault, California,*GSA* ," *Abstracts with Programs*, Spring 1991 SSA/GSA-Cordilleran meeting.

Working Group

J.H. Dietrich, C. R. Allen, L.S. Cluff, C.A. Cornell, W.L. Ellsworth, L.R. Johnson, A.G. Lindh, S.P. Nishenko, C.H. Scholz, D.P. Schwartz, W. Thatcher, P.L. Williams, "Probabilities of Large Earthquakes in the San Francisco Bay Region, California," *USGS Circ. 1053*, 51pp. 1990.

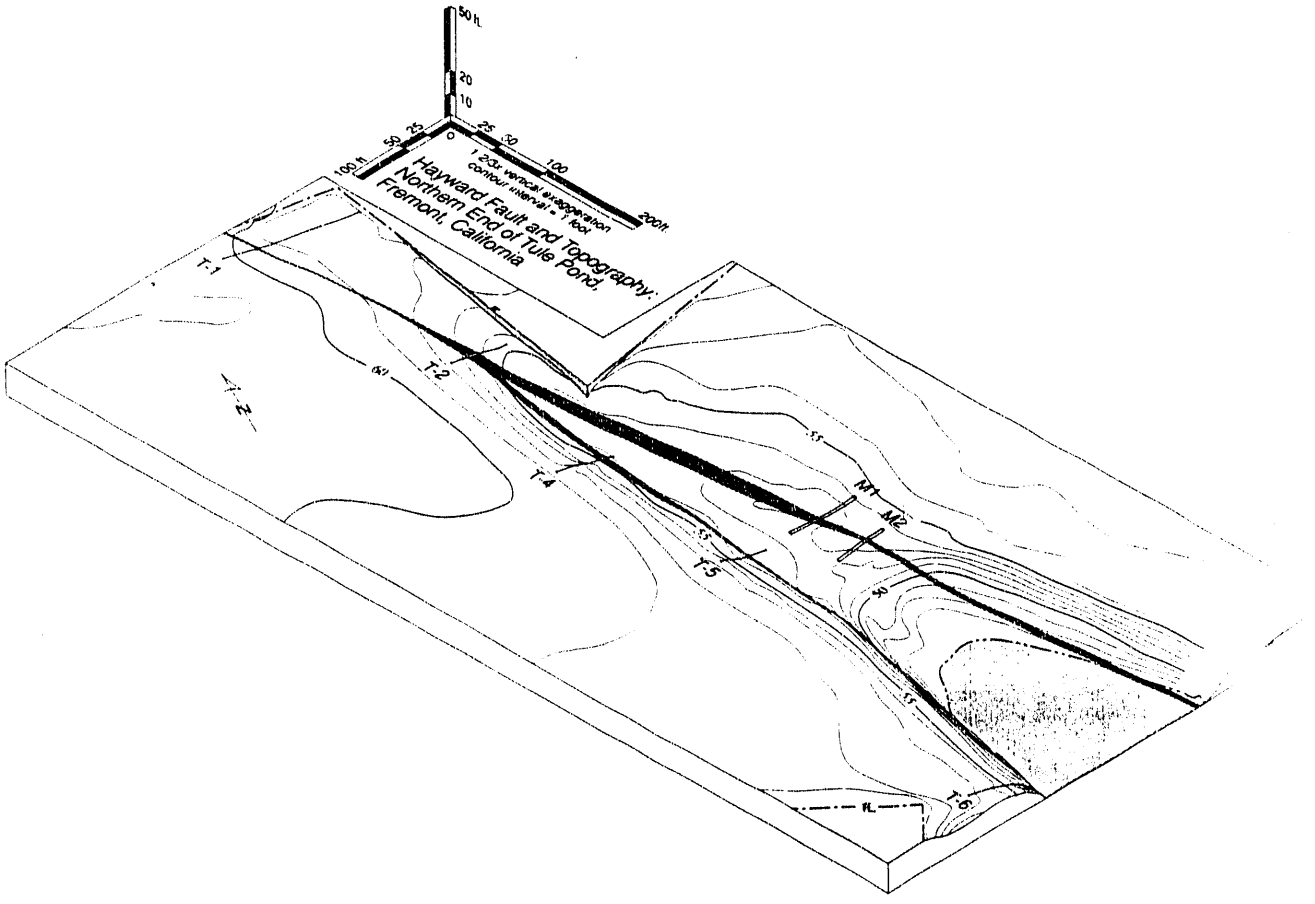

Fig. 2. Orthometric view map of Tule Pond. Map shows the topographic expression o the Tule Pond fault graben. The graben results from extension across a right double-bend of the west trace. Note the shallow swale intersecting the T..le Pond depression from the east near trench M1. This probably expresses an intersecting buried channel that flowed along the fault between trenches M1 and M2. Artificial fill subdues topographic expression of the graben north of the 47' contour.

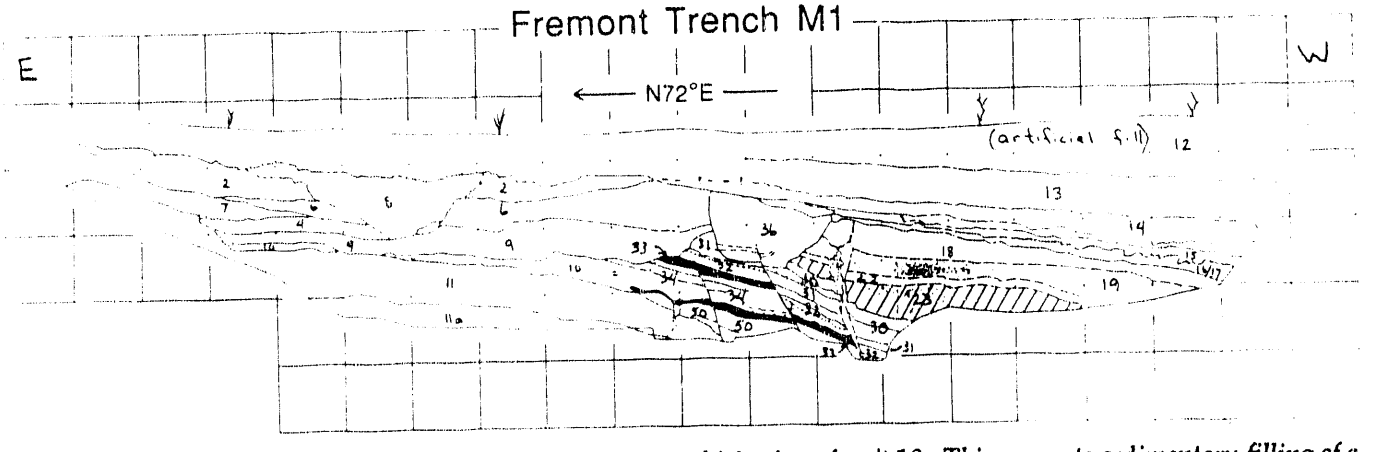

Fig. 3. Overview of Trench M1 sough wall. Note the eastward-thickening of unit 18. This suggests sedimentary-filling of a tectonic depression subsequent to deposition of unit 19. The westward-thickening of units 14 to 16/17 suggests later down-to-the-west tilt of the graben. The tabular geometry of unit 13 capping the unit 14-to-16/17 wedge suggests it was originally flat lying and was tilted in the latest (probably 1868) fault rupture. Units 8, 9, and 36 are cut-and-fill fluvial deposits. Shaded units were deposited prior to candidate fault ruptures F, 1-1'(?), O (2 events?), and R.

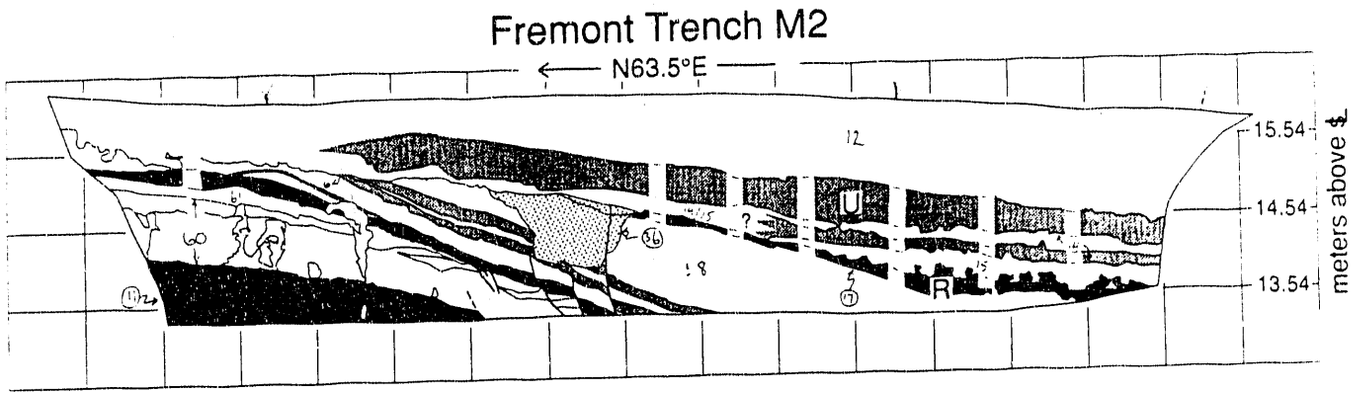

Fig. 4. Overview of Trench M2, south wall. Shaded layers are composed of slit to clay sized particles. The darker tones represent higher clay, and to a lesser extent, organic content. The light gray vertical features at the east end of the trench are liquifaction structures. The stippled feature near the middle of the trench is a channel-filling deposit. Event R is indicated by 19° westward dip of unit 17 and subsequent onlap of units 14 and 15. The 9° westward dip of units 13, 14 and 15 suggests the 19° dip of unit 17 was produced in two events. The tabular geometry of unit 13 indicates deposition on a flat-lying surface and tilt in the latest (probably 1868) fault rupture. Unit 13 contains historical artifacts.

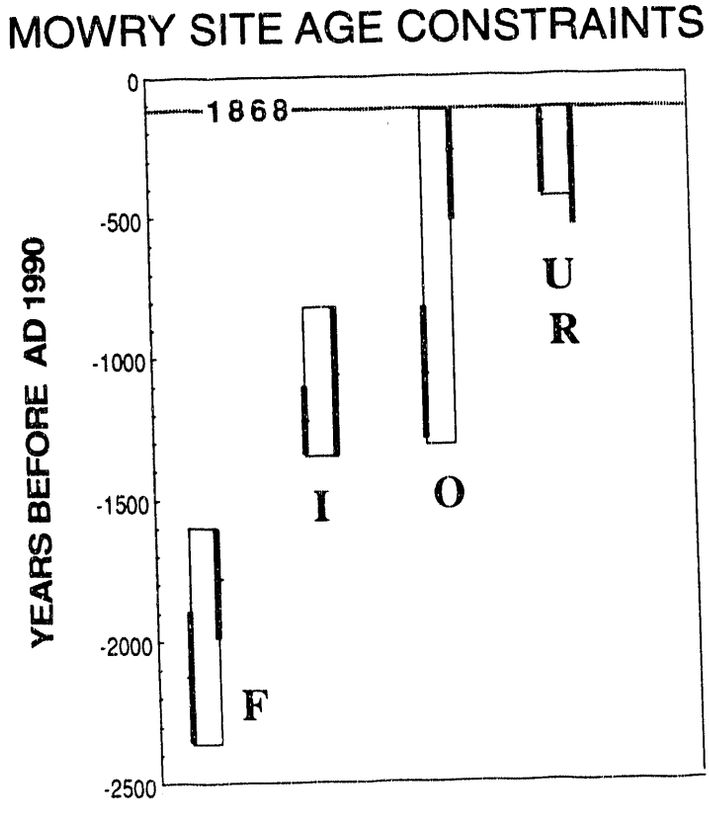

Fig. 5. Graph of bracketing ages of seismic evidence in Trenches M1 and M2. Bars indicate maximum (left) and minimum (right) bounding ages with their associated uncertainties (1 sigma, dendrocorrected).

Engineering Division

Search for Dark Matter with Silicon Detectors

Principal Investigator: Frederick S. Goulding

Funding: $60,300 (third year of funding)

Project Description

Work on a silicon detector system for direct detection of dark matter particles was completed. This work was done at the Oroville Low-Background Counting Facility.

Accomplishments

A detector system containing four silicon detectors with a total volume of 30 cm^3 (66 gm) of silicon was fabricated and installed in the Oroville Low-Background Counting Facility. This facility was designed and used for a number of years for detection of double-beta decay in the ^{76}Ge contained in an array of germanium detectors. It was used later for detection of dark matter particles by sensing the signals produced by impact of these particles with the germanium atoms in germanium detectors. Three advantages accrue from the use of silicon detectors in place of the germanium detectors in the shield:

1) Because the silicon atom is more than two times lighter than germanium, the impact of a dark matter particle will impact much more energy to a silicon atom.

2) A larger proportion of the energy of the recoiling atom is converted into ionization. Together with 1) this results in larger signals or, since noise sets the minimum signal detection threshold, improves the lower mass limit for detection of dark matter particles.

3) The lower leakage current of silicon detectors (as compared with germanium) results in lower noise thereby further reducing the mass threshold of dark matter particle detection.

The first four-detector silicon system was installed in FY1989 and the data-acquisition system and signal processing equipment was modified to accommodate the silicon system, and a six-month run was started. This run was completed in FY 1990, and the data was analyzed. The data set is shown in Fig. 1 together with fits to 4 GeV/c^2 and 10 GeV/c^2 dark matter particles. The same data are plotted in Fig. 2 converted into a cross section vs. dark matter particle mass plot with two assumptions regarding the rms velocity of the earth through a stationary sea of dark matter particles. On this same plot, the theoretical limits are shown for cosmions, weakly interacting massive particles that have been postulated to provide dark matter and to explain the deficit of ^8B neutrinos from the sun. The theoretical limits are determined from astrophysical constraints. This figure shows that cosmions are almost excluded by the observed results although a small region is not excluded if the lower velocity assumption applies.

The existence of this small region of uncertainty led to removal of the silicon detector system and its rework to lower the noise threshold. As seen in Fig. 1, the earlier results show a noise threshold just above 1.1 keV. In order to lower this threshold, the system was equipped with smaller area and lower capacitance detectors. Laboratory tests indicate that a threshold of 0.9 keV has been achieved. The new four-detector system as been installed in the Oroville shield and counting has started. It is anticipated that a six-month counting period will again be used.

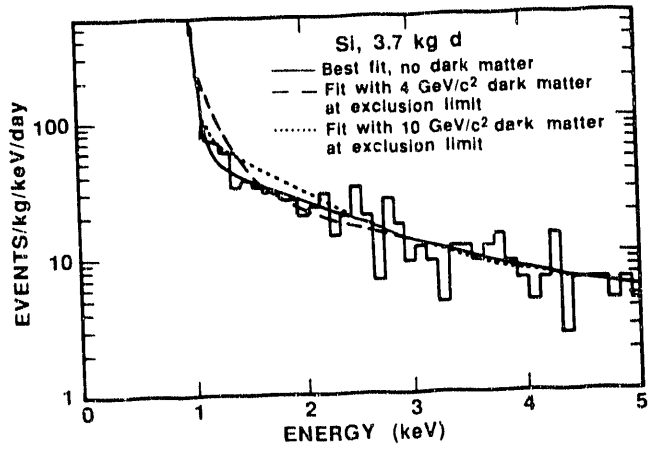

Fig. 1. Low-energy region of the ionization detected in a Si counter for 3.7 kg days of data. Figs are shown with no dark matter and with addition of signals due to masses of 4 or 10 GeV/c^2 with cross sections on the exclusion contour of Fig. 2.

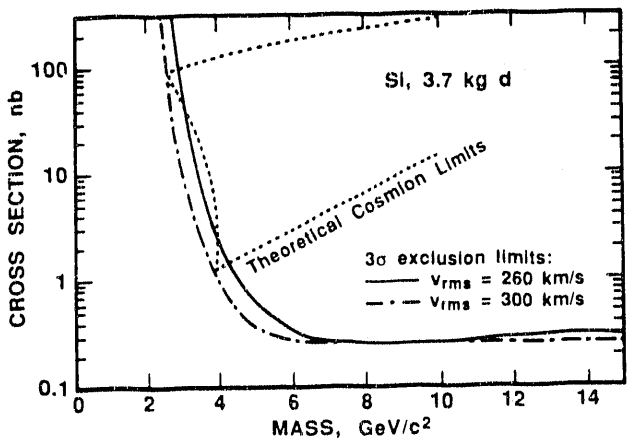

Fig. 2. Exclusion plots for two values of the velocity of dark-matter particles as functions of their mass and elastic cross section on Si. Coherently scattering cosmions are expected to lie within the dashed lines, if they are to solve the solar-neutrino problem.

Publications

Journals and Proceedings

D.O. Caldwell et al. "Searching for the Cosmion by Scattering in Silicon Detectors," *Phys. Rev. Lett.* 65, 11, 1205 (1990).

G. Gerbier et al., "Measurement of the Ionization of Slow Silicon Nuclei in Silicon," *Phys. Rev. D* 42, 9, 211 (1990).

Information and Computing Sciences Division

Distributed Scientific Data Management in a Heterogeneous Environment

Principal Investigators: Dennis Hall and William Greiman

Funding: $150,800 (second year of funding)

Project Description

The goal of this project was to establish LBL as a participant in a proposed new National Initiative in High Performance Computing. This required demonstrating that the proposed programmatic approach was a practical way to establish collaborations among government, universities, and industry for the development and marketing of commercial software products vital to both scientific research and to the success of the High Performance Computing Initiative.

Accomplishments

Initial industrial collaboration efforts focused on the FindIt system that served as a proving ground for the distributed data-management facilities developed under ERF funding in FY 1989. The FindIt software was developed to monitor detector equipment and identify malfunctioning components in real time. The system was designed to be quite general, and is capable of being applied to a wide variety of problems in industrial process control as well as scientific data acquisition. Copyrights to the software packages were requested from the Department of Energy. Presentations were then given at a series of meetings of the East Bay Emerging Technologies Advisory Board. Although a great deal of interest was expressed, an industrial partnership was not forged based on the FindIt software. It was recognized that a successful partnership would require a technology that could be transferred to industry with minimal consultation.

The distributed data-management tools were generalized and have been used for magnet field measurement systems. The power of the approach was demonstrated by the ability of the software to access and control different magnet measurement data-acquisition systems. The success of these applications resulted in an invitation to submit a Field Task Proposal to the Department of Energy's High Performance Computing and Communications program starting in FY 1993.

Publications

Presentations and Seminars

W. Greiman, D. Hall, and C. Day, "Experience Using a Software Bus to Build Reusable Scientific Software," Computing in High Energy Physics, Santa Fe, New Mexico, April 1990.

D. Olson, W. Greiman, D. Hall, D. Balaban, C. Day, "Experience Using an Automated Fault Location System with a Time-of-Flight Wall Detector Array," Computing in High Energy Physics, Santa Fe, New Mexico, April 1990.

Materials Sciences Division

Noise in High-T_c Superconductors

Principal Investigator: John Clarke

Funding: $46,400

Purpose

The purpose of this project is to study the dynamics of flux vortices in high-transition temperature (T_c) superconductors through measurements of the low-frequency magnetic noise generated by this motion. The project has two goals: an understanding of the fundamental physics, and the reduction of noise in practical devices.

The flux noise is measured in flux transformers fabricated from $YBa_2Cu_3O_{7-x}$ (YBCO) films in the configuration shown in Fig. 1. The flux transformer, which consists of a single-turn pickup loop coupled to a ten-turn spiral input coil, is mounted roughly 100 μm away from a Nb-based dc Superconducting Quantum Interference Device (SQUID) maintained at 4.2 K. The temperature of the flux transformer can be raised to above T_c. The application of a small magnetic field to the pickup loop induces a supercurrent I in the transformer, enabling one to measure the noise induced in the SQUID as a function of this current.

Accomplishments

Figure 2(a) shows the spectral density of the flux noise $S_\Phi(f)$ measured by the SQUID for I = 0 and I = 2 mA. The 2 mA current reduces the noise power by an order of magnitude; when the current is removed, the noise is restored to its original value. The spectral density of the noise varies as 1/f below about 100 Hz, but flattens at higher frequencies. However, when the I = 2 mA spectrum is subtracted from the I = 0 spectrum, the noise scales as 1/f over the entire frequency range [Fig. 2(b)]. The reduction in noise is independent of the direction of the current and varies with temperature, as illustrated in Fig. 3.

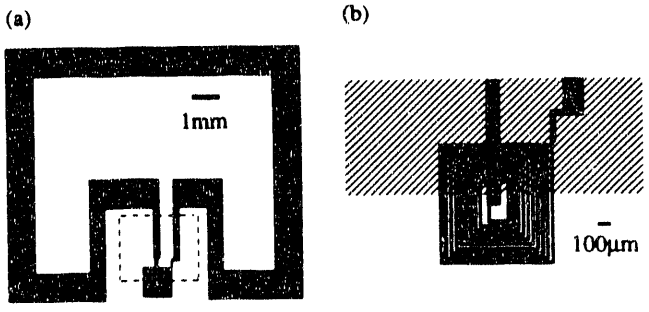

Fig. 1. YBCO flux transformer. (a) Pickup loop formed by wide lines, input coil centered on bottom edge, insulating $SrTiO_3$ layer indicated by dashed box. (b) Enlargement of input coil: $SrTiO_3$ is shaded region, crossunder is vertical strip connected to center of coil.

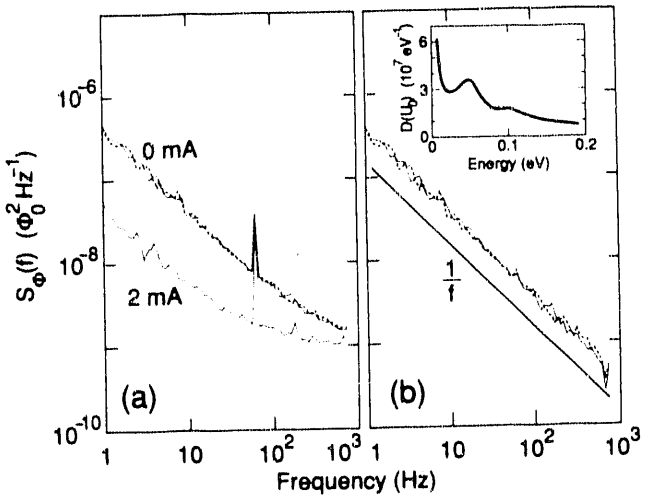

Fig. 2. (a) Noise power vs. frequency with transformer at 39.2 K. Light curve: initial spectrum (I = 0); heavy curve: application of I = 2 mA; dashed curve: subsequent return to I = 0. (b) Spectra for I = 0; line indicates 1/f scaling. Inset: distribution of activation energies.

The current-induced reduction can be explained by our model for 1/f noise, which postulates an ensemble of thermally activated bistable switching processes such as the one shown in Fig. 4. In the absence of a current, a given flux vortex hops between sites 1 and 2 [Fig. 4(a)], that is, between the two symmetric wells shown in Fig. 4(b). When a current is applied, however, there is a Lorentz force on the vortex in a direction perpendicular to the current, causing the two wells to shift as illustrated in Fig. 4(c). Thus, the lifetime of the vortex in state 1 is decreased while that in state 2 is increased; however, the net hopping rate is reduced, thereby lowering the observed noise.

A detailed model for the process has been developed, and gives rise to the solid lines shown in Fig. 3. The model, which requires only a single fitting parameter, namely the vortex hopping length l(T), fits the data remarkably well. From the results of the theory, one can deduce the following results: over the tempera-

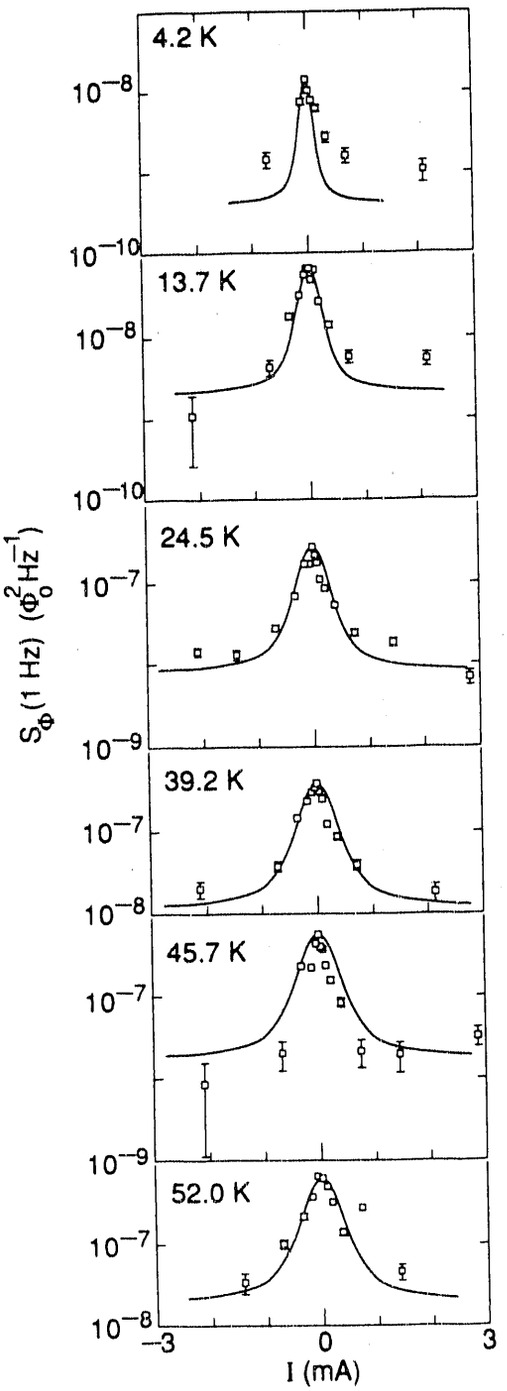

Fig. 3. Noise power S_Φ (1 Hz) vs. current in transformer for six temperatures. Points are experimental data, curves are theoretical predictions.

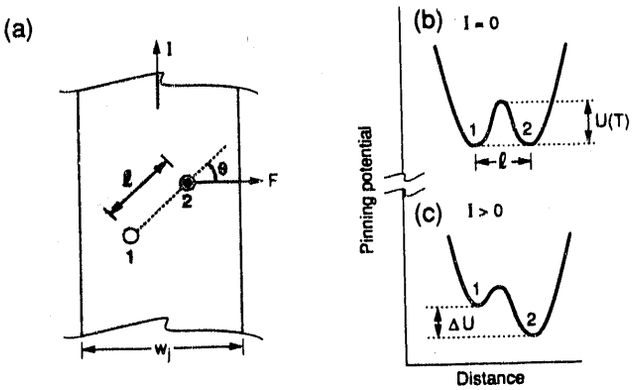

Fig. 4. (a) Schematic of single hopping process in line of width w_j. Current I exerts force F on vortex which hops distance ℓ between pinning sites 1 and 2 at angle θ with F. Scale of ℓ exaggerated. (b) Schematic pinning potential for I = 0. (c) Potential for I > 0.

ture range from 4.2 K to 60 K, the characteristic pinning energy varies from 8.5 meV to 190 meV, while the hopping length varies from 15 to 70 nm. The number density of vortices is about 0.02 μm^{-2} for a film cooled in zero field, corresponding to an *effective* cooling field of about 40 μT. These are the first experiments to produce direct measurements of the hopping length and zero-field vortex density, and provide a graphic demonstration of the validity of the thermally activated flux hopping model.

These results have important practical implications. It is now clear that, to achieve a minimum in the low frequency noise, high-T_c devices such as a flux transformer should be operated with a persistent supercurrent. Thus, one can envisage a magnetometer with a "noise reduction scheme" that consists of the application of a static magnetic field. As an example, in the system described above, the rms flux noise at 10 Hz in a transformer at 52 K was reduced to 10^{-13} tesla $Hz^{-1/2}$. This value is low enough for one to contemplate magnetocardiology using a hybrid system consisting of a low-T_c SQUID coupled to a high-T_c flux transformer that can be brought very close to the subject.

The low magnetic field noise demonstrated in this project played a significant role in obtaining a grant of $373,000 from the California Competitive Technology Program. In turn, this grant will greatly expedite the transfer of the LBL high-T_c SQUID technology to Conductus, Inc.

High Energy Photoelectron Spectroscopy

Principal Investigator: Charles S. Fadley

Funding: $14,500

Project Description

High energy photoelectron spectroscopy is being used in several ways to characterize the surfaces of both semiconductors and metals. In particular, the angular distributions of the photoelectrons emitted can be used to derive several useful types of structural information, including the locations of bond directions and low-index directions, as well as more subtle details such as the positions of adsorbed atoms and the degree of interlayer relaxation involved in the development and assessment of photoelectron holography, in which the observed intensities are inverted via Fourier transform methods to yield approximate direct images of the atomic structure near a surface. Photoelectron spectroscopy is being combined with scanning tunneling microscopy, another powerful probe of surface structures that is complementary to it.

Accomplishments

Fourier transform software was used to carry out a number of calculations to assess the accuracy of photoelectron holography, as well as to explore better methods of data analysis. This has been applied to several systems, including the Si(111) surface, silver adsorbed on the Si(111) surface, the Ge(111) surface, sulfur adsorbed on the Ni(001) surface, and small models of microclusters of only 2–5 atoms. The work on microclusters has resulted in the development of a new method for analyzing such data that appears to dramatically improve the quality of the atomic images.

The work on Si and Ge shows promise for determining near-neighbor atomic positions, with both experimental and theoretical results yielding similar atomic images and thus good agreement. The work on sulfur on Ni also shows good structural accuracy, provided that our method for analyzing the data is followed.

Role of Oxygen in High-Temperature Superconductors

Principal Investigator: Donald E. Morris

Funding: $134,300

Project Description

The purpose of this research is to advance the technology of high-temperature superconductors. Objectives are to determine the oxygen pressure/composition phase diagrams in the Y-Ba-Cu-O system, including the effects of La and Fe substitution. Observation of possible enhanced solubility of the substituents in high oxygen pressure, and/or stabilization of the 123 structure at higher levels of substitution is to be investigated.

The approach planned for this research is to utilize our experience with, and apparatus for, high-oxygen pressure synthesis of the high-temperature superconductors. Novel materials will be synthesized, both to determine the phase diagrams in these systems, and to perform physical and chemical characterization of the resulting compounds to clarify the nature of the superconductivity. For example, during our earlier work on nonisovalent substitution of Ca in place of Y in the Y-Ba-Cu-O system, we observed (1) enhancements of T_c (transition temperature), (2) enhanced solubility of dopant with oxygen pressure, (3) stabilization of 123 in preference to 124, and (4) conversion of orthorhombic 123 to tetragonal 123.

Accomplishments

It was determined that lanthanum substitution in the Y-Ba-Cu-O system at elevated $P(O_2)$ (oxygen pressure) results in superconducting compositions which throw interesting light on the effects of nonisovalent substitution. (The La^{3+} ion primarily occupies the site of the Ba^{2+} ion.) Like Ca substitution, La substitution also shifts the phase formation boundary between 123, 247, and 124 phases to higher $P(O_2)$, and stabilizes a tetragonal 123 structure at moderately elevated $P(O_2)$. However, in contrast with Ca substitution, T_c de-

creases continuously and rapidly with increasing La content. The tetragonal 123 structure formed at higher La contents is not superconducting at all, down to 5 K. This is only partly explained by the expected decrease of the hole concentration.

To extend the work on Ca and La substitution, the effects of Fe were investigated. Ca and La are known to enter primarily at the Y and Ba sites, respectively. Iron, on the other hand, occupies the Cu sites. Single-phase iron-substituted 124 ($YBa_2Cu_{4-x}Fe_xO_y$) has been obtained in the range of $0 < x < 0.05$ at oxygen pressures of 200 bar and 100 bar. Greater Fe substitution at elevated $P(O_2)$ destabilized the 124 and 247 phases in favor of a tetragonal 123 phase (FeT-123). The solubility of Fe in FeT-123 phase increases with oxygen pressure. The lattice parameters do not change significantly with Fe content and $P(O_2)$. The formal average copper valency (FACV) of single phase FeT-123 samples is high (e.g., 2.58 for x=0.65). The reduction of T_c caused by Fe substitution is about 6° K over the range $0 < x < 0.2$, for samples prepared at 200 bar oxygen pressure and cooled slowly under pressure.

Based on this work, it appears that under fairly general conditions, phase formation boundaries shift and the 123 structure is stabilized by chemical substitutions. Three very different types of substitutions, namely, Ca at Y sites, La at Ba sites, and Fe at Cu sites, give similar effects. Incorporation of Ca, La, or Fe in the 247 structure is accompanied by a phase change to the tetragonal 123 structure with elimination of the 247 phase, while the 124 phase accepts substitution only to a very limited extent before a 123 phase appears (10% for Ca, 5% for La, 1% for Fe). In all three cases, elevated oxygen pressure extends the 123 region. Furthermore, in all three cases the 123 in the extended region remains tetragonal upon cooling. As far as changes in T_c are concerned, the effect of Fe substitution is markedly different from that of Ca, which enhances the T_c of 124 and leaves the T_c of 123 unchanged. Both Fe and La have drastic and deleterious effects on T_c, even when the formal average copper valency is maintained at or above 2.2.

A new study of the phase diagram of the undoped Y-Ba-Cu-O system was undertaken to clarify its nature at high oxygen pressure. At 980 C and 200 bar oxygen pressure, highly oxidized phases are stabilized, compared with the atmospheric pressure (1 bar) diagram: BaO_2 instead of BaO, and $YBa_2Cu_4O_8$ instead of $YBa_2Cu_3O_{7-x}$. Two new phases have been observed: $YBa_5Cu_2O_{10-x'}$ which has a tetragonal unit cell with a = 5.88 and c = 8.04 angstroms, and $YBa_2Cu_2O_{26-x'}$ which appears to be isomorphous with the superconductor $La_{1.6}Sr_{0.4}CaCu_2O_6$. Both of these new compounds have a high-formal average copper valency and are therefore good candidates for high-temperature superconductivity.

The high-oxygen pressure synthesis techniques, so successful for Y-124, were applied to the analogous Er and Dy compounds $ErBa_2Cu_4O_8$ and $DyBa_2Cu_4O_8$. The specimens were analyzed for two- and three-dimensional magnetic ordering by neutron scattering. The magnetic properties of oxide superconductors are of interest because the Cu magnetism may be related in a fundamental way to the pairing mechanism in these materials, and also because it is of interest to examine the interaction between rare-earth magnetism and the superconducting order parameter, which should be coupled via the electromagnetic interaction. For the Er system a simple three-dimensional (3-D) antiferromagnetic structure is observed, in which the magnetic unit cell is twice the chemical unit cell along the a axis, with a Neel temperature $T_N = 0.49$ K. In the vicinity of the Neel temperature, however, scattering characteristic of 2-D behavior is observed. 2-D behavior is also observed in the Dy material near its Neel temperature of 0.9 K. However, the scattering in the Dy system does not cross over to the expected 3-D Bragg peaks at low temperatures. Instead, the 2-D line shape persists to the lowest temperatures measured. We explain this result as originating from a geometric cancellation of interactions between c-axis layers for the specific Dy a-b spin configuration, which together with the weak intrinsic c-axis interaction renders the net interaction along the c-axis much smaller than all other known "2-D magnets." We anticipate that a similar cancellation of interactions is likely to occur in other $RBa_2Cu_4O_8$ (R = rare earth element) systems.

Excite and Probe Studies of High-T_c Superconductors in the TH_z Regime

Principal Investigator: Joseph W. Orenstein

Funding: $45,400

Project Description

This is an experimental program to study elementary excitations in high-T_c superconductors at low temperature. These experiments apply excite and probe techniques developed in semiconductor physics to superconductors. Ultrashort laser pulse methods are being used to inject quasiparticles and to probe their electrodynamic response. The injection of quasipar-

ticles will be accomplished either with optical pulses whose photon energy is comparable to the superconducting gap, 2Δ, or with electrical pulses whose peak voltage exceeds Δ/e. The electrodynamic response of these quasiparticles in the THz frequency range is measured using short electric pulse techniques pioneered by Auston. These measurements test for a breakdown in the Fermi-liquid description of the Cu-O based metals, a central issue in the theory of high-T_c superconductivity.

Accomplishments

Design of terahertz spectroscopy facility. The goal of the project is to develop the capability for measuring the electromagnetic properties of materials in the terahertz region of the spectrum. This requires the development of four basic subsystems: 1) ultra-short pulse laser; 2) terahertz spectrometer; 3) superconducting magnet cryostat; and 4) data acquisition system. In this initial phase of the project, key design decisions were made in each of these areas.

Two separate short-pulse laser systems are to be constructed. The first system to be built will be a colliding-pulse mode-locked (CPM) dye laser. Once it is operating, we will build a second mode-locked laser based on Ti:Al_2O_3 as a gain medium. The Ti:Al_2O_3 laser has the potential for greater stability and higher power, both of which will be advantageous for our application.

Each of these lasers requires a high power argon-ion laser as an excitation source. The dye-laser will be pumped with a Coherent I-90 laser on loan from AT&T Bell Labs. It has arrived in Berkeley, where it has been set up and tested. The laser now generates 4.5 watts (all lines) in the TEM mode, which should be adequate to pump the CPM dye-laser. Another argon laser is required for the Ti:Al_2O_3- based laser.

The measurements planned require that materials under test be maintained at temperatures as low as 0.3 K and in magnetic fields up to approximately 9 T. In addition, optical access to the samples is required along two perpendicular axes. These requirements are not met by standard commercial cryostat systems. We are working on a design which will be cost effective in addition to meeting the specifications.

Work has begun on the design of antenna and receivers for the terahertz spectrometer. The key component of these devices are lithographically patterned metal layers deposited on silicon-on-sapphire wafers. At present we have prepared designs for the antenna and receiver lithography masks, and for the supports for the antenna and receiver. We have begun a collaboration with Prof. Paul Richards and his group, who have considerable experience in the design and fabrication of similar antenna structures for submillimeter wave astronomy.

Unprocessed data will emerge from the spectrometer in the form of a voltage vs. delay between the generating and gating pulses. To be useful, these waveforms must be co-added to increase signal-to-noise ratio, Fourier transformed, and stored for plotting and analysis. Efforts have begun to implement the software required for signal averaging, data analysis and computer control of the experiment. We have also completed an analysis of all of the factors influencing the signal-to-noise ratio. From our analysis we have concluded that rapid scanning of the delay is the optimal procedure for minimizing the $1/f$ noise due to laser amplitude fluctuations. We have designed our data-acquisition system to accommodate rapid scan operation.

Antenna-Coupled High T_c Bolometer

Principal Investigator: Paul L. Richards

Funding: $54,000

Project Description

The discovery of high T_c superconductivity offers the possibility of constructing sensitive transition edge bolometers for use as detectors of far infrared and millimeter waves. These detectors are intended to bridge the gap between liquid helium-cooled bolometers and room temperature detectors such as the Golay cell, the pyroelectric detector, and the bismuth microbolometer. Recent estimates indicate that high T_c bolometric detectors can potentially be two orders of magnitude more sensitive than any competing direct detector at or above liquid-nitrogen temperatures for infrared wavelengths longer than 20 μm.

Accomplishments

We have fabricated and measured the performance of antenna-coupled microbolometers based on the resistive transition of a high T_c superconducting film for use as detectors of far-infrared and millimeter waves. A planar lithographed antenna (log-periodic or log-spiral) is used to couple the radiation to a thin YBCO film with dimensions ($\approx 6 \times 13$ μm^2) that are much smaller than the wavelength to be measured. This film acts both as the resistor to thermalize the RF currents and as a transition edge thermometer to

measure the resulting temperature rise. Because of its small size, both the thermal conductance from the film into the bulk of the substrate and the heat capacity of the thermally active region are small. Consequently, the microbolometer has low noise, fast response, and a high voltage responsivity. We have measured a phonon limited electrical NEP of 4.5×10^{-12} $WHz^{-1/2}$ at a 10 kHz modulation frequency and a responsivity of 478 V/W at a bias of 550 μA. Measurements of the optical efficiency are in progress.

The quasi-optical coupling scheme that is able to couple long infrared wavelengths into the much smaller thermally active area of the microbolometer is shown in Fig. 5. The experimentally measured noise equivalent power (NEP) of the microbolometer shown in Fig. 6 is very close to the theoretical calculation based on the properties and dimensions of the materials involved. The NEP reaches the fundamental limit set by thermal fluctuations (phonon noise limited NEP).

In the course of this work, the concept for a low T_c version of this detector was originated, which has very useful properties. The active area of the low T_c microbolometer is thermally decoupled both by its small size and by the thermal resistance of the boundaries with the substrate and the antenna terminals. Design calculations based on a 2×2 μm square film of a superconductor with $T_c \approx 0.1$ K give an NEP $\approx 10^{-18}$ $WHz^{-1/2}$, time constant $\approx 10^{-6}$ s and responsivities up to $\approx 10^9$ V/W. These specifications meet the requirements for NASA's Space Infrared Telescope

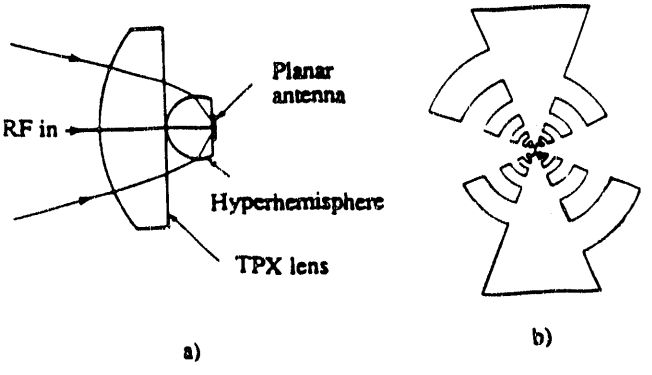

Fig. 5. Quasi-optical coupling scheme. a) Cross section. The substrate is mounted on the flat side of a hyperhemispherical sapphire lens (D=0.5″). A TPX lens (f/1.16) is used to further narrow the beam. b) Planar log-periodic antenna. This self-complementary structure gives a frequency-independent real antenna impedance and very broadband response. In addition, it has a nearly Gaussian beam pattern.

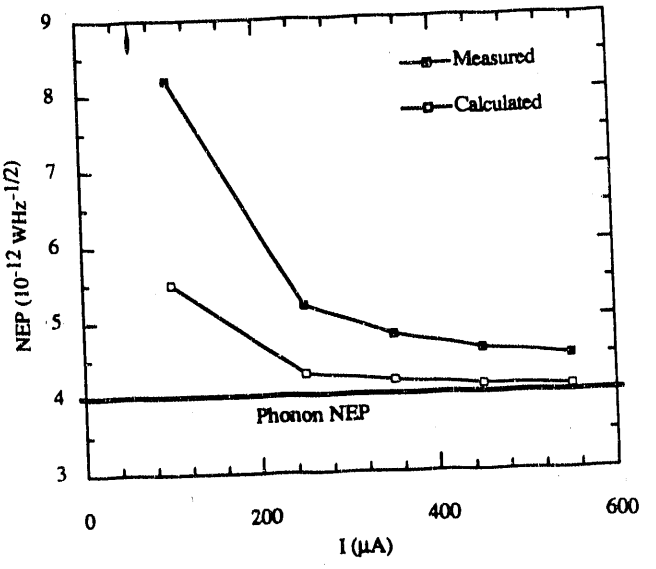

Fig. 6. Frequency-dependence of the electrical NEP measured at a bias of 100 μA and at the optimum operating temperature. The solid line is the calculated NEP in the absence of 1/f noise.

Facility and Sub-Millimeter Moderate Mission. Useful applications also exist at ^{3}He and ^{4}He temperatures. The calculated NEP scales as $T^{5/2}$.

This project was carried out in collaboration with staff members at Conductus, Inc., of Sunnyvale, CA, who produced the epitaxial c-axis YBCO films on YSZ substrates that were used to make the bolometers.

Raman Studies of Materials and High Temperature Systems

Principal Investigator: Gerd M. Rosenblatt

Funding: $252,800

Project Description

The purpose of this project is to investigate the effect of changes in molecular or crystalline structure on the properties of materials, interfaces, and high temperature systems, utilizing Raman spectroscopy and related optical techniques. Particular emphasis is placed on understanding changes in vibrational Raman spectra produced by changes in processing, defects and inhomogeneities, crystalline character, strain, and temperature.

The project utilizes a unique high-sensitivity Raman instrument that makes use of the two-dimensional detection capability of an imaging photomultiplier to obtain up to a thousand spatially-resolved Raman spectra simultaneously. Combined with real-time computer data analysis and sample movement, these spectra provide the data needed to profile or map chemical, physical, or mechanical properties at or near the surfaces of materials, with unprecedented speed.

Accomplishments

Carbon fibers. Carbon fibers are widely used as a structural material in composites because of their high tensile strength-to-weight ratio (up to ten times that of steel). The first-order Raman spectrum of single crystal graphite (e.g., highly ordered pyrolytic graphite or HOPG) consists of a single peak (G-band). In disordered graphites, such as commercial carbon fibers, a second peak (D-band) appears at lower frequency. The relative intensities of the D- and G-bands are related to the average microcrystallite size.

During the Raman characterization of single carbon fibers, the fine fiber is heated by the laser in the probed area. Because the frequencies of both the G- and D-bands are temperature dependent, changes in the Raman spectrum occur. At sufficiently high laser powers, permanent changes in the physical structure of the fibers are produced. In this work, changes in the Raman spectra of carbon fibers resulting from different processing conditions are separated from changes caused by laser heating.

The Raman spectra of individual 8 μm diameter PAN-derived carbon fibers that had been annealed at five temperatures from 1700 C to 2800 C were measured over a broad range of incident laser power. In all the fibers, the frequencies of the G- and D-bands shift to lower frequency with increasing laser power, and at powers above 30 mW the linewidths and the relatives intensities change irreversibly. The irreversible changes extend several hundred μm away from the 2 μm spot illuminated by the laser.

To quantify the degree of laser heating, the temperature dependence of the frequency of the Raman G-band in pure bulk HOPG was measured. Using the HOPG data, the fiber experiments show that a laser power of 30 mW heats an 8 μm fiber to 330°C and that the irreversible changes above 330°C are produced by erosion of the fiber. Even a laser power as low as 10 mW causes a temperature increase of ~100° and a significant shift in the position of the Raman G-band in a 2800°C annealed fiber. To study the fiber heating in more detail, a Raman imaging experiment was carried out in which a 0.1 mm spot on a fiber was heated by a focused laser beam while the fiber was illuminated for Raman characterization along a 1.6 mm length by a low power probe beam. The spatially resolved Raman shifts measured in this experiment, when combined with the HOPG frequency-temperature calibration, yield the *in-situ* temperature profile of the laser heated fiber, as shown in Fig. 7.

The observations show that reproducible room-temperature characterization of the bonding and microstructure in fine carbon fibers by Raman spectroscopy must be carried out at very low incident laser power and/or by extrapolating measurements back to zero laser power. Upon doing this for these PAN-derived fibers, the G-band frequency and the D-band relative intensity both decrease with increasing heat treatment temperature, indicating that the microcrystallite size is larger in the fibers annealed at higher temperature. In addition, the results indicate that the D-band relative intensity may be larger in the interior of the fiber than in the surface layer.

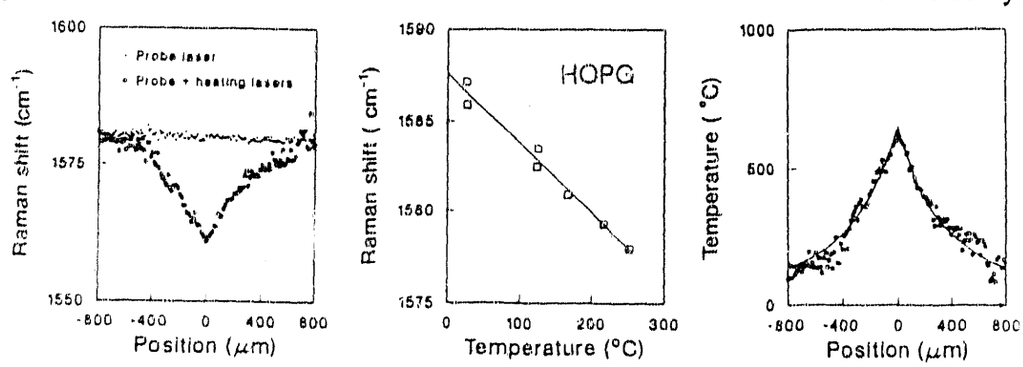

Fig. 7. Spatially resolved Raman spectroscopy showing laser heating of a single carbon fiber. Left graph: the frequency of the Raman G-band as a function of vertical position along the fiber; the upper trace is for the low-power probe laser beam only and the lower trace results from addition of a second focused laser beam. Middle graph: the dependence of the Raman band of bulk graphite upon temperature. Right graph: the in-situ temperature profile of the fiber determined from the first two graphs. The solid line is a fit to a simple heat transfer model.

Amorphous "hard carbon" films. Amorphous carbon films are used as protective coatings on hard disks in the computer industry. The wear of such films critically affects the lifetime and reliability of the manufactured disks. The G- and D- Raman bands in amorphous carbon films are very broad and change in their relative intensity and in their central band frequency with film structure and morphology. These changes in the Raman spectrum are related to the mechanical and optical properties of the films. The effects of short range order, bonding, and internal stress on the shape of the Raman bands are not well understood.

In collaborative work with Seagate Magnetics, features in the Raman spectra of amorphous carbon films have been correlated with the rates of specific types of wear. Changes in the G-band position correlate with the rate of tribochemical wear and changes in the relative intensities of the G- and D- band correlate with the rate of abrasive wear. The results are consistent with a structural model of amorphous carbon films in which ~20 Å trigonally bonded, graphitic domains are cross-linked by a few tetrahedral (diamond-like) bonds. This work led to the funding of a DOE Industry-Laboratory Exchange research program with Seagate Magnetics in FY 1991.

Diamond films. Chemically synthesized diamond films are a new field of interest in industry, both in the US and in Japan and Europe. Diamond films possess the attractive properties of natural diamonds such as hardness and high thermal conductivity. Potential applications include heat sinks, x-ray optics, tool coatings, abrasives, and high-band gap semiconductors. Raman spectroscopy uniquely and unambiguously verifies the presence of diamond. The focus of this work is to gain information concerning residual stress and defect density from the frequency and shape of the diamond Raman line and then to relate this to the electronic and mechanical properties of the film.

To obtain insight into the nature of diamond films, the frequency and lineshape of the diamond Raman line were measured and examined in detail for a series of microwave-plasma-assisted CVD films grown on Si. The Raman lines in the films appear at higher frequency than that of natural diamond and the observed lines are symmetric but broader than for natural diamond. In addition, spatially resolved Raman spectra show that the line frequencies and linewidths are correlated: film regions with the highest vibrational frequencies have the largest linewidths (Fig. 8). The data include 500 data points from different positions on a single film and single point measurements on eight films grown under different conditions. The primary contribution to the frequency shift

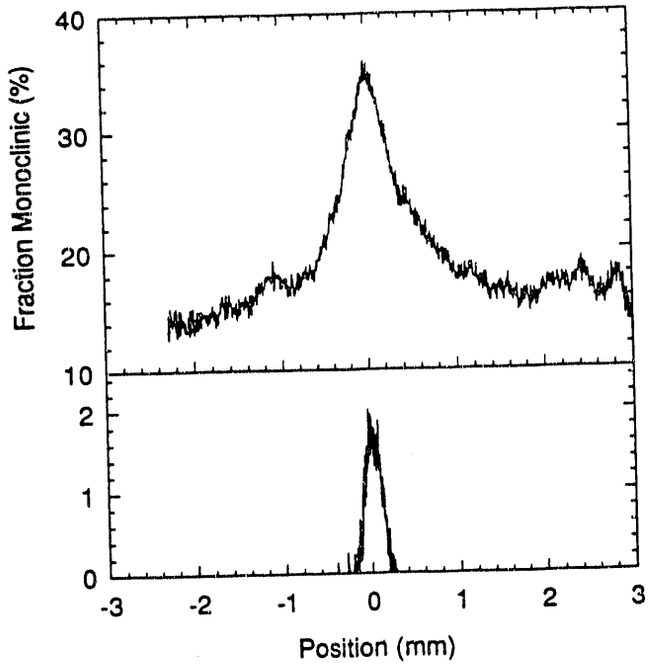

Fig. 8. Profiles across crack-induced transformation zones in microengineered zirconias obtained from imaging Raman spectroscopy. The upper graph shows MgO-stabilized zirconia with 22% maximum transformation and a zone width of 1 mm; the lower graph shows CeO_2-stabilized zirconia with 2% maximum transformation and a zone width of 200 μm.

appears to be compressive stress although the several mechanisms for the frequency shift and the correlation of the linewidth with frequency that were evaluated, including phonon confinement, residual stress, and defect scattering. The correlation between Raman line frequency and width suggests that the degree of compressive stress may be associated with the density of microcrystalline defects in the films.

Phase stabilized zirconia ceramics. In a continuing collaboration with R.O. Ritchie and R. Dauskardt of LBL's Center for Advanced Materials, spatially resolved Raman spectroscopy is being used for the quantitative measurement of phase-transformed zones in phase stabilized zirconias (PSZs). Fracture of these materials induces a martensitic transformation from the tetragonal to the monoclinic phase in the vicinity of a propagating crack. The degree of toughening is related to the spatial extent and the amount of transformation of the transformed zone. Spatially resolved Raman spectroscopy has revealed zone sizes ranging from 230 to 1500 μm and amounts of transformations ranging from 0.2% to 20%. The sensitivity of the technique is shown by the first quantitative measurement of the transformation zone in a CeO_2 stabilized

zirconia, as shown in Fig. 9. In CeO_2-TZP, the transformed zone is only 230 μm across and only 2% of the material is transformed.

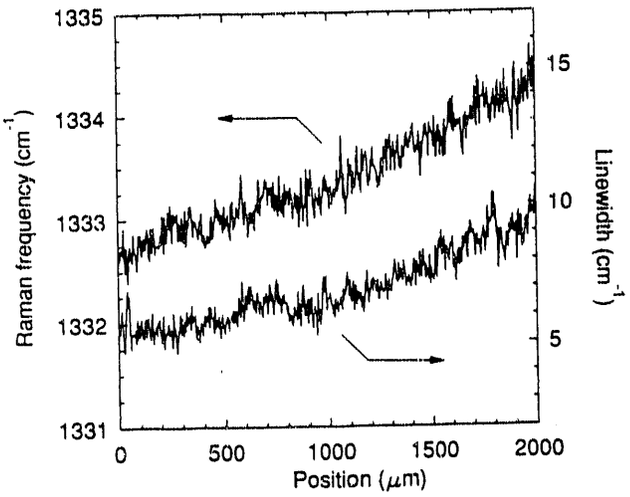

Fig. 9. Spatially resolved Raman analysis of a chemically synthesized diamond film. The observed Raman linewidth is smaller and the line frequency is closer to that of single crystal diamond in the center of the sample. The changes in the frequency and width of the Raman line are correlated and these values change with the quality of the film.

Femtosecond Dynamics in Condensed Matter

Principal Investigator: Charles V. Shank

Funding: $296,500

Project Description

Investigation of ultrafast processes in materials using optical and electronic techniques. Emphasis is on the development and application of femtosecond optical techniques to probe the properties of solids, molecules, and surfaces.

Accomplishments

A new program has been established to perform investigations of ultrafast processes with femtosecond time resolution. A colliding pulse dye laser system with a copper vapor laser amplifier was set up. This system is capable of generating optical pulses as short as 6 femtoseconds. The spectral coverage of this laser system ranges from 600 nm to 900 nm.

The spectral coverage of ultrashort optical pulse laser systems has been limited to the red and infrared region of the spectrum. In the last year we have developed a new laser system that is capable of producing pulses of 22 femtoseconds duration over the spectral region 450–500 nm region of the spectrum with an energy of 2 microjoules. Pulses at 500 nm have been compressed to less than 10 femtoseconds duration using an optical fiber with pairs of gratings and prisms for phase compensation. The extension of femtosecond pulse generation and compression to shorter wavelengths provides the temporal resolution and photon energy necessary for investigation of ultrafast processes in a variety of organic and solid-state material systems.

A new effect never before seen in a solid state material system has been observed in GaAs. We term this effect "Resonant Intervalley Scattering." The dynamics of intervalley scattering of electrons has been investigated in GaAs with 6 femtosecond optical pulses at room temperature. We have observed a "resonant coupling" between the Γ and X conduction bands in this material. This effect slows the apparent rate of scattering of carriers in the Γ valley at energies near the minimum of the X valley. These are the first experiments ever performed with this resolution to monitor nonequilibrium intervalley scattering processes.

Raman Spectroscopy for Advanced Characterization of Materials

Principal Investigator: D. Kirk Veirs

Funding: $57,700

Project Description

Raman spectroscopy probes the atomic vibrations of a material and can yield important information about the chemical, physical, and mechanical properties of materials. Measurements of chemical composition, thermodynamic phase, temperature, or stress can be made with Raman spectroscopy with a spatial resolution approaching 1 μm. We have developed a technique, including instrumentation and software, that allows us to obtain and analyze many Raman spectra, encompassing a significant area of a sample, in a reasonable period of time, in order to profile or map the property of interest. Producing a detailed map of

the chemical or physical properties of a material may require collection and analysis of tens of thousands of spectra. Previously, it was not possible to produce such maps, because of the time taken to acquire and analyze Raman spectra from many individual points.

Accomplishments

In our approach, Raman scattered light is collected from a slit-like illuminated area on the sample and imaged onto the entrance slit of a spectrometer. A two-dimensional detector is used to detect the dispersed light. We use a microchannel plate PMT detector with a position-sensitive resistive anode, but the method can also be implemented with a charge coupled device (CCD) detector. Up to 1024 Raman spectra are collected simultaneously, each representing one spatial position along the illuminated line on the sample. The data are analyzed to produce a one-dimensional profile of the desired chemical or physical property. Successive sample translations build up a two-dimensional map of the desired property from successive one-dimensional profiles. The spatial resolution and spectral precision are currently 5 μm and 0.16 cm^{-1}, respectively. Although our experiments have utilized Raman scattering, the approach can be adapted to the collection and analysis of data from other spectroscopic techniques that disperse light collected from a sample, e.g., photoluminescence.

Practical implementation of spatially resolved spectroscopy requires computer control of spectra acquisition, analysis, and storage and of sample movement. Specialized software developed in our group (copyrighted as CHEMMAP, University of California, 1990) controls acquisition of data, performs real-time data analysis and displays the results (profiles and maps) in an easily understandable form. Developments in this software include a factor of five increase in the analysis speed and the implementation of an integrated, menu-driven, mapping environment.

Spatially resolved spectroscopy can be performed with other two-dimensional detectors. In a recent collaborative effort with Photometrics, Ltd., the imaging performance of a state of the art CCD camera was compared to that of the microchannel plate photomultiplier currently used in our system. The signal to noise of the CCD camera is slightly higher than that of the imaging PMT; the improvement arises from the higher quantum efficiency of the CCD camera (30% vs. 10%).

Publications

Journals and Proceedings

G.M. Rosenblatt and D.K. Veirs, "Raman Characterization of High Temperature Materials Using an Imaging Detector," *High Temp. Sci. 26*, 31 (1989), LBL-27621.

D.K. Veirs, J.W. Ager III, E.T. Loucks, and G.M. Rosenblatt, "Mapping Materials Properties with Raman Spectroscopy Utilizing a Two-dimensional Detector," *Appl. Opt. 29*, 4969 (1990), LBL-28369.

R.W. Schoenlein, J.Y. Bigot, M.T. Portella and C.V. Shank, "Generation of Blue-Green 10 fs Pulses Using an Excimer Pumped Dye Amplifier," *Appl. Phys. Lett.* 58 (8), 801, 25 February 1991.

J.Y. Bigot, M.T. Portella, R.W. Schoenlein, J.E. Cunningham, and C.V. Shank, "Resonant Intervalley Scattering in GaAs," *Phys. Lett.* 65 (27), 3429, Dec. 31, 1990.

G.M. Rosenblatt and D.K. Veirs, "Raman Characterization of High Temperature Materials Using an Imaging Detector," *High Temp. Sci. 26*, 31 (1989), LBL-27621.

J.W. Ager III, D.K. Veirs, J. Shamir, and G.M. Rosenblatt, "Laser Heating Effects in the Characterization of Carbon Fibers by Raman Spectroscopy," *J. Appl. Phys. 68*, 3598 (1990), LBL-28370.

N.-H. Cho, K.M. Krishnan, D.K. Veirs, M.D. Rubin, C.B. Hopper, B. Bhushan, and D.B. Bogy, "Chemical Structure and Physical Properties of Diamond-like Amorphous Carbon Films Prepared by Magnetron Sputtering," *J. Mater. Res.* 5, 2543 (1990), LBL-28908.

R.H. Dauskardt, W.C. Carter, D.K. Veirs, and R.O. Ritchie, "Transient Subcritical Crack-growth Behavior in Transformation-toughened Ceramics," *Acta. Metal. Mater.* 38, 2327 (1990), LBL-26682.

B. Marchon, N. Heiman, M.R. Khan, A. Lautie, J.W. Ager III, and D.K. Veirs, "Raman and Resistivity Investigations of Carbon Overcoats of Thin Films Media – Correlations with Tribological Properties," *J. Appl. Phys.*, in press.

G.M. Rosenblatt, D.K. Veirs, J.W. Ager III, and J. Shamir, "Characterization of Materials with Raman Spectroscopy," in *Proceedings of the Symposium on High Temperature and Materials Chemistry*, LBL-27905.

G.M. Rosenblatt and D.K. Veirs, "Raman Characterization of High Temperature Materials Using an Imaging Detector," in *Materials Chemistry at High Temperature*, ed. J.W. Hastie (Humana Press, Clifton, NJ, 1990), Vol. 1.

S. Verghese, P.L. Richards, K. Char, and S.A. Sachtjen, "Fabrication of a High T_c Superconducting Bolometer," *SPIE Superconductivity Applications for Infrared and Microwave Devices Proc.* vol. 1292, p. 137, 1990. LBL-28885.

M. Nahum, Q. Hu, P.L. Richards, and S.A. Sachtjen, "Fabrication and Measurement of a High T_c Superconducting Microbolometer," *Bull. Am. Phys. Soc.*, vol. 35, p. 377, 1990. LBL-28133 Abs.

S. Verghese, P.L. Richards, S.A. Sachtjen, K. Char, and N. Newman, "Low Frequency Voltage Noise Measurements in HTSC Thin Films," *Bull. Am. Phys. Soc.*, vol. 35, p. 425, 1990. LBL-28135 Abs.

H. Zhang, J.W. Lynn, W-H. Li, T.W. Clinton, and D.E. Morris, "Two- and Three-Dimensional Magnetic Order of the Rare-Earth Ions in $RBa_2Cu_4O_8$," *Phys. Rev. B 41*, 229, 1990.

M.R. Chandrachood, D.E. Morris, and A.P.B. Sinha, "Phase Diagram and New Phases in the Y-Ba-Cu-O System at High Oxygen Pressure," *Physica C 171*, 187 (1990).

D.E. Morris, N.G. Asmar, J.Y.T. Wei, R.L. Sid, J.H. Nickel, J.S. Scott, and J.E. Post, "Rare Earth Substituted 124 and 247 Superconductors," *Physica C 955*, 162 (1989).

D.E. Morris, A.P. Marathe, and A.P.B. Sinha, "Destabilisation of 124 and 247 of Y-Ba-Cu-O by Fe Substitution at Elevated Oxygen Pressures," *Physica C 386*, 169 (1990).

D.E. Morris, P.K. Narwankar, A.P.B. Sinha, K. Takano, and V.T, Shum, "Lanthanum-Substitued Y-Ba-Cu-O Superconductors Synthesized at Elevated Oxygen Pressures," *Appl. Phys. Lett. 57*, 7 (1990).

D.E. Morris, N.G. Asmar, J.Y.T. Wei, J.H. Nickel, R.L. Sid, J.S. Scott, and J.E. Post, "Synthesis and Properties of the 2:4:7 Superconductors $RBa_2Cu_7O_{15-x}$ (R =Y, Eu, Gd, Dy, Ho, Er)," *Phys. Rev. B 40*, 406, (1989).

S. Thevuthasan, G.S. Herman, A.P. Kaduwela, R.S. Saiki, Y.J. Kim, and C.S. Fadley, "Electron Emission Holography: Prospects and Limitations," submitted to *Physical Review Letters*.

G.S. Herman, S. Thevuthasan, T. Tran, and C.S. Fadley, "Photoelectron Holography from Si(111) and Ge(111)," to be submitted to *Physical Review B.*, Rapid Communications.

R.S. Saiki, A.P. Kaduwela, Y.J. Kim, and C.S. Fadley, "The Structure of c(2x2)S on Ni(001) as Determined by High-Resolution X-ray Photoelectron Diffraction and Holography," to be submitted to *Surface Science*.

M.J. Ferrari, M. Johnson, F.C. Wellstood, J. Clarke, D. Mitzi, P.A. Rosenthal, C.B. Eom. T.H. Geballe, A. Kapitulnik and M.R. Beasley, "Distribution of Flux Pinning Energies in $YBa_2Cu_3O_{7-\delta}$ and $Bi_2Sr_2CaCu_2O_{8+\delta}$ from Flux Noise," *Phys. Rev. Lett. 64*, 72 (1990), LBL-27651.

M.J. Ferrari, M. Johnson, F.C. Wellstood and J. Clarke, "Flux Pinning Energies in High-T_c Superconductors: Ferrari *et al* Reply," *Phys. Rev. Lett. 65*, 279 (1990), LBL-29275.

F.C. Wellstood, J.J. Kingston, M.J. Ferrari and J. Clarke, "Superconducting Thin-Film Flux Transformers of $YBa_2Cu_3O_{7-x}$," *Appl. Phys. Lett. 57*, 1930 (1990), LBL-29274.

M. Johnson, M.J. Ferrari, F.C. Wellstood, J. Clarke, M.R. Beasley, A. Inam, X.D. Wu, L. Nazar and T. Venkatesan, "Random Telegraph Signals in High Temperature Superconductors," *Phys. Rev. Rapid Communication* 42, 10792 (1990), LBL-29510.

S. Verghese, P.L. Richards, K. Char, and S.A. Sachtjen, "Fabrication of an Infrared Bolometer With a High T_c Superconducting Thermometer," *Applied Superconductivity Conf. Proc., IEEE Trans. Magn.* (in press) LBL-28989.

M. Nahum, Q. Hu, P.L. Richards, N. Newman, S.A. Sachtjen, and B.F. Cole, "Fabrication and Measurement of High T_c Superconducting Microbolometers," *Applied Superconductivity Conf. Proc., IEEE Trans. Magn.* (in press) LBL-28990.

M. Nahum and P.L. Richards, "Design Analysis of a Novel Low Temperature Bolometer," *Applied Superconductivity Conf. Proc., IEEE Trans. Magn.* (in press) LBL-28992.

M.J. Ferrari, J.J. Kingston, F.C. Wellstood and J. Clarke, "Flux Noise from Superconducting $YBa_2Cu_3O_{7-x}$ Flux Transformers," *Appl. Phys. Lett. 5B*, 1106 (1991), LBL-29613.

F.C. Wellstood, J.J. Kingston, M.J. Ferrari, and J. Clarke, "Thin-Film Flux Transformers of $YBa_2Cu_3O_{7-x}$," *IEEE Trans. Magn.* 27, 2569 (1991), LBL-28890.

A.H. Miklich, F.C. Wellstood, J.J. Kingston, J. Clarke, M.S. Colclough, A.H. Cardona, L.C. Bourne, W.L. Olson and M.M. Eddy, "High-T_c Thin-Film Magnetometer," *IEEE Trans. Magn. Mag.* 27, 3219 (1991), LBL-28892.

J. Clarke, M.S. Colclough, D. Quan, M.J. Ferrari, J.J. Kingston, A.H. Miklich and F.C. Wellstood, "High-T_c Thin-Film Microelectronics," Proc. 3rd Int'l. Symposium on Superconductivity, Springer Verlag, Tokyo (1991), LBL-29794.

G.M. Rosenblatt and D.K. Veirs, "Raman Characterization of High Temperature Materials Using an Imaging Detector," in *Materials Chemistry at High Temperature*, ed. J.W. Hastie (Humana Press, Clifton, NJ, 1990), Vol. 1.

D.K. Veirs, J.W. Ager III, E.T. Loucks, and G.M. Rosenblatt, "Mapping Chemical Properties of Advanced Materials Using Imaging Raman Spectroscopy," in *Digest of Topical Meeting on Laser Applications to Chemical Analysis*, 1990 (Optical Society of America, Washington, DC 1990), Vol. 2, p. 10.

D. Kirk Veirs, J.W. Ager III, and G.M. Rosenblatt, "Mapping Chemical and Physical Properties of Advanced Materials Using Spatially Resolved Raman Spectroscopy," in *XXII International Conference on Raman Spectroscopy*, ed. J.R. Durig and J.F. Sullivan (Wiley, Chichester, UK, 1990). p. 898.

Presentations and Seminars

G.M. Rosenblatt, D.K. Veirs, and E.T. Loucks, "CHEMMAP: Software for Two Dimensional Surface Analysis," East Bay Emerging Technology Ventures Briefing, Oakland, CA, October 1989.

D.K. Veirs, "Spectroscopic Imaging of Materials' Properties," NMT Seminar, Los Alamos, NH, February 1990

D.K. Veirs, "Imaging Using Vibrational Raman Spectroscopy," Gordon Research Conference on Vibrational Spectroscopy, Wolfeboro, NH, August 1990.

G.M. Rosenblatt, D.K. Veirs, J.W. Ager III, and J. Shamir, "Characterization of Materials by Raman Spectroscopy," Symposium on High Temperature and Materials Chemistry, Berkeley, CA, October 1989.

G.M. Rosenblatt, "Cluster Impact Fusion," Heavy Ion Fusion Seminar, Lawrence Berkeley Laboratory, Berkeley, CA, October 1989.

G.M. Rosenblatt, "Symposium Overview," Symposium on High Temperature and Materials Chemistry, Berkeley, CA, October 1989.

G.M. Rosenblatt, D.K. Veirs, J.W. Ager III, and J. Shamir, "Characterization of Materials by Raman Spectroscopy," Symposium on High Temperature and Materials Chemistry, Berkeley, CA, October 1989.

J. Shamir (Hebrew University of Jerusalem), "Structure of Solid Complexed Salts by Raman Spectroscopy," Materials and Chemical Sciences Division, Lawrence Berkeley Laboratory, October, 1989.

N.-H. Cho, M.D. Rubin, K.M. Krishnan, D.K. Veirs, B. Bhushan, and D.B. Bogy, "Characterization of Diamond-like Amorphous Carbon Thin Films," International Conference on Metallurgical Coatings, San Diego, CA, March 1990.

G.M. Rosenblatt, "Recent Developments in the Raman Characterization of Materials," Gordon Research Conference on High Temperature Chemistry, Meridan, NH, July, 1990.

J.W. Ager III, D.K. Veirs, and G.M. Rosenblatt, "Characterization of CVD Diamond Thin Films by Imaging Raman Spectroscopy," 13th Surface & Interface Research Meeting, Northern California Chapter, American Vacuum Society, Menlo Park, CA, June 1990.

Q. Hu and P.L. Richards, "Quasiparticle Mixers and Detectors," in *Modern Superconducting Devices*, eds. Steven T. Ruggiero and David A. Rudman, pp. 169-196, Academic Press, San Diego, California 1990. LBL-26535.

P.L. Richards, "Bolometric Infrared Sensors: Non-Superconducting and Superconducting," 1989 Superconducting Electronics Workshop, St. Michaels, MD, October 1-5, 1989.

P.L. Richards, "High T_c Applications: Infrared and Millimeter Wave Sensors," American Vacuum Society 36th National Symposium and Topical Conference, Boston, MA, October 23, 1989.

Q. Hu, "A High T_c Superconducting Bolometer," Seminar at the National Institute of Standards and Technology, Boulder, CO, December 22, 1989.

M. Nahum, "Fabrication of Sensitive High T_c Bolometers," Workshop on Innovative Long Wavelength Infrared Detectors, Pasadena, CA, April 26, 1990.

S. Verghese, "Low Frequency Voltage Noise Measurements in HTSC Thin Films," American Physical Society March Meeting, Anaheim, CA, March 12-16, 1990.

S. Verghese, "Fabrication of a High T_c Superconducting Bolometer," SPIE's Technical Symposium on Optical Engineering and Photonics in Aerospace Sensing, Superconductivity Applications for Infrared and Microwave Devices, Orlando, FL, April 19-20, 1990.

C.S. Fadley, "Spectroscopy, Diffraction, and Holography with High-Energy Photoelectrons," invited talk at the Workshop on Opportunities in High Brightness Soft-X-Ray Science in the 1–4 keV Range, Stanford Synchrotron Radiation Laboratory, October 1, 1990.

J. Clarke, "Flux Noise and Pinning Energies in High Temperature Superconductors," colloquium, Physics Department, UCSD, February 8, 1990.

J. Clarke, "1/f Noise in High-T_c Superconductors," colloquium, Applied Science Department, UC Davis, Livermore, California, May 15, 1990.

F.C. Wellstood and J. Clarke, "Vortex Motion and Noise in YBCO Flux Transformers," Condensed Matter Colloquium, Dept. of Physics and Astronomy, University of Maryland, College Park, MD, September 6, 1990.

J. Clarke, "Thermally Activated Noise Processes in High Transition Temperature Superconductors," invited talk, NATO Advanced Research Workshop "Rate Processes in Dissipative Systems: 50 Years after Kramers," Tutzing, W. Germany, September 10-13, 1990.

J. Clarke, "Progress towards an Electronics Technology with Thin Films of High-T_c Superconductors," opening plenary address, Third International Symposium on Superconductivity, Sendai, Japan, November 7-9, 1990.

J. Clarke, "Current Dependence of Flux Noise and Pinning Energies in $YBa_2Cu_3O_{7-x}$ Films," LT-Satellite Conference on High-T_c Superconductivity, Cambridge, England, August 13-15, 1990.

Nuclear Science Division

Exotic Beams at the 88-Inch Cyclotron

Principal Investigator: Robert G. Stokstad

Funding: $80,700

Project Description

The purpose of this program was to develop the basis for a radioactive beam capability at the 88-Inch Cyclotron.

Accomplishments

This project developed the scientific justification for producing radioactive beams at the 88-Inch Cyclotron, a technical overview of the components, and an approximate cost and schedule. The project was presented to Director of the Division of Nuclear Physics in the DOE and to the scientific community at a Workshop on the Science of Intense Radioactive Beams at Los Alamos. The project was also presented to a subcommittee of the Nuclear Science Advisory Committee that reviewed the scientific program and plans for the future at the 88-Inch Cyclotron.

The scientific justification was coordinated and developed through a series of meetings that began in late October 1989 and concluded in March of 1990. Interested members of the Nuclear Science Division (NSD) and visitors attended these discussions and contributed ideas. In January 1990 the NSD decided to pursue EB-88, that is, the double cyclotron concept, instead of an alternate suggestion involving the SuperHILAC. Following this decision, work continued to improve the scientific justification, build a larger community of interested supporters including outside users, and improve the technical design. A nuclear physicist from Los Alamos, D. Vieira, who was organizing a workshop in April to promote a national high-intensity facility, was invited to LBL in February to review the plans for EB-88, and a delegation of three people from the NSD visited TRIUMF in March to inspect the ECR source and Isotope Separator on Line (ISOL) built by J. D'Auria and to discuss the EB-88 project with him. A visiting scientist, P. Haustein, made measurements of the yields of radioactive products from a boron nitride target; shielding calculations and activation estimates were checked by K. Gregorich. Both these R&D efforts made use of proton beams from the 88-Inch Cyclotron.

At the same time, the engineering staff at the Cyclotron and NSD scientists were exploring alternate designs for the shielding of the primary cyclotron and the caves for the production target. A system of three similar caves with adjacent facilities for remote handling of radioactive production targets was selected. At this point the project was ready to present to the DOE and this was done in Washington on March 26, 1990. The presentation was favorably received. In April 1990, the workshop was held at Los Alamos and the benefits of EB-88 for the development of a national high-intensity facility explained. Members of the NSD played significant roles in this workshop (J.M. Nitschke was a summary speaker on facilities, and R.G. Stokstad was the chairman of a working group on reaction mechanisms) and these contributions gave additional visibility to EB-88.

EB-88 was a prominent element in the category of Major Future Initiatives for the 88-Inch Cyclotron and was presented to the NSAC review panel during their site visit in August 1990. Because the preparations for this project had begun in October and it had received exposure in the community, EB-88 was better developed as a project and generally farther along than a similar effort begun at a later date by another low-energy facility undergoing the same review. Our exploratory R&D effort to develop radioactive beams at the 88-Inch Cyclotron thus helped us in this competitive review and also, later, in the negotiations to site Gammasphere here.

Physics Division

Calorimeter Electronics R&D

Principal Investigators: Gerald Abrams, Fred Kirsten, Michael Levi, Jasper Siegrist, George Trilling

Funding: $70,600

Project Description

Considerable effort at LBL and elsewhere has been devoted to developing sophisticated data-acquisition electronics for silicon tracking detectors. The intent of this project was to employ the techniques and methods developed in silicon tracking electronics to initiate similar advances in calorimeter readout electronics. These advances in front-end electronics for calorimetry are essential for the successful operation of calorimeter detectors in future high-luminosity experiments. The high-rate, high-density, low-power, radiation-hard electronics required by these experiments are well beyond current practices and certainly at or beyond the current state-of-the-art. This project had two primary objectives: (1) develop design goals and criteria for low-noise calorimeter readout amplifiers, and (2) apply these rules in the development of an amplifier readout applicable to liquid argon, warm liquid, or scintillator calorimetry.

The tradeoffs considered in our analysis included the issues of input thermal noise, power dissipation, amplifier topologies, radiation hardness, and integrated circuit technology (e.g. JFET, CMOS, Bipolar). The designs considered had to be producible in integrated circuit form as opposed to other approaches involving hybrid fabrication that are not appropriate for many channel application. Additionally, we had to contend with the practicality of connecting preamplifiers to detectors with high source capacitances.

Accomplishments

Methods of detector-to-amplifier capacitive matching were investigated. The conventional technique to reduce electronic noise is to match the detector capacitance to the input capacitance of the preamplifier via a transformer. In order to understand how to best make electronics connections to the calorimeter stack, a model for simulation of the electrical properties of the stack had to first be generated. A lumped element model was considered with an attempt to understand the signal parameters. A small test calorimeter stack was constructed in order to better analyze the high frequency interactions of the detector amplifier combination.

An alternate method of impedance matching is through the use of large capacitance amplifiers. This method has serious consequences for any design due to the large power consumption; however, it has significant fabrication advantages due to the lack of a transformer. Two large area JFET amplifiers were constructed as part of this analysis. One was based on a 2SK147 and the second was based on eleven matched 2SK152 JFET's in parallel. A third design used several BRF992 MOSFET's in parallel. All three designs addressed the need for very low noise (series resistance of less than 5 ohms) at high bandwidths (50 MHz).

In further work we considered how these amplifiers could be connected to both trigger and readout data acquisition chains as would be found in a typical future high-rate experiment. An outgrowth of this project lead to the involvement by LBL in the Front-End Electronics Collaboration.

New Postdoctoral Fellowship in Mathematics

Principal Investigators: Alexandre Chorin and Paul Concus

Funding: $25,000

Project Description

The new Hans Lewy Postdoctoral Fellowship at LBL was initiated to foster research by recent Ph.D.s in areas of computational and applied mathematics related to the numerical solution of partial differential equations and the concomitant use of advanced-architecture computers.

Accomplishments

The first Hans Lewy Fellow selected was Jingyi Zhu, who received his Ph.D. from the New York University

Courant Institute of Mathematical Sciences in 1989. His research at LBL is in the area of computational fluid dynamics, especially in methods related to higher-order finite differences.

One physical problem of interest for which new techniques were developed is the propagation of combusting interfaces in viscous fluids. Consider a flame burning in a viscous incompressible fluid with volume expansion and baroclinic vorticity production along the flame fronts. Computational solution of this problem would incorporate several aspects of computational fluid dynamics and interface propagation. Among recent advances in the field are the second-order projection methods for viscous, incompressible flows developed by Bell, Colella, and Glaz and the level set method for interface propagation developed by Osher and Sethian. In a collaboration with James Sethian, Zhu merged the above methods and solved the cold flame propagation problem numerically for viscous, incompressible flows; in particular, he concentrated on cold flames burning in several fluid flows with strong vorticity dominance. Of major interest is the interplay between fluid velocity and flame burning, and the effect of curvature-dependence on the moving front. The technique that was developed was shown to be strikingly effective in handling the formation of corners in the flames, with consistent curvature-dependent smoothing.

A related area is on the use of numerical techniques for solving problems that are physically unstable. One such problem of interest—both theoretical and practical—is high Reynolds number flow through a channel with a backwards-facing step. The study of turbulent combustion in the recirculation zone behind the step has been a challenging problem of long-standing general interest, for which there is a rich history of experimental results that can be used to corroborate computational findings. The problem poses extreme difficulty for any numerical method, and most finite difference calculations so far have given reasonable results only for a limited range of restrictively small Reynolds numbers. It is the strength of the second-order projection method, upon which the method being developed is based, that makes feasible an attempt to capture all the basic phenomena observed in experiments and, at the same time, improves the resolution over that available with other methods. Preliminary calculations for two-dimensional problems with reasonably large Reynolds numbers have been found to agree very well with the basic experimental results. Extension to three dimensions, which is natural for the projection method/level set interface technique, has been initiated.

SSC Detector Optimization

Principal Investigator: Chris Quigg

Funding: $122,800

Project Description

The principal physics research interest was in the scientific possibilities of multi-TeV hadron colliders. The purpose of the project was to understand more clearly the range of physics goals appropriate for a solenoid detector and to help ensure that potentially interesting phenomena had not been overlooked in the design and optimization of the detector.

Related to this focus was work addressing data in hand—or soon to be acquired—from the CDF and D0 experiments at the Tevatron Collider. There are natural links, both fundamental and instrumental, between current and future detectors and their experimental programs. In its first runs, the CDF detector has emphasized physics at the highest energy scales. The recent reconstruction of B mesons in CDF opens a second front that emphasizes copious production of relatively light objects. A similar breadth must be anticipated for the principal instruments designed for the SSC; it is not only the rarest processes that bring new insights.

Methods used ranged from analytic to computational to Monte Carlo simulation. Topics studied included the production of strong-interaction resonances such as axigluons, the effects of heavy top quarks on discovery channels, strongly interacting gauge bosons, and the properties of particles containing heavy quarks.

Accomplishments

During the fall of 1989, a preliminary study was made of the influence of top-quark decays into real W-bosons on the signatures for heavy Higgs bosons and other electroweak resonances. This work has been extended by others and is now a staple of SSC and LHC detector simulations.

The production of axigluons—observed as two-jet resonances—was incorporated into the PAPAGINO event generator, and the discovery limits for SSC experiments and for CDF were assessed. The same analysis that leads to compositeness limits can be used to search for strong resonances.

New calculations on the physics reach of colliders with varying energies and luminosities were carried out, and the machine options under consideration for the SSC were characterized in terms of parton-parton luminosities.

Various possibilities for gauge-boson scattering at energies approaching 1 TeV were investigated to understand how resonant and nonresonant structures in low partial waves can distinguish among models for electroweak symmetry breaking.

New Liquid-Crystalline Polymer Composite Materials through Sol-Gel Processes

Principal Investigator: Bruce M. Novak

Funding: $30,600

Project Description

A key thrust in the area of ultra-light, advanced materials research lies in the design of new composite systems. Composites embody a general class of materials that is extremely broad, ranging from polymer blends and reinforced plastics to chopped-fiber and filled polymer composites. Advanced composites, formed by aligning extremely strong and stiff inorganic fibers in a polymer resin matrix or binder, display exceptional mechanical properties. The combination of a brittle fiber in a brittle matrix produces a material that is much tougher than either of the two single components. In this work, a new program was initiated designed to turn this traditional picture of a composite around and use essentially organic polymers to reinforce low-density, inorganic glass matrices. Although these new materials are "inverted," the basic composite principles remain intact, but now the synergistic relationship results from the combination of a rigid-rod organic polymer (for high tensile strength) with a three-dimensionally cross-linked, inorganic matrix (for high compressive strength).

Our basic approach involves incorporating liquid-crystalline, organic polymers into sol-gel solutions that can be hydrolyzed to form low-density SiO_2 networks that act to lock-in the ordered organic polymer. As an alternative approach, we are exploring the formation of inorganic-organic SIPNs formed through the simultaneous formation of both the cross-linked inorganic glass and a cross-linked organic polymer. This approach has proved highly successful, by providing composite materials that display unparalleled mixture between the two chemically dissimilar phases.

Accomplishments

During preliminary studies in this area, we have been able to show that a select number of polymers are soluble in the sol-gel solutions and that they remain homogeneously embedded within the SiO_2 glass formed as a result of the hydrolysis procedure. For example, polymers with basic functional groups such as amines and pyridines are soluble in the acid catalyzed, pregelled, sol-gel solutions. (A limited number of polyacid materials appear to be soluble in base catalyzed, pregelled solutions.) Specifically, poly(2-vinylpyridine), poly(vinylpyrrolidone) and polyacrylonitrile can be dissolved in tetraethoxy orthosilicate (TEOS)/H_2O solution (tetramethoxy orthosilicates (TMOS) can also be used), using organic acids as cosolvents. Under the proper conditions, subsequent hydrolysis and condensation of the TEOS produces composite materials in which the organic polymer remains homogeneously embedded within the three-dimensional SiO_2 network. By controlling the rate of the TEOS hydrolysis, monolithic samples of material can be produced. These monolithic glassy materials display excellent optical clarity and mechanical strength (Scheme I).

Scheme I

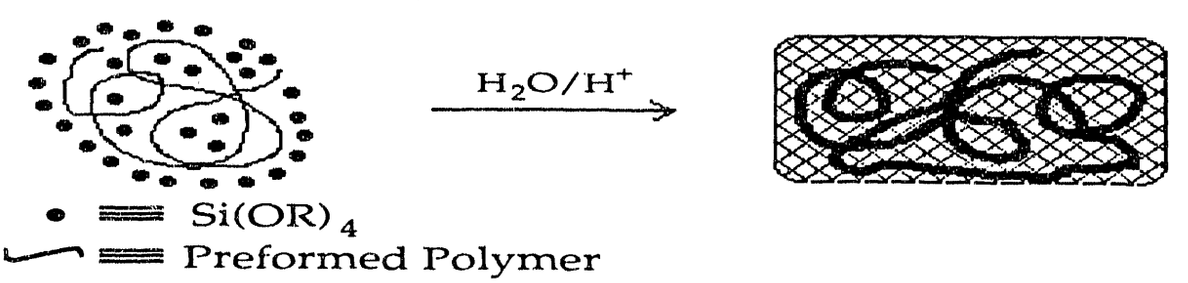

The incorporation of order, liquid-crystalline polymers has also been examined. We have found that when liquid crystalline polymers are substituted for the amorphous, random-coiled polymers in these glasses, anisotropic materials are obtained that exhibit strong birefringence. For example, cellulose derivatives can be used in the sol-gel process to form homogeneous, optically transparent, monolithic, composite glasses (Scheme II).

The utility of this technique is illustrated by the fact that poly-I (Scheme III) is an intractable, completely insoluble polymer and yet it can be homogeneously embedded within the glass matrix in concentrations up to ~60% without undergoing macro-phase separation. SEM studies show that in comparison to the composites formed by incorporating preformed polymers, the SIPN composite materials show far

Scheme II

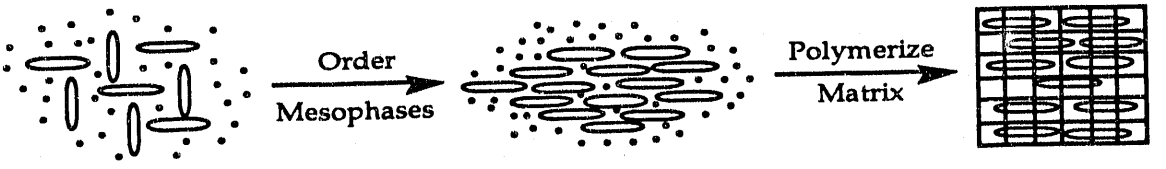

Although the mechanical properties of these new composites have yet to be systematically measured, preliminary results indicate that these composites are exceptionally tough and impact resistant (i.e., vigorous pounding in a mortar and pestle does not crack or shatter these composites).

In order to circumvent the solubility problem associated with trying to incorporate preformed polymers and to provide better homogeneity between the two phases, investigations were begun into the formation of simultaneous interpenetrating networks (SIPNs) by the synchronous formation of both the organic polymer and the inorganic glass network. Two organic polymerization methods were identified that restrictive conditions imposed by the sol-gel reaction (i.e., aqueous acidic or basic medium): vinyl, free radical polymerizations and aqueous ring-opening metathesis polymerizations (aqueous ROMP) catalyzed by a variety of Ru^{3+} and Ru^{2+} salts. A ROMP example of this SIPN process is shown in Scheme III.

greater homogeneity and small domain sizes (average polymer domain sizes are less than 1000 Å).

A serious limitation to sol-gel technology is the tremendous shrinkage that occurs during the drying of the glass samples. (Shrinkages of up to 75% are common.) As with standard sol-gel glasses, shrinkage remains a problem in these SIPNs. In an effort to surmount this problem, we have synthesized a series of tetraalkoxysilane derivatives possessing polymerizable alkoxide groups in place of the standard ethoxide or methoxide groups. The hydrolysis and condensation of these siloxane derivatives liberates a polymerizable alcohol. In the presence of the appropriate catalyst (free radical or ROMP), and by using a stoichiometric amount of water and the corresponding alcohol as cosolvent, all components of these derivatives are polymerized. Since both the cosolvent and the liberated alcohol polymerize, gel drying is unnecessary and no gel shrinkage occurs. This overall process is illustrated in Scheme IV.

Scheme III

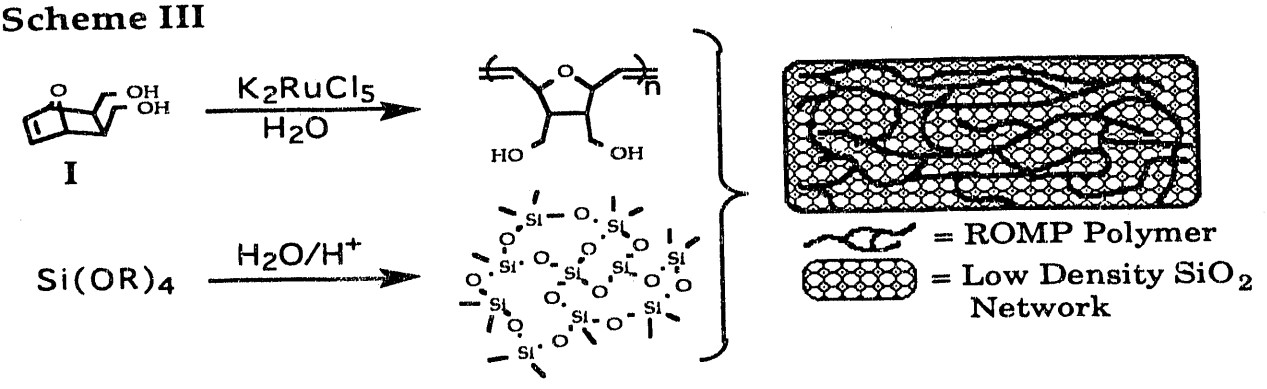

Scheme IV

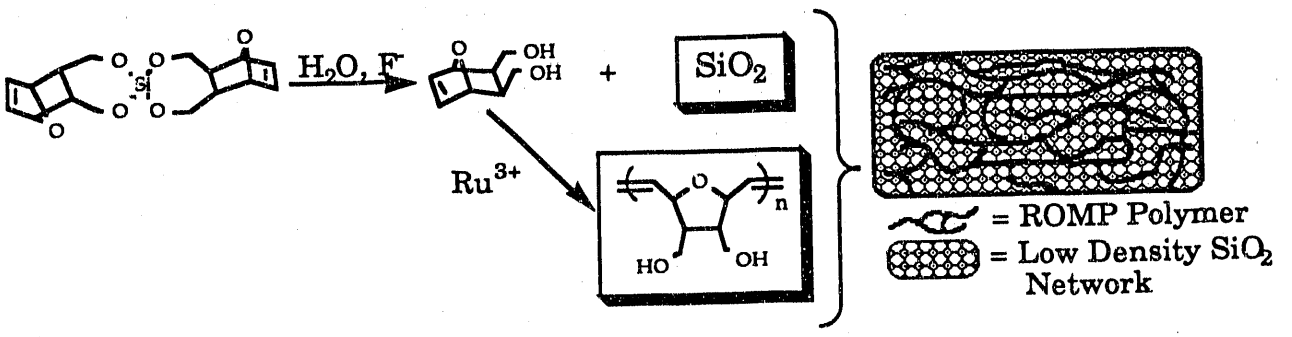

There has been considerable industrial and government interest in this project. We are currently receiving direct funding from Du Pont, Chevron and Exxon Chemical Company and are slated for support from Amoco and 3M. Funding for this work from the Office of Naval Research is scheduled to begin in February 1, 1991.

Cluster Formation in the Vapor Produced by Laser Pulsing of the YBCO Superconducting Solid

Principal Investigator: Donald R. Olander

Funding: $29,100

Project Description

In the intense research effort on industrial utilization of high-T_c superconductors, laser evaporation has been established as the leading method for deposition of thin films. However, formation and growth of large clusters in the evaporated plume can have a detrimental effect on the quality of the film. The project aims at characterizing the clusters and investigating methods of breaking up the clusters before they reach the substrate. The specific objectives of the project were as follows:

i) To identify various species contained in the laser-evaporated plumes of $Y_1Ba_2Cu_3O_7$ by time-of-flight and quadrupole mass spectrometry and by high-resolution-microscopic examination of deposited species. Since UO_2 evaporates primarily into a single monomer species, UO_2 plumes were investigated first. Vapor plumes of YBCO were then examined.

ii) To investigate the possibility of lowering cluster yields by re-evaporating the clusters in flight by intense radiation. For this purpose two sources of radiation, a Xe flash lamp and a focused laser beam, are being investigated.

Accomplishments

Three experimental setups and four techniques were used as follows:

Laser ionization/time -of -flight mass spectrometry. UO_2 and YBCO targets were irradiated with laser pulses of 266 nm wavelength and 5 ns duration (power density exceeding 10^{10} W/cm^2). The resulting ions were identified by time-of-flight mass spectrometry.

Laser vaporization/time-of-flight mass spectrometry. UO_2 and YBCO targets were vaporized by laser pulses of 1060 nm wavelength and 1.75 ms duration (power density < 10^5). The neutral species were ionized by a pulsed electron gun and identified by time-of-flight mass spectrometry.

Laser vaporization/quadrupole mass spectrometry. YBCO targets were vaporized as above and the signals of various monomers and clusters at a quadrupole mass spectrometer were monitored as a function of time.

Laser vaporization/scanning microscopy. UO_2 and YBCO targets were vaporized as above and deposited on substrate coupons for microscopic examination. Highly-oriented pyrolitic graphite was used as substrate for scanning tunneling microscopy and silicon was used for atomic force microscopy.

The following results were obtained:

- Clusters can form a significant part of deposited species depending on a number of factors:
  - At low power densities of the incident laser beam (10^4 to 10^5 W/cm^2 with peak surface temperatures not exceeding 2200 K), laser evaporation primarily generates monomer species.

- As incident power density is increased, significant cluster formation is observed. Clusters with masses up to and beyond 3500 amu were observed. Only a small portion of the plume consists of monomer species that initially evaporated from the surface. For UO_2, clusters consist of combinations of UO, UO_2, and UO_3. The YBCO system, owing to its multi-component nature, is much more complex and clusters formed by various combinations of Y, YO, Ba, BaO, Cu, and Cu_2O were observed.
- At very high power densities obtained in laser-ionization experiments, a reduction in high-mass cluster yields was observed indicating the possibility of cluster breakdown due to absorption of radiation.

- Microscopic examination of deposited films also verified the cluster nature of the plume. Clusters deposited on pyrolitic graphite have diameters of the order of 3 nm. Films of 100 nm thickness were examined by atomic force microscopy. They appear to be primarily formed of clusters with an occasional ejected liquid drop of micron size. Lack of liquid droplets is the primary advantage of long-pulse technique over the short pulse method of film deposition. The role of clusters, however, requires further study.
- Research effort on the methods of re-evaporating the clusters is underway and most of required experimental modifications have already been completed. The following methods are being examined:
  - Flashing a high-intensity Xe flash lamp after ejection of the plume.
  - Extending the length of contact of the plume with the vaporizing laser.

Publications

Journals and Proceedings

B.M. Novak, M. Ellsworth, T. Wallow, and C. Davies, "Simultaneous Interpenetrating Networks of Inorganic Glasses and Organic Polymers. New Routes into Nonshrinking Sol-Gel Derived Composites," *Polymer Preprints*, *31*, 698 (1990).

M.W. Ellsworth and B.M. Novak, "Mutually Interpenetrating Inorganic-Organic Networks. New Routes into Non-Shrinking Sol-Gel Composite Materials," *J. Am. Chem. Soc.*, submitted for publication.

M.W. Ellsworth and B.M. Novak, "Mutually Interpenetrating Inorganic-Organic Networks. New Routes into Non-Shrinking Sol-Gel Composite Materials," US Patent pending (1990).

C. Quigg, "Hadron Supercolliders: The 1-TeV Scale and Beyond," LBL-29453, August 10, 1990, to appear in the *Proceedings of the Workshop/Symposium on TeV Physics*, Beijing, May 28-June 8, 1990 (Gordon and Breach, London, in press).

C. Quigg, "Gauge Boson Dynamics," Fermilab-Pub-91/58-T, to appear in the *Proceedings of Beyond the Standard Model II*, University of Oklahoma, October 31-November 3, 1990 (World Scientific, Singapore, in press).

J. Zhu and J. Sethian, "Projection Methods Coupled to Level Set Interface Techniques," LBL-30183, 1990; submitted to *J. of Comp. Phys.*

Presentations and Seminars

D.R. Olander, "Cluster Formation in Laser Vaporization of YBCO Superconducting Ceramics," High-Temperature Superconductivity Program Review Meeting, Lawrence Berkeley Laboratory, Oct. 3, 1990.

W. Wang, "Characterization of Clusters in Plumes of Laser-Evaporated Refractory Ceramics," Bay Area High-Temperature Society meeting, Lawrence Berkeley Laboratory, Fall 1990.

"Liquid-Crystalline Organic-Inorganic Composite Materials," Dow Chemical Company, Walnut Creek, CA., January 4, 1990.

B.M. Novak, "Organic-Inorganic Composite Materials," Du Pont, Wilmington, DE., April 12, 1990.

B.M. Novak, "Simultaneous Interpenetrating Networks of Inorganic Glasses and Organic Polymers. New Routes into Nonshrinking Sol-Gel Derived Composites," National Meeting, American Chemical Society, Washington, D. C., August 26, 1990.

B.M. Novak, "Organic-Inorganic Composite Materials Using Aqueous ROMP Techniques," B. F. Goodrich Company, Brecksville, OH., September 26, 1990.

B.M. Novak, "Polymer Synthesis: From Inorganic-Organic Composite Materials to Photodoped Conducting Polymers," 3M, St. Paul, MN, October 26, 1990.

B.M. Novak, "Polymer Synthesis: From Inorganic-Organic Composite Materials to Photodoped Conducting Polymers," Lawrence Livermore National Laboratories, Livermore, CA., December 18, 1990.

B.M. Novak, "'Inverse' Organic-Inorganic Composite Materials. New Routes into *Nonshrinking* Sol-Gel Composites," Japan-US Joint Seminar on Inorganic and Organometallic Polymers;" Nagoya, Japan, March 24-27, 1991.

J. Zhu, Applied Mathematics Seminar, Stanford University, May 1990.

J. Zhu, Conference on Computational Methods for Fluid Dynamics and the Evolution of Fronts and Interfaces, University of Utah, October 1990.

Other Publications

C. Quigg, S.D. Drell et al., "Report of the 1990 HEAPAP Subpanel on SSC Physics," DOE/ER-0434 (1990).

Research Medicine and Radiation Biophysics Division

Viability in Synchrotron Microscopy

Principal Investigators: Thomas L. Hayes, Patrick Echlin, and Edward N. Ashworth

Funding: $77,400

Project Description

The possibility for viable biological specimens to be examined by soft x-ray microscopy was evaluated, with particular attention to the viability of frozen-hydrated material in whole cell mounts or just prior to cryosectioning for frozen hydrated tissue section specimens.

Accomplishments

Test of low-temperature viability and selection of plant tissue for soft x-ray irradiation studies. Three levels of dehydration were selected for evaluation of cold resistant properties, a highly dehydrated, embryonic seed tissue of the higher plant *Raphanus sativus* (radish) was selected because of its rapid germination time and suitable size and form of the embryonic tissue for microscopic identification. A partially dehydrated cell from a commercially prepared (dry) activated yeast was selected for low-temperature viability tests based on the production of carbon dioxide following low-temperature exposure. A completely dehydrated tissue was selected from the specialized leaf structure (turion) of the water plant *Lemna*, which had previously been shown by others to have a moderate degree of cold resistance. The embryonic seed tissue of *Raphanus sativus* was 100% viable after exposure to liquid nitrogen temperature (-196 C) for up to 90 minutes and will be an excellent specimen for future studies that utilize low-temperature microscope stage systems. The partially dehydrated yeast cells were also viable after exposure to liquid nitrogen temperature but the more hydrated turion of *Lemna* lost viability in ice when the ice temperature fell below -20 C. Based on these preliminary experiments, the embryonic tissue of the *Raphanus* seed was selected for further studies of the environmental factors (vacuum, radiation) associated with high resolution soft x-ray microscopy.

Viability in vacuum conditions. No loss of viability was detected in *Raphanus* seed germination following exposure to 3×10^{-6} Torr in the low-temperature preparation chamber of the scanning electron microscope. Tests were carried out at both low temperature (-196 C) and room temperature with exposure up to one-half hour.

Viability as a function of rehydration. In order to evaluate the effects of condensation during preparation of the *Raphanus* seeds, cold resistance of seeds placed in a high humidity (100%) chamber for varying amounts of time was studied. Cold resistance to exposure to liquid nitrogen temperature was maintained through 15 minutes of rehydration in the high-humidity chamber, but was reduced by a 30-minute exposure, and the seeds lost all viability if two hours of rehydration preceded the exposure to liquid nitrogen.

Scanning electron microscopy of viable seed embryos at liquid nitrogen temperature. Figure 1 shows the scanning electron micrograph images at increasing magnification of the seed embryo following cryo fracture in the low temperature preparation chamber of the scanning microscope. Figure 1a, taken at 20 times original magnification, shows the entire embryo in cross section, as well as the low-temperature holder and calibration grid in the background. Figure 1b, taken at 200 times original magnification, shows a cross section of one component of the embryo with the surface cells clearly distinguishable from the cryo fractured surface. Figure 1c, taken at 500 times original magnification, shows the edge between the surface and the cryo fractured component, and Fig. 1d, taken at 5000 times original magnification, shows the frozen hydrated single cell from the embryo that was viable up to the time of SEM imaging. Figure 1e shows the stability of the system in the scanning microscope following several minutes of the specimen exposure to the vacuum and radiation conditions of the beam. Gross structure is completely preserved.

Single cell and thick cryo section investigations. One of the unique characteristics of the future soft x-ray scanning microscope at the ALS will be the ability to image thicker specimens at higher resolutions than can be obtained with present electron microscope or light microscope techniques. The light microscope can

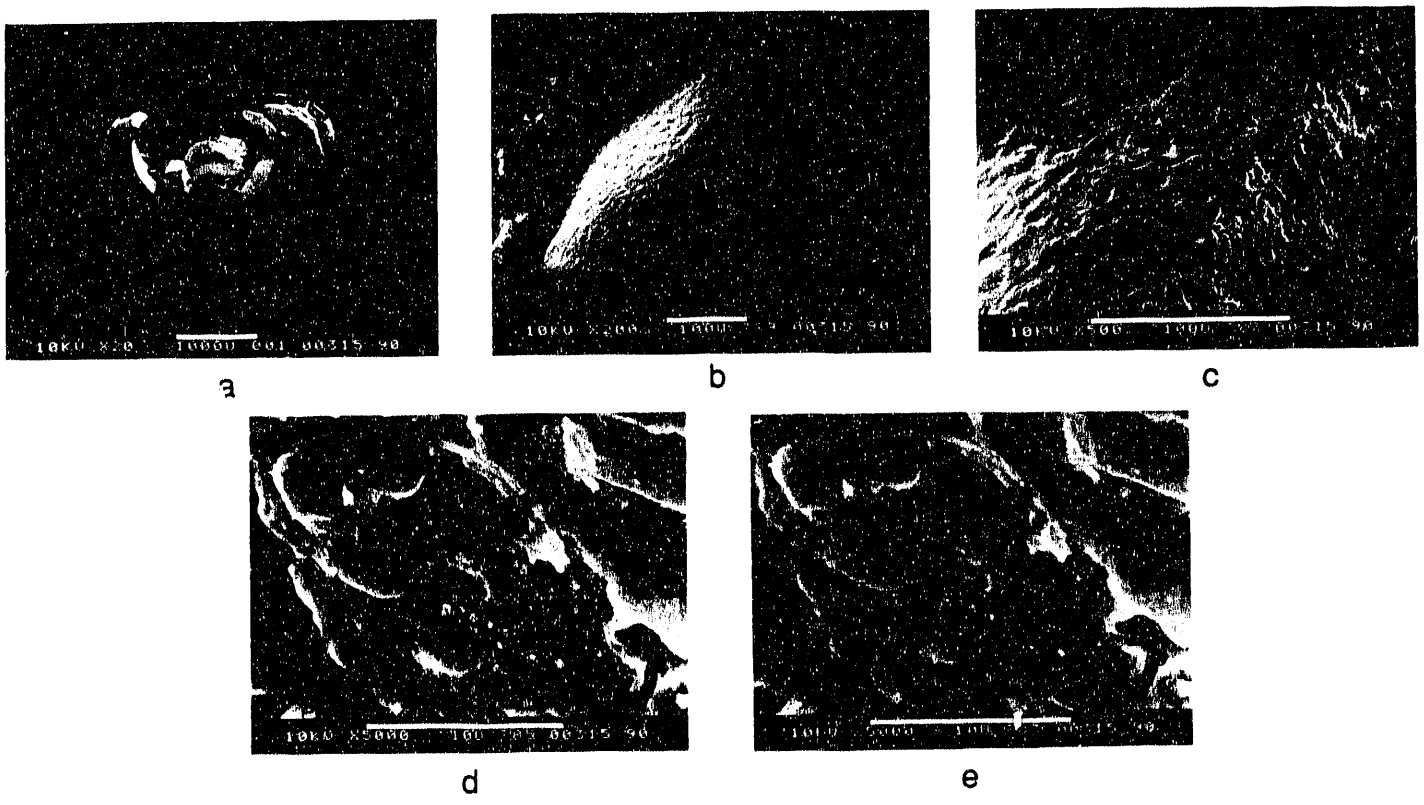

Fig. 1. Low-temperature scanning electron microscope images of cryofractured seed of Raphanns sativus. Seed was viable under environmental conditions of temperature and pressure used during specimen preparation and viewing. (a) Bar represents 1,000 μm. (b) Bar represents 100 μm. (c) Bar represents 100 μm. (d) Bar represents 10 μm. (e) Bar represents 10 μm.

image specimens up to a size of ~1 mm but smallest feature resolution is limited to about 0.5 micrometers. Electron microscopes have very high resolution (2 Å) but there is a severe limit on the thickness of the specimen, usually requiring specimens of ultra thin dimensions, and even with high voltage electron microscopy specimens thicker than 0.5 micrometers are difficult to image. The scanning x-ray microscope will be able to image specimens up to 10 micrometers in thickness with smallest feature resolution approaching 300 Å. Cultured cells and cryo sections can be imaged, therefore, at thicknesses that both improve the amount of information available in three dimensions and also are technically feasible with current cryo sectioning techniques. The ability to localize ionic concentrations of major elements is one of the goals of the tissue work currently underway on the bulk seed embryo specimens described above. The low-temperature specimen holder for such specimens has been developed in our laboratory and tested in the low-temperature scanning electron microscope.

Publications

Journals and Proceedings

T. Hayes, "Low Temperature Microscopy of Cold Resistant Plant Cells," *The Proceedings of the Low-temperature Biological Microscopy and Analysis Meeting*, Cambridge University, Cambridge, England, April 2-6, 1990.

J. Bastacky, C. Goodman, and T.L. Hayes, "A Specimen Holder for Low-Temperature Scanning Electron Microscopy," *J. Electron Microscopic Techniques*, Vol. 14, 83(1990).

Innovative Project Reports

Accelerator and Fusion Research Division

Thin Film Diamond Synthesis

Principal Investigators: Ian Brown and Kannan Krishnan

Funding: $84,000 (second year of funding)

Project Description

The synthesis of diamond at high pressure and temperature is well known. Recently, a few laboratories have accomplished synthesis of diamond under metastable conditions, i.e., in the graphite stable region. The attractiveness of such vapor/plasma deposition techniques for synthesizing large areas of controlled structure and composition is clear. These developments open a new area in thin-film technology and offer the potential for exploiting the unique properties of diamond for applications such as electronics (heat sinks, insulating gates, active devices), optical (antireflective and protective coatings) and mechanical (wear-resistant, low friction coatings). This subject is also pertinent to the study of carbon in interstellar space and the origin of diamond in the earth.

The rapid development of this field, in spite of its immense technological implications, has been impeded by the following attributes:

- Nucleation of the diamond crystallites on the substrate surface and the subsequent growth mechanism is not well understood.
- Characterization of such thin film diamond is not simple.
- There is a large number of experimentally controllable parameters.

These problems motivated this coordinated study of the synthesis and characterization of plasma-synthesized diamond films. The program involves the growth and investigation of high quality polycrystalline diamond thin films. Films were synthesized using a plasma CVD method and characterized with a variety of electron optical techniques. Measurements were aimed at understanding the fundamentals of the nucleation, growth and structure of the films.

Diamond thin films were synthesized using plasma CVD techniques. Characterization of the films provided continuous feedback and guidance for optimization of the synthesis process as well as fundamental information on the films' structural properties.

The emphasis of this program was placed on the characterization aspects of films grown by a microwave-produced plasma technique. Considerable time and effort were invested in the safety aspects of the facility. Detailed microstructural characterization was performed using the unique capabilities available at LBL's National Center for Electron Microscopy. Nucleation and growth of the films was investigated by high-resolution electron microscopy, and supportive Raman spectroscopy was carried out by collaborators in LBL's Materials Sciences Division.

Accomplishments

A microwave plasma CVD diamond synthesis facility was designed and fabricated, and used for growing diamond films of excellent quality. The diamond synthesis facility is of the kind known generically and informally as a "bell jar system." Microwave power is provided by a 500-W magnetron generator (taken from a standard microwave oven) at a frequency of 2.45 GHz, and is delivered to the plasma chamber via a simple waveguide feed to a pyramidal cavity. A 3-inch-diameter quartz bell jar is located within the microwave cavity, in which a hydrogen/methane plasma is established by microwave power absorption in the gas. During processing, a 1-inch diameter substrate is positioned on a pedestal inside the quartz reactor and immersed in the discharge. The hydrogen and methane gas flow rates and mixture ratios are controlled and the total pressure is monitored. The hydrogen/methane gas pressure ratio is kept in a range near 99% : 1%, and the system pressure in the

range 10–100 torr. The facility has operated outstandingly; it is stable and reliable, it has operated for long periods of time without any problems, and its results are reproducible.

High-quality diamond films have been grown, as determined by Raman spectroscopy, uniformly on 1-inch diameter silicon substrates under a variety of conditions. The film growth characteristics have been explored. One important study that was completed is an investigation of the effect of a graphite holder (the device that locates the substrate in the correct location within the plasma) on the quality of the diamond film synthesized on its substrate. A high-quality diamond film grows on the graphite holder itself, which in turn influences the quality of the film grown on the substrate. It is beneficial to use a holder that is fabricated of graphite and on which a diamond film has been grown.

Publications

Journals and Proceedings

G.J. Vandentop, M. Kawasaki, R.M. Nix, I.G. Brown, M. Salmeron and G.A. Somorjai, "Formation of Hydrogenated Amorphous Carbon Films of Controlled Hardness from a Methane Plasma," *Phys. Rev B* 41, 3200 (1990).

Presentations

M.C. Salvadori, M. Brewer, J. Ager, I.G. Brown and K.M. Krishnan, "The Effect of a Graphite Holder on Diamond Synthesis by Microwave Plasma Chemical Vapor Deposition," paper to be presented at the Second International Symposium on Diamond Materials, Washington, DC, May 5–10, 1991.

Applied Science Division

Photochemical Vapor Deposition of Mixed-Metal and Oxide Thin Films

Principal Investigator: David K. Liu

Funding: $57,000 (second year of funding)

Project Description

A novel photochemical vapor deposition (PCVD) method was developed for the preparation of magnetic thin films at ambient temperature using volatile organometallic precursors

Accomplishments

Thin films of iron-cobalt and iron-nickel have been prepared at ambient temperature using a photochemical vapor deposition (PCVD) apparatus built in-house. The major advantage of this PCVD technique is the low temperature employed, thus permitting the preparation of amorphous materials as well as the use of a wide variety of substrates. Other problems associated with thermal CVD, such as the diffusion of impurities from the reactor or substrate into the growing film, may also be circumvented using this technique.

One of the most important findings of our study is that these mixed-metal thin films can be prepared by two different methods: (1) using two separate organometallic sources, such as $Fe(CO)_5/Co(CO)_3NO$ or $Fe(CO)_5/Co_2(CO)_8$, and (2) using a single heteronuclear organometallic precursor containing one or more metal-metal bonds, such as $CpFeCo(CO)_6$, $CpFe_2Co(CO)_9$, $HFeCo_3(CO)_{12}$, and $Cp_2FeNi(CO)_3$, where Cp represents a η^5-C_5H_5 ligand. Each of these methods has its own merits. Using the first approach, it was demonstrated that by varying either the excitation wavelength (Table 1) or the vaporization temperatures (Table 2) of the Fe and Co carbonyl precursors, the Fe/Co ratios of the resultant thin films can be manipulated. On the other hand, by using a single heteronuclear compound, the Fe/Co ratio of the precursor can be preserved in the thin films in most of the cases studied (Table 3). Therefore, this low-temperature PCVD process can provide the ability to

Table 1. Fe/Co ratio of thin films prepared by wavelength-selective PCVD using $Fe(CO)_5$ and $Co(CO)_3NO$ precursors at 20°C.

Photolysis Condition	Fe/Co Ratio
With 325 nm band pass filter	1.31
No filter	1.00
With 345 nm long pass filter	0.52

Table 2. Fe/Co ratio of thin films prepared by PCVD using $Fe(CO)_5/Co(CO)_3NO$ and $Fe(CO)_5/Co_2(CO)_8$ precursors at different vaporization temperatures.

T°, $Fe(CO)_5$ (°C)	T°, $Co(CO)_3NO$ (°C)	T°, $Co_2(CO)_8$ (°C)	Fe/Co Ratio
20	–1	—	1.40
20	4	—	1.25
20	20	—	1.00
2	20	—	0.78
20	—	45	0.66
5	—	45	0.21
0	—	45	0.13

Table 3. Fe/Co and Fe/Ni ratios of alloy thin films on Al substrates prepared by PCVD using a single heteronuclear precursor.

Precursor	Fe/Co (theor.)	Fe/Co (found)	Fe/Ni (theor.)	Fe/Ni (found)
$CpFe_2Co(CO)_9$	2.00	0.85	—	—
$CpFeCo(CO)_6$	1.00	1.19	—	—
$HFeCo_3(CO)_{12}$	0.33	0.31	—	—
$Cp_2FeNi(CO)_3$	—	—	1.00	0.98

control the metal compositions and possibly the magnetic properties of alloy and mixed-metal oxide thin films.

This PCVD procedure consistently produced thin Fe-Co and Fe-Ni films which were metallic in appearance and were coherent and adherent in nature. Using two separate precursors and photolysis times of 10 min, film thickness and deposition rates of 0.03-0.06 μm and 0.2-0.4 μm/h were obtained, as measured by stylus profilometry. For experiments using a single heteronuclear precursor and photolysis times of 1-2 h, typical film thickness was 0.1-0.2 μm and deposition rates for $CpFeCo(CO)_6$ and $HFeCo_3(CO)_{12}$, were 0.20 and 0.05 μm/h, respectively. The absence of observable lines except for those of the substrates in x-ray powder diffraction (XRD) spectra suggested that the deposited films are amorphous. Scanning electron microscopy (SEM) analysis of the deposited films revealed granular surfaces with particle sizes of 0.1-0.4 μm. The fact that both mixed-metal and oxide thin films can be prepared at ambient temperature by PCVD was confirmed by Auger electron spectroscopy (AES). The AES depth profile of a typical $CpFeCo(CO)_6$-derived film revealed that Fe and Co are present in approximately stoichiometric ratio and are homogeneously distributed throughout the entire thickness of the deposit. The amounts of C and O present in the film were ~4% and ~8%, respectively, and these contaminant levels could probably be reduced if lower pressure can be achieved during film deposition. However, when the same PCVD process was carried out with added O_2, a thin film containing ~25% O was obtained, implying a more or less fully oxidized Fe-Co film was formed in this case. Therefore, both mixed-metal and oxide thin films can be prepared *in situ* using this PCVD procedure. Electrical conductivity measurement of a 1:1 Fe-Co film using the four-point probe technique gave a resistivity of 34.4 μΩ-cm. The saturation magnetization, σ_{sat}, of the same Fe-Co film was 24.2 emu/g, as measured by a vibrating sample magnetometer (VSM). This translates to a saturation moment, μ_{sat}, of 0.50 Bohr magneton per atom, which is substantially lower than the theoretical value of 2.3 Bohr magneton per atom predicted by the Slater-Pauling curves for a 1:1 Fe-Co thin film. The lower saturation moment is probably due to the presence of antiferromagnetic iron and cobalt oxides in these films, as suggested by Auger analysis results.

Optical Fiber Sensors Based on Thermal Lens Spectroscopy

Principal Investigator: Richard E. Russo

Funding: $88,000 (second year of funding)

Project Description

The development of optical fiber sensors based on thermal lens spectroscopy (TLS) was continued. A primary purpose for investigating TLS optical fiber sensors is their potential application for remote and *in situ* monitoring of actinide species in mixed waste environments. The monitoring and clean-up of waste sites containing radionuclides is an area of importance to DOE, DOD, and EPA.

The proposed TLS sensors differ from other optical fiber sensors in that the distal fiber end does not contain immobilized reagents, i.e., a miniature chemical laboratory at the end of the fiber (cf., antibody/antigen receptor sites). These agents can become poisoned with use so that frequent standardization and replacement is necessary. In contrast, the optical fiber TLS sensor relies on wavelength selectivity alone to provide a measure of the actinide level and its oxidation state.

TLS is an ultra-sensitive optical absorption technique. The concept of TLS is straightforward. A pulsed or modulated continuous-wave (cw) laser beam induces a transient refractive index gradient in the sample medium by optical absorption and non-radiative relaxation (heating) processes. If the spatial profile of this excitation laser is near-Gaussian, the induced refractive index gradient will resemble a divergent lens. The defocusing of the excitation beam, or of a second paraxial probe beam, is measured using a pinhole (spatial filter) and photodetector. The change in measured intensity through the pinhole is directly proportional to the Beers Law absorbance. Actinide ions in solution release absorbed optical energy thermally with no fluorescence quantum yield, and are therefore ideal candidates for detection by TLS. The ability to measure optical absorption at low levels, and to provide oxidation state information as well, makes TLS an ideally suited technique for monitoring radionuclides in mixed waste samples. Our approach was

to implement the TLS technique using optical fibers to deliver the light to the sample medium and record the intensity change due to absorption.

Accomplishments

The technology for optical fiber sensors based on thermal lens spectroscopy was successfully developed. A fiber optic sensor based on photoacoustic spectroscopy was also developed. The first prototype for a TLS optical fiber spectrometer/sensor is shown in Fig. 1. For this sensor, a conventional dye laser system was employed as the excitation source. Such a system is unsuitable for field applications. However, the section enclosed by the dashed box was placed remotely from the large laser system. Excellent sensitivity for the measurement of neodymium in aqueous solution was achieved, comparable to those obtained in the laboratory without fibers. Figure 2 shows a second prototype optical fiber TLS spectrometer that incorporated a small semiconductor diode laser as the excitation source. In this case, the spectrometer/sensor was specific to neodymium and plutonium. The overall size of this spectrometer was small and field portable. Based on experience using optical fibers from the development of these TLS spectrometers, we also developed an optical fiber sensor using photoacoustic spectroscopy. Figures 3 and 4 present a diagram and photograph of this spectrometer. The spectrometer/sensor has already been used at the Lawrence

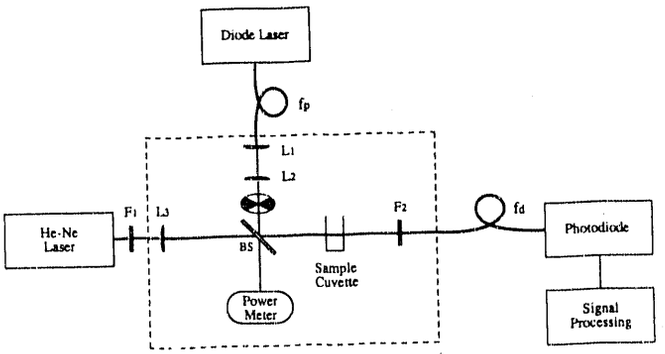

Fig. 2. Prototype of a diode-laser based TLS optical fiber spectrometer/sensor.

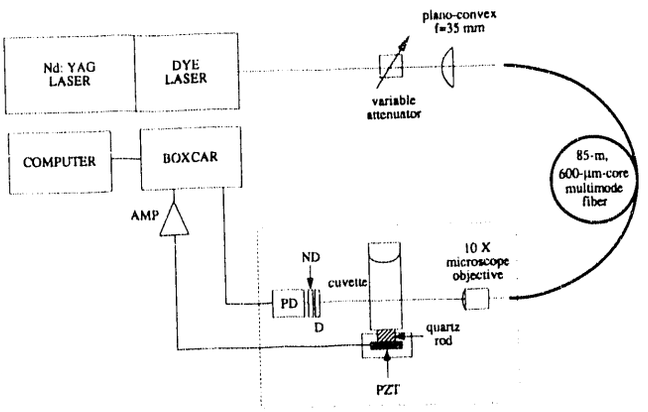

Fig. 3. Diagram of an optical fiber photoacoustic spectrometer.

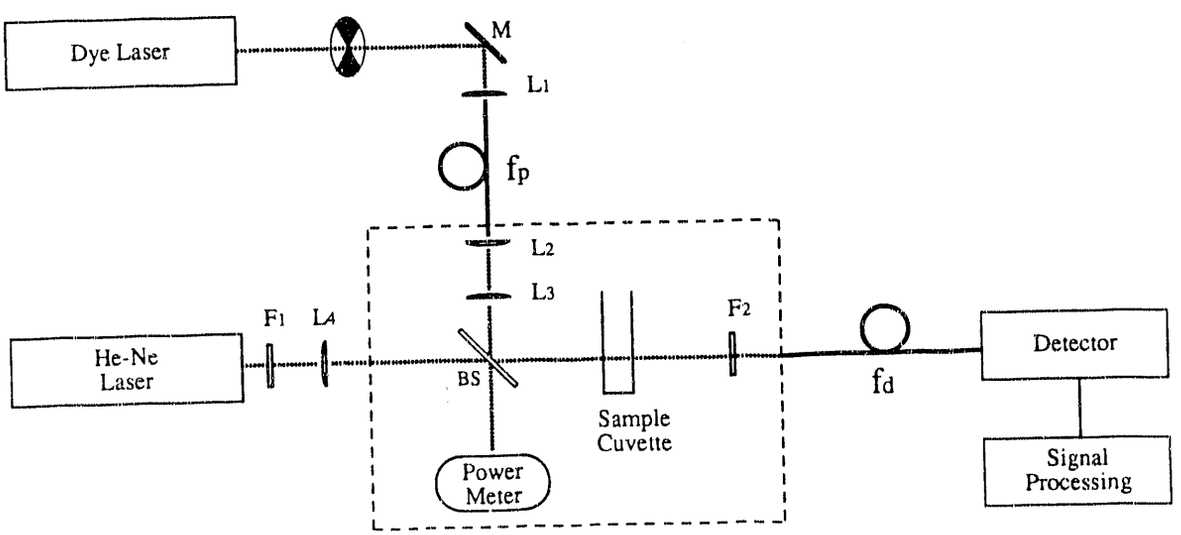

Fig. 1. Prototype of a dye-laser based TLS optical fiber spectrometer/sensor.

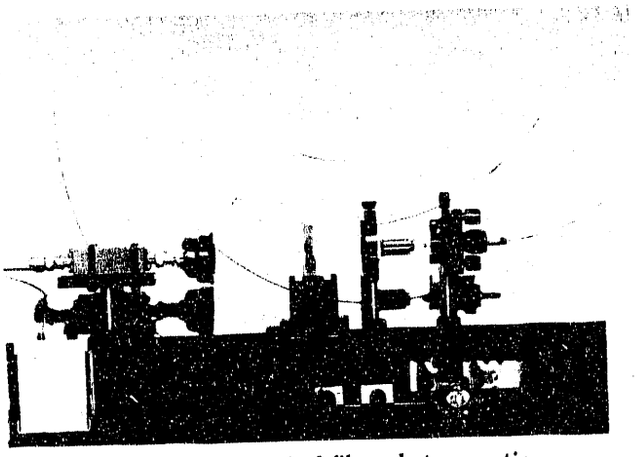

Fig. 4. Photograph of the optical fiber photoacoustic spectrometer.

Livermore National Laboratory for actinide chemical measurements in a hot-box. Optical absorption spectra for uranium, americium, and plutonium were measured in the glove box.

These studies are very important to the nuclear repository program. Numerous requests have been received from several other DOE laboratories for constructing similar actinide sensors, as well as other agencies and private industry concerning the suitability of these optical fiber sensors for measuring pesticides and organic pollutants in the environment. There is excellent probability that this fiber optic thermal lens spectroscopy and photoacoustic technology can be extended into these areas.

Publications

Journals and Proceedings

D. Rojas, R.J. Silva, and R.E. Russo, "Thermal Lens Spectroscopy Using a Diode Laser and Optical Fibers," submitted to *Anal. Chem.*, January 1991.

D. Rojas, R.J. Silva, J.D. Spear, and R.E. Russo, "Dual Beam Optical Fiber Thermal Lens Spectrometry," submitted to *Anal. Chem.*, January 1991.

D.K. Liu, A.L. Lai and R.J. Chin, "Photochemical Vapor Deposition of Mixed-Metal Thin Films from Organometallic Precursors Containing Heteronuclear Metal-Metal Bonds," *Mater. Lett.*, in press.

D.K. Liu, R.J. Chin and A.L. Lai, "Photochemical Vapor Deposition of Iron Cobalt Thin Films: Wavelength and Temperature Control of Film Compositions," *Chem. Mater.*, in press.

R.E. Russo, D. Rojas, P. Robouch, and R.J. Silva, "Remote Photoacoustic Measurements In Aqueous Solutions Using An Optical Fiber," *Rev. Sci. Instrum.* 61, 3729 (1990).

R.E. Russo, P.B. Robouch, and R.J. Silva, "Remote Measurements of Actinide Species in Aqueous Solutions using an Optical Fiber Photoacoustic Spectrometer," *MRS Proceedings*, November 1990.

Presentations

D.K. Liu, "Photochemical Vapor Deposition of Alloy and Mixed-Metal Oxide Thin Films," Paper INOR-579 presented at the International Chemical Congress of Pacific Basin Societies at Honolulu, HI, December 1989.

R.E. Russo, "Optical Fiber Photothermal Spectroscopies for *In-Situ* Monitoring and Characterization," DOE Real-Time Subsurface Monitoring of Groundwater Workshop, April 17, 1990, Dallas, TX.

R.E. Russo, "Remote Measurements of Actinide Species In Aqueous Solutions Using An Optical Fiber Photoacoustic Spectrometer," Materials Research Society Meeting, December 1990, Boston, MA.

R.E. Russo, "Thermal Lens Spectroscopy using Tunable Diode Lasers," American Chemical Society Meeting (invited), August 27-30, 1990, Washington, DC.

R.E. Russo, D. Rojas, and R.J. Silva, "Remote Thermal Lens Spectroscopy," FACSS VI (invited), October 1-6, 1989, Chicago, IL.

R.E. Russo, J.D. Spear, and R.J.Silva, "Differential Thermal Lens Spectrometer for Ultrasensitive Absorption Measurements," FACSS XVI (invited), October 1-6, 1989, Chicago, IL.

R.E. Russo, R.J. Silva, and D. Rojas, "Remote Detection of Actinide Species by Photoacoustic Spectroscopy," Migration 89, November 6-10, 1989, Monterey, CA.

Biological Analysis in Transgenic Mice of Large Defined Segments of the Human Genome Cloned in Yeast Artificial Chromosomes

Principal Investigator: Edward Rubin

Funding: $108,000 (second year of funding)

Project Description

The transgenic mouse system has proven to be an extremely useful means for examining gene expression in the whole organism. A major limitation in the introduction of foreign DNA into the mouse's genome by this approach has been the availability of only conventionally cloned DNA fragments of relatively small size. This has prevented the analysis of large genes or several interrelated genes. Creation of transgenic animals with DNA from yeast artificial chromosomes (YAC) vectors containing large human inserts could potentially solve this problem. The goals of this project were 1) the creation of a transgenic mouse system at LBL; 2) preparative isolation of large intact fragments of DNA containing genes or gene clusters cloned into YACs; and 3) creation of transgenic mice containing the large intact fragments of DNA isolated from YACs.

Accomplishments

Transgenic mouse facility. A considerable amount of effort has gone into the development of a transgenic mouse facility. This has involved the assembly of necessary equipment, the development of a mouse breeding colony, and training personnel in mouse embryo collection, microinjection of DNA into fertilized embryos, and cultivation of embryos and reimplantation of injected embryos into recipient females. The many steps of this complicated procedure are now functioning smoothly and transgenic mice are being produced.

Isolation of YAC DNA from total yeast DNA. A variety of approaches were taken to isolate and solubilize large MW DNA from the agarose gel matrix so that the DNA would be suitable for passage through a microinjection needle. The method which proved to be most successful used the enzyme agarase to solubilize the agarose matrix. By this approach it was possible to derive highly enriched YAC DNA largely intact. This DNA is essentially free of particulate matter and passes easily through the 1-micron needle tip used in microinjecting DNA into mouse embryos. The DNA, which was agarase treated in 10 mM Tris, 0.25 mM EDTA pH 7.5, had minimal effect on the initial survival and eventual development of embryos to term after pronuclear injections.

The DNA concentration injected into fertilized mouse embryos has been shown to have a major effect on the success of creating transgenic mice with cloned DNA, with 0.2-3.0 ng/μl being optimal. The concentration of DNA typically isolated from the pulse field preparative agarose gels is many fold lower than this. Several methods of DNA concentration were attempted, but all led to marked degradation of the YAC DNA. In an attempt to stabilize the DNA for the concentration procedure as well as for passage through the needle tip the YAC DNA was condensed with spermine. This proved to be extremely successful in stabilizing DNA which was then concentrated on an Amicon centricon 10 microconcentrator.

Though the size of the DNA after passage through the needle tip has not yet been determined, we have been using L-CA YAC DNA, prepared as described above, to microinject mouse embryos. Over 700 fertilized mouse embryos have undergone pronuclear microinjections with gel-purified, spermine-treated YAC DNA. Of these embryos, 330 were transplanted into pseudopregnant female mice. Of the 121 live born pups, none contained the injected YAC-cloned DNA.

Molecular Analysis of Human Chromosome 21 Region Associated with Down's Syndrome

Principal Investigator: David Schild

Funding: $56,500

Project Description

The genes located on the terminal third of chromosome 21 were analyzed to increase the understanding of the pathogenesis of Down's Syndrome. This project includes physical mapping of restriction sites, determination of coding regions, and isolation and sequencing of the cDNAs corresponding to these coding regions with the eventual goal of determining the function of these genes.

Accomplishments

The cloning of the human GART cDNA (which maps on human chromosome 21) and two other multifunctional genes involved in purine biosynthesis, using functional complementation of yeast mutations, has been completed. This study included the DNA sequence of one domain of the large trifunctional GART cDNA, and the sequences of the rest of this cDNA and another bifunctional cDNA are currently being completed in collaboration with Philip Barr (Chiron Corp.). In collaboration with M. Olson and A. Gnirke (Washington Univ.), a YAC (yeast artificial chromosome) clone containing the entire genomic copy of the human GART gene has been isolated. This YAC is ~350 kilobases in length and presumably encodes additional genes which we hope to identify. The GART cDNA has been cloned into a mammalian expression vector and in collaboration with D. Patterson (Eleanor Roosevelt Inst.), this cDNA has been shown to complement CHO mutations in each of the three functions of this trifunctional gene. The YAC genomic clone has also recently been shown to complement one of these mutations. Efforts have also continued to isolate additional human cDNAs by complementation of yeast mutations. Inadvertently, a cDNA encoding a human ribosomal protein (S11), and a second different cDNA, have been isolated because they function as omnipotent suppressors in yeast, suppressing both amber and ochre nonsense mutations. These results suggest that the human S11 protein is probably assembled into some yeast ribosomes, resulting in translational misreading, and implicate the S11 subunit in translational fidelity. Although these cDNAs are interesting from a translational point of view, they can also be considered as unwelcome cloning artifacts, since increasingly complementation of yeast mutations is being used for cloning genes from various organisms. Several ways for avoiding such artifacts have been devised.

Detection of Viral Integration

Principal Investigator: Richard Schwarz

Funding: $44,800

Project Description

The aim of this project was to develop a system for reliable and definitive detection of viral integration into the genome. The default technology was to rely on viral protein expression with detection based on a variety of antibody techniques. However, it has become increasing clear that the virus can coexist in a silent state and then be activated by conditions that are not well understood. When dealing with an oncogenic virus, such as *Rous sarcoma* virus (RSV), it becomes difficult, in certain situations, to assess whether initiation of tumorigenesis requires new infection or only activation of existing viral genes. In addition to the primary goal of viral detection, the ability to detect unique DNA sequences would be an asset for tagging cells or whole animals. These could be used in developmental studies in order to map the lineage of specific cell types or simply as a marker to identify certain cells in a mix of other cells. The latter would become the method of choice in several projects ongoing or proposed in the Cell and Molecular Biology Division.

The scheme we proposed was to detect a 20 base-pair promotor sequence for T7 RNA polymerase when incorporated into the chicken genome of 2×10^9 base-pairs: a detection of 1 in 10 billion. Such selectivity, while difficult to imagine in the macro world, is commonplace for a polymerase. In earlier studies by others, the promotor sequence for T7 polymerase had been genetically engineered into mammalian cells along with the sequence for the polymerase itself. Inside the living cell, the polymerase was synthesized, found its 20 base-pair promotor sequence, and this combination directed the synthesis of a reporter protein. So the polymerase was clearly capable of this selective task.

In our case, we wanted to add only the DNA encoding the small promotor sequence but still be able to detect

it in fixed cells in order to identify infected cells from their uninfected neighbors. For this purpose, purified T7 polymerase would be added to the fixed cells *in situ*, making use of the fact that the RNA being made could be tagged with radioactive-labeled or a non-radioactive identifier. As a consequence, a 20 base-pair sequence could give rise to thousands of incorporated, tagged nucleotides in RNA. This amplification step should be sufficient to definitively detect the RNA sequences.

The project divided itself into two parts:

1) Genetically engineering an RSV to include a T7 promotor site;

2) Developing methods to *in vitro* synthesize labeled RNA inside a fixed cell using T7 RNA polymerase and then detect it.

Accomplishments

The first part was accomplished in a few months. Its major complication was that we wanted to keep the insert with the T7 promotor site as small as possible in order to minimize the impact of this added DNA on the function of the virus. Small fragments are harder to genetically engineer. In addition, the T7 promotor site was first inserted into a vector such that it was flanked by multiple cloning sites. In the future, this step would facilitate insertion of the T7 promotor sequence into a variety of other vectors.

The small T7 promotor site with flanking multiple cloning sites was placed into a plasmid encoding a replication defective RSV genome. When this vector was transfected into a packaging cell line that supplemented the missing viral genes needed for replication, a replication defective virus was produced that contained the T7 promotor site as well as a protein reporter gene, lac Z. The latter, if expressed, is very stable and its enzyme activity can be detected by a simple color reaction. Under the appropriate assay conditions, the lac Z enzyme caused infected cells to turn blue. This enabled a simple control that showed that the virus was produced, that the virus could infect cells, and that some of the cells could express the genes encoded within the virus.

Our second aim was to show that cells expressing lac Z, or cells infected but not expressing viral genes, could be detected by the inclusion of the T7 promotor site. The conditions for optimal expression of the T7 polymerase *in vitro* had been worked out by others. Under these conditions we could show that the vector containing the promotor site would incorporate 40-fold more ^{32}P labeled nucleotides into RNA than a vector without this site (false starts of a few nucleotides probably account for the incorporation in this case). Several difficulties exist with performing this reaction *in situ*. Using fixed cells could inhibit the polymerase, which is about 100,000 MW, from reaching the promotor site in the nucleus. On the other hand, if the cell is permeabilized too much, the newly made RNA could escape during the washing steps needed to remove unincorporated nucleotides. In addition, it was unclear whether various proteins bound to the DNA might block the polymerase from interaction with its promotor site. These are not independent variables so it is impossible to optimize them one at a time.

We started with a standard protocol for fixing cells (4% paraformaldehyde) and a standard protocol for a T7 polymerase reaction using either ^{32}P labeled nucleotides or biotin labeled nucleotides. After running the reaction, one detects the ^{32}P at the single cell level using autoradiography or biotin by fluorescence, using a fluorescent probe conjugated to strepavidin. Using either detection scheme, no specific signal was initially detected. The first set of variables to be tested focused on increasing the permeability of the cells and extracting DNA bound proteins. A variety of protocols had been established for this purpose by others. One approach used strong acid (1 M HCl) to remove proteins bound to the DNA through ionic bounds. This procedure caused all cells to label with the T7 polymerase reaction. Strong acid causes depurination of the DNA and this is suspected of causing a number of false start sites for the polymerase and a strong signal to be generated in all cells. While not a true success, this procedure did show that the polymerase could enter the cell, synthesize labeled RNA, and this RNA was retained during the wash procedures. However, we needed to optimize the method for one start site and the resulting small amounts of RNA produced by the reaction.

While it was not possible to increase the number of T7 promotor sites, other parameters in the reaction could be increased. The polymerase itself could be purchased from one company (USB) at high concentration, allowing the amount in the *in situ* reaction to be increased by 100 to 1000 fold. The non-labeled nucleotides, already in vast excess, were increased another 4 fold. In discussions with other scientists who use T7 polymerase, we found out that the reaction could be run overnight at room temperature, thereby giving more time for the polymerase to diffuse to the promotor site. However, biotin-labeled nucleotide could not be raised in concentration and instead had to be reduced in order to lower non-specific background

signal (the focus had been placed on biotin labeling over radioactivity due to its speed and lower hazard). The high background or stickiness of biotin probes had been seen with other procedures as well.

In performing *in situ* hybridization, biotin probes had given poor results due to non-specific binding that was difficult to remove by extensive washing. One company (Boehringer Mannheim) has improved upon the technique by using another label that can be detected by antibody binding. This has significantly improved the signal to noise ratio for *in situ* hybridization and promises to improve our detection as well. Similarly another company (BRL) has come out with a nucleotide with a linker group ending with a free amino group. This modified nucleotide could replace an unlabeled nucleotide at equal concentration but with the advantage that the amino group would allow the synthesized RNA to be fixed to the cell after the reaction using paraformaldehyde. This would ensure that any RNA made by the polymerase would not be lost in the washing steps. Furthermore, a new procedure for the T7 polymerase reaction has been published for extending the size of the transcript made during the reaction by the inclusion of a pyrophosphatase. These improvements have the potential to significantly improve the signal-to-noise ratio and push the technique to a successful conclusion.

In conclusion, this is an important new technique that has many important applications. The genetic engineering has been accomplished and preliminary procedures for its use have been developed. New commercially available reagents should allow us to improve the signal-to-noise ratio that appears to be the critical factor for success. These will be tested as soon as a source can be found to fund future research.

Procarcinogen Activation in Human Mammary Epithelial Cells

Principal Investigator: Allan N. Tischler

Funding: $66,200 (second year of funding)

Project Description

Efforts were continued to establish the pathway(s) for the activation of relevant procarcinogens in human mammary epithelial cells (HMEC) and evaluate the synergistic potential of logical combinations of carcinogens, particularly nicotine-derived nitrosamines and benzo[a]pyrene, both of which occur in cigarette smoke.

Accomplishments

Work has continued in our ongoing attempt to understand how procarcinogens (e.g., benzo[a]pyrene), which are in themselves innocuous, are metabolically activated into potent carcinogens in susceptible cells (e.g., human mammary epithelial cells). In the specific case of benzo[a]pyrene (BP), activation is a two-step process: the conversion of BP to benzo[a]pyrene-7,8-dihydrodiol (BP-diol), and the conversion of BP-diol to the "ultimate carcinogen," benzo[a]pyrene-7,8-dihydroxy-9,10-epoxide (BPDE).

Considerable progress has been made in our understanding of the mechanism of BP metabolism in human mammary epithelial cells (HMEC). The metabolism of BP and BP-diol was compared in HMEC grown in the serum-free medium MCDB-170. Conversion of ^{3}H-BP-diol to the carcinogen BPDE, as measured by analysis of BPDE-derived tetraols, was observed to proceed more than four-times faster in cultures incubated with ^{3}H-BP-diol than in cultures incubated with ^{3}H-BP. In cultures pretreated with cold BP (100-400 nM), the conversion of ^{3}H-BP to ^{3}H-BP-diol is enhanced while the conversion of ^{3}H-BP-diol to ^{3}H-tetraols is inhibited. This observation led to the identification of a major BP-derived metabolite as 7-hydroxybenzo[a]pyrene (BP-7-ol), which was found to be an extremely potent and selective inhibitor of the BP-diol to BPDE conversion ($K_I < 12$ nM). Thus BP activation in HMEC appears to be significantly limited by a feedback inhibition pathway induced by BP-7-ol. The potency of the BP-7-ol-induced inhibition, together with the observation that the cyclooxygenase inhibitor, indomethacin, does not inhibit BP-diol metabolism suggests that the BP-diol to BPDE conversion is induced by a selective oxygenase in HMEC. These findings demonstrate the possibility of developing means to prevent the activation of common, environmental carcinogens in humans.

A carefully conducted time course of BP metabolism in conjunction with a collaboration with Tony Leadon has led to the observation that two distinct pathways leading to bulky adducts are operating in HMEC. In addition to the well-characterized BPDE pathway discussed above, which requires self-induction and becomes the predominant pathway after approximately 8 hours of BP exposure, there is a second pathway requiring no induction that is predominant for the first 4-6 hours of BP exposure. This pathway probably involves the formation of a BP radical cation

at the 6-position. This intermediate can either react directly with DNA to form bulky adducts or can be further oxidized to quinone metabolites that can be observed in cell extracts. While both pathways result in oxidative DNA damage as measured be thymine glycols, the radical cation pathway is significantly more proficient.

Most recently we have embarked on a study of the effects of components of cigarette smoke on the metabolism of BP in HMEC. After many attempts to optimize such effects, we have developed a system whereby the cells are exposed to low levels (0.1 μM) of cigarette smoke components for 16 hours followed by incubation with ^{3}H-BP for 4 hours. Table 1 summarizes our results thus far.

These results show that most of the cigarette smoke components studied enhance BP activation along either the BPDE pathway (as measured by diol production) and/or the radical cation pathway (as measured by quinone production). Benzo[e]pyrene (BeP) significantly enhances the BPDE pathway while inhibiting the radical cation pathway. Squalene is the only chemical studied that preferentially enhances the radical cation pathway. NNK, itself a procarcinogen, and catechol are particularly effective at enhancing the BPDE pathway. These cigarette smoke components will also be investigated for their effects on the formation of BP-derived bulky adducts and oxidative DNA damage.

Perhaps the most significant accomplishment of this past year was the procurement of a grant from the State of California Tobacco-Related Disease Research Program. Success in obtaining this grant rested largely on the preliminary results that this ERF grant allowed.

Publications

Journals and Proceedings

A.N. Tischler, G.A. Levine, and J. Bartley, "Metabolism Of Benzo[a]pyrene and Benzo[a]pyrene-7,8-dihydrodiol in Human Mammary Epithelial Cells: Feedback Inhibition by 7-Hydroxybenzo[a]pyrene," *Carcinogenesis*, in press (1991).

D. Schild, "A Human Ribosomal Protein Functions in Yeast as an Omnipotent Suppressor," *Yeast 6*, S391 (1990). (Abstract of paper presented at the 15th International Conference on Yeast Genetics and Molecular Biology, The Hague, Netherlands, July, 1990.)

D. Schild, A.J. Brake, M.C. Kiefer, D. Young, and P.J. Barr, "Cloning of the Human GART Gene and Two Other Multifunctional *de novo* Purine Biosynthetic Genes by Functional Complementation of Yeast Mutations," *Proc. Natl. Acad. Sci. USA* **87**: 2916-2920 (1990).

E. Spangler, K. Andrews, and E. Rubin, "Developmental Specific Expression of the Human z-globin Gene in Transgenic Mice," *Nuc. Acid. Res.*, in press (1991).

E.M. Rubin, B. Isheda, S. Clift, and R. Krauss, "Expression of Human Apolipoprotein AI in Transgenic Mice Results in the Reduction in Murine Apolipoprotein AI and the Appearance of Two New High Density Lipoprotein Particles," *Proc. Natl. Acad. Sci.*, in press (1991).

Table 1. Effect of potential cocarcinogens On B[a]P metabolism in HMEC.

Averages	Total Met	% Change	Polar (% Change)	Diol (% Change)	Quinone (% Change)	7-ol (% Change)
Control	6.54%					
BeP	7.50%	14.73	14.23	37.34	–11.99	24.61
Squalene	7.56%	15.61	7.81	10.69	22.46	18.03
Oleate	7.21%	10.32	6.88	26.96	3.09	9.92
Decane	6.80%	4.03	1.54	15.37	3.70	2.88
NNK	8.09%	3.73	16.71	50.95	24.30	5.35
Catecho	18.18%	25.08	18.28	44.90	4.34	30.86

E.M. Rubin, E. Witowska, E. Spangler, P. Curtin, B. Lubin, N. Mohandas, and S. Clift, "Sickling of Mouse Red Cells: a Transgenic Mouse Model for Sickle Cell Anemia," *J. Clin. Invest.*, in press (1991).

E.M. Rubin, R. Krauss, E. Spangler, S. Verstuyft, and S. Clift, "Expression of Human Apolipoprotein AI in Transgenic Mice Raises HDL and Inhibits Atherosclerosis," submitted to *Science* (1991).

L. Couto, E. Spangler, and E.M. Rubin, "A Method for the Introduction of High Molecular Weight DNA into Mouse Embryos," *Nuc. Acid. Res.*, 17:8010 (1989).

Other Publications

A.N. Tischler and S.A. Leadon, "Benzo[a]pyrene-Induced Oxidative DNA Damage in Human Mammary Epithelial Cells: Effects of Metabolic Intermediates and Arachidonic Acid Cascade Inhibitors," in preparation (1991).

E. Rubin and E. Spangler, "Developmental Specific Expression of the Human z-globin Gene in Transgenic Mice," in *Globin Gene Expression In Hematopoietic Differentiation*, Stamatoyannopoulos and Nienhuis, eds., New York, Alan R. Liss, Inc., in press (1991).

F. Chang, T. Barnes, J. Bleskan, D. Schild, and D. Patterson, "Functional Expression of Human cDNA Encoded Multifunctional Protein with GAR Synthetase, AIR Synthetase and GAR Transformylase in CHO Mutant Cells Deficient in *de novo* Purine Biosynthesis," in preparation.

L. Couto and E.M. Rubin, "Methods for the Quantitative Isolation of Large Molecular DNA," *Methods in Enzymology 1991*, in preparation.

Chemical Biodynamics Division

X-Ray Spectroscopy of Sulfur in Biology

Principal Investigators: Melvin P. Klein and Alexandre Quintanilha

Funding: $63,300

Project Description

Sulfur is an important element in chemistry and biology. Sulfur atoms occur in biological systems as constituents of the three amino acids cysteine, cystine and methionine, and in the nucleic acids as the base thiouracil. These sulfur bearing amino acid residues provide secondary and tertiary structural stability to proteins and provide ligands to many metal species that perform a variety of functions. For example, the iron-sulfur proteins are an important class of metalloproteins where sulfur in the form of sulfide and cysteinyl thiolate binds the Fe atoms. The redox properties of these ubiquitous Fe-S proteins ranges from 350 mV to -700 mV. The reasons for these differences are largely unknown and it is thought that the sulfur ligands modulate the electronic structure of the Fe-S clusters by interaction with the protein backbone. Additionally, sulfur is present in thiolated sugars, sulfur-containing lipids, sulfonates, and thioesters as well as reducing agents such as dithiothreitol and dithioerythritol. Many organisms contain enzymes that reduce sulfite with sulfite reductases and certain photosynthetic bacteria are able to use sulfite as the final electron donor in the electron transport chain. Importantly, one tripeptide, glutathione, has been recognized for many years as an important intracellular reducing agent providing protection against oxidative and radiation induced damage.

In all cases, however, there has been no spectroscopic tool that could provide direct observation of these important sulfur moieties, of their oxidation state or states and how they are transformed during metabolism. X-ray absorption spectroscopy (EXAFS) at the sulfur K-edge of 2.4 keV now provides such a tool. The precise energy at which absorption commences and the shape at the edge has now been demonstrated to correlate well with the oxidation state of sulfur; it is anticipated that EXAFS analysis will provide complementary site specific structural information. Operation of the LBL/EXXON/SSRL beamline VI-2 in the undulator mode has been demonstrated to yield large photon fluxes at the sulfur K-edge energy. Our objective is to apply the methods of x-ray absorption spectroscopy to study problems in cellular metabolism, metallo-protein structure and implicitly to problems in the structure and redox chemistry of sulfur for which there are no other direct methods. These studies will lead to expanded opportunities for the study of other low Z-elements that could be fruitfully exploited with the Advanced Light Source.

Accomplishments

The main objectives of the proposal were: 1) to obtain experience on beamline VI-2, operating in the undulator mode, with a variety of samples of inorganic, organic, and biochemical origin; 2) non-invasive spectroscopic determination of the oxidation states of the intracellular thiol groups in general and of glutathione in particular; 3) time resolution of the reversible oxidation-reduction of the thiol groups during increased oxidative stress (inflammation, drug detoxification, etc.); and 4) intracellular spatial resolution of the distribution of the different thiol groups.

X-ray beam time at SSRL at Stanford has been scarce over the past two years due to the upgrades in progress: the construction of the injector and the booster for the SPEAR storage ring. There has not been sufficient beam time to complete all of the experiments proposed. However, significant results pertaining to items 1 and 2 above have been obtained.

The results of the group at Stanford which showed that the position of the sulfur K-edge correlates with the oxidation state have been reproduced. The oxidation state of sulfur ranges from -2 in sulfide to +6 in sulfate, with intermediate oxidation states for elemental sulfur, sulfite, thiosulfate and persulfate. The K-edge inflection point changes about 10 eV corresponding to a change in oxidation state of –2 to +6, and the spectra exhibit a rich XANES structure. The sulfur K-edge spectra of the amino acids cystine, cysteine, and methionine was obtained. Interestingly, the spectra were clearly different for the three amino acids, although the oxidation state of S is similar in all three species. The main difference is structural, with sulfur present as C-S-S-C, C-S-H and C-S-C in cystine,

cysteine, and methionine respectively. This result is very encouraging since it suggests that the dominant intracellular components, which are thiols and disulfides, will be resolved.

Glutathione is the most ubiquitous and perhaps the most important non-protein thiol in living organisms; it is a tripeptide made up of glutamate-cysteine-glycine. In its free form, it is present intracellularly mainly in the thiol-reduced form (GSH), while the disulfide-oxidized form (GSSG) is present at much lower concentrations. The activity of many enzymes is known to be very sensitive to the intracellular ratio of GSH to GSSG. It is also known that oxidative stress raises the levels of GSSG. Other pathways of thiol oxidation are also known which involve the oxidation of methionine to the sulfoxide form. The sulfur K-edge spectra of reduced glutathione GSH, oxidized disulfide form GSSG, and methionine sulfoxide have been obtained. The spectra of each form is clearly distinct, which makes the method of x-ray spectroscopy an important and viable method for determining the ratios of these moities *in vivo*.

Finally, the sulfur K-edge spectra of blood was determined to investigate if indeed the method is suitable for distinguishing the forms of sulfur present in cellular systems. As mentioned earlier, the ratio of GSH to GSSG *in vivo* can be as high 10:1000, depending on the conditions. Preliminary results clearly show that the dominant form of sulfur in blood is in the reduced GSH form.

Labeling and NMR Studies of Nucleic Acids

Principal Investigators: David E. Wemmer, Philip G. Williams, and Henry Rapoport

Funding: $44,200 (second year of funding)

Project Description

The intent of this project was to develop tritium labeling methods that would allow site-specific incorporation into nucleic acids with high-specific activity. The labeled nucleic acids are to be used in structural biology studies of structure and function of DNA and RNA, and their interactions with other molecules. The work was extended somewhat to also include labeling of substrate molecules that interact with proteins, since both the principles of the NMR work and the labeling methodology are of value in continuing work in these areas. The sections below cover progress in the second year of the project.

Accomplishments

Oligonucleotide synthesis: 2'-deoxyadenosine derivatives. Tritium NMR provides an effective means to study molecular structure and is particularly attractive for investigating biological systems where the size of the system makes proton NMR intractable. Tritium-labeled oligonucleotides of a desired sequence can be prepared from corresponding site-specific tritiated nucleoside. The preparation of high specific activity 2-deoxy -[2-^{3}H]adenosine requires a halogenated precursor. A synthetic route for 2-chloro-2'-deoxyadenosine shown schematically below has been developed.

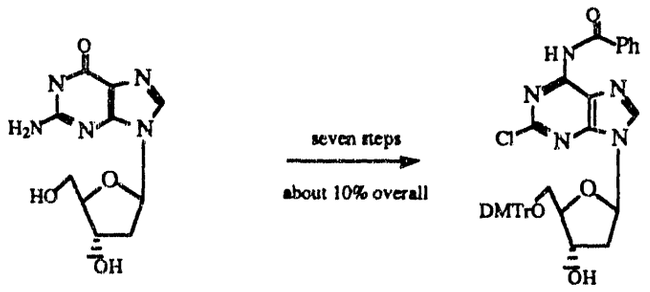

The modified nucleotide has been incorporated into a 12-mer using solid phase oligonucleotide synthesis with a DNA synthesizer. The sequence CGCGXXTTCGCG will be made first, where X is the 2-chloro-2'-deoxyadenosine.

Work continues on tritiodehalogenation of 2-chloro-2'-deoxyadenosine derivatives to corresponding tritiated 2'-adenosine derivatives and their incorporation into the oligonucleotides as well as tritiodehalogenation of halogenated oligonucleotide. This is an an important modification of the previous scheme because it minimizes the chemistry and purification which must be done after the labeling step. This approach will make use of the methodology more practical. The site-specific tritiated oligonucleotides will be used in studies on drug-DNA interactions using ^{3}H NMR. Distamycin-A has been characterized in complexes with similar DNAs and this oligomer and related compounds will be used in studies of relative binding affinities, and drug exchange kinetics.

Other adenosine derivatives. Tritium-labeled adenosine 5'-triphosphate of high-specific activity has been required for studies on its binding to the S1 fragment of myosin in relation to chemomechanical energy transduction and in synthesis of tritiated adenosine incorporated into self-cleaving RNA molecule. The

2-bromoadenosine 5'-triphosphate, a precursor for the desired labeled ATP, was prepared through a synthetic route involving conversion of guanosine to 2-bromoadenosine, analogous to the approach for the deoxynucleotide above. This was then phosphorylated in two steps to give the 2-BrATP. The tritiodehalogenation of this compound using PdO catalyst yielded tritium-labeled ATP with a specific activity of 26 Ci/mmol, far greater than that obtained by a reported catalytic exchange procedure (~10 Ci/mmol).

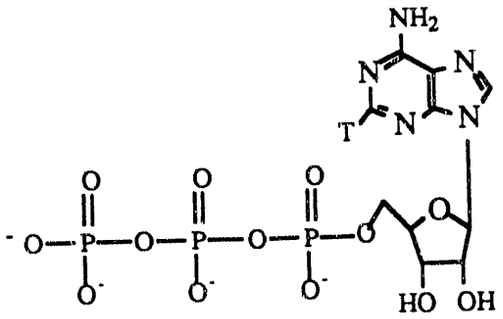

The studies on the binding of tritiated adenosine 5'-triphosphate with S1 fragment of myosin are currently being pursued using ^3H NMR spectroscopy at 533 MHz, the first high-field biophysical NMR studies using tritium.

Synthesis of tritium-labeled transition state analog hapten for ^3H NMR studies with catalytic antibodies: [2,6-$^3H_2$]-4-nitrophenyl phosphate. A wide variety of catalytic antibodies have been generated using a transition state analog hapten. However, characterization of the residues involved in catalysis has remained difficult. Exploration of one system has begun using NMR spectroscopy and an antibody that catalyses cleavage of nitrophenyl phosphate esters and carbonates. The hapten selected in this case is a p-nitrophenyl phosphate (NPP), which has been tritiated on the aromatic ring. This compound is formed by the reaction of 4-nitrophenol (NP) with phosphoryl chloride. Tritium labeling of the substrate in the aromatic ring can thus be achieved through labeled NP. The labeling of nitro compounds based on the catalytic dehalogenation reactions has a potential problem of simultaneous reduction of nitro functionality. Therefore, a procedure based on catalytic dehalogenation of 2,6-dibromophenol to phenol and subsequent nitration to nitrophenol has been developed. The procedure was performed with deuterium labeling of NPP and the intermediates were characterized with ^1H and ^2H NMR and mass spectral data. In the tritiation experiments with 20% (T/H), the 2,6-[^3H]-NP was obtained with a specific activity of 10.1 Ci/mmol and was converted to 2,6-[^3H]-NPP; the distribution of tritium in both compounds was confirmed by ^3H NMR. The procedure developed is thus suitable for preparation of high-specific activity 2,6-[^3H]-NPP. The work on preparing monoclonal antibodies for binding studies with the hapten by ^3H NMR is currently in progress.

^3H-maltose interaction with MBP. Work continued on tritiated maltose oligomers and their interaction with maltose binding protein (MBP). Efforts concentrated on the binding of oligomers with 3, 4, 5 and 6 glucose units. It was found that there is a higher anomeric specificity in binding of these than for maltose itself, and that there are at least two binding modes for the β anomer. The NMR evidence from the bound forms is that any two of the sugars can bind in the primary site in fast exchange with one another unless the terminal sugar binds in the primary site. This is unexpected behavior, which is generally important in understanding ligand binding specificity and dynamics. Tritium is really the only nucleus that could have been used in these studies because of the high sensitivity and resolution, making it possible to detect broad lines in exchanging systems.

NMR spectroscopy. Initial NMR experiments were carried out at 320 MHz at the NTLF. In many of the biomolecular systems of interest, the sensitivity and resolution at this field strength are minimally sufficient, and better results would be obtained at higher field. To this end, modifications were made on the GN-500 housed in the Calvin Lab for observation of tritium. This required retuning of one of the receiver filters and building a new amplifier with broader bandwidth. With these modifications completed and addition of a new probe, it is now possible to observe tritium at 533 MHz, with the expected two+ fold greater sensitivity and 60% greater resolution. This has already been important for work on ^3H-ATP binding to S1. It will also be significant for all future biomolecular tritium studies.

Chemistry of Hydrophilic Gels for Separation of Solutes from Dilute Aqueous Solution

Principal Investigator: John M. Prausnitz

Funding: $57,300 (second year of funding)

Project Description

The goal of this project is to develop a fundamental, molecular-thermodynamic framework for design of novel, environmentally-sensitive polymeric gels. The water-absorbency properties of reversible gels are extremely sensitive to environment. Under certain conditions, small perturbations in gel temperature or pH can induce order-of-magnitude changes in gel volume. This unique material property of reversible gels is currently being applied in novel separation processes, controlled-release systems, and environmentally-responsive membrane devices. This work will provide a rational framework for designing and tailoring gel properties to meet the needs of specific applications.

A combined approach of theory, experiment, and computer simulation was used to elucidate and quantify the dependence of gel swelling properties on gel and solution conditions. Systematic experiments are conducted to isolate the effects of relevant gel and solution properties (i.e., gel charge density, solution ionic strength) on swelling behavior. Experimental results are used to test predictions of a gel-swelling model currently under development, and to determine where further model improvements are needed. Finally, Monte Carlo computer-simulation studies of single, isolated polyelectrolyte chains on a lattice were conducted. These simulation studies enable us to examine in detail the effects of charge density, temperature, and ionic strength on polymer configurational properties; such information will allow for further (theoretically based) improvements in the gel-swelling model.

Accomplishments

Significant progress was made in this second year of this project. First, Monte Carlo simulations were used to study the configurational properties of a lattice-model isolated polyelectrolyte with attractive segment-segment interaction potentials. This model provides a simple representation of a hydrophobic polyelectrolyte. Configurational properties were investigated as a function of chain ionization, Debye screening length, and segment-segment potential. For chains with highly attractive segment-segment potentials, large, global changes in polymer dimensions were observed with increasing ionization. The transformation from a collapsed chain at low ionization to an expanded chain at high ionization becomes increasingly sharp with increasing chain hydrophobicity. The ionization-induced structural transitions for this model hydrophobic polyelectrolyte are analogous to pH-induced transitions seen in real polyelectrolytes and gels. These studies suggest a simple explanation for such transitions based on competing hydrophilic and hydrophobic interactions.

The newly developed oriented-lattice model for correlating quantitatively the collapse of uncharged gels in response to temperature increases was then extended to describe isothermal swelling equilibria of ionized gels. A series of ionized acrylamide gels was synthesized, and their swelling properties were compared with model predictions. Good agreement was obtained for the effects of charge density and solution ionic strength on gel swelling. However, existing elasticity theories were found inadequate to describe quantitatively the effect of gel monomer concentration at preparation on swelling equilibria.

Monte Carlo simulations were also performed for a lattice model of an isolated, partially ionized polyelectrolyte whose charge groups interact through screened Coulombic potentials. Configurational properties are reported as a function of chain ionization and Debye screening length for chains containing 20-140 segments. At high screening between fixed charges, the chains exhibit power law scaling behavior for the dependence of the mean-square end-to-end distance on chain length. At lower screenings, the chains undergo a transformation from flexible to stiff conformations as ionization rises. Simulation results for poly-ion electrostatic energies and expansion factors are compared with predictions based on the theory of Katchalsky and Lifson and the uniform-expansion extension of this theory. Large discrepancies between theory and simulation were found and are probably

due to the assumed theoretical expressions used for describing distance probability distributions between charged groups.

Finally, Monte Carlo simulations were performed for a lattice model of an isolated, partially ionized polyelectrolyte near an impenetrable, oppositely ionized surface. The effects of chain ionization, chain hydrophobicity, surface charge density, and solution ionic strength on the conformational and interfacial properties were considered for the model system. The overall dimensions of model polyelectrolytes in the adsorbed state were found to be similar to those of isolated polyelectrolytes in solution; however, the conformational isotropy characteristic of isolated chains is lost when the polymer adsorbs at an interface.

Laser Produced Microparticle Suspensions

Principal Investigator: Richard J. Saykally

Funding: $64,700

Project Description

Plasmas of a given nonvolatile material are produced by laser vaporization in an atmosphere of nonreactive buffer gas. Microparticles (clusters containing 103–106 atoms) nucleate and cool. We are attempting to study the properties of these microparticles (absorption cross sections, polarizabilities, size distributions) and investigating how to control their sizes. The use of these particles as highly dispersed media for catalysis and synthesis is being explored as the primary goal of this research.

Accomplishments

Silver particles were produced in laser vaporization and studied *in situ* by UV-visible absorption spectroscopy. Size distributions were deduced by analysis of the shift in plasmon resonance; particle sizes could be controlled by variation of the buffer gas pressure and composition. Diffusion lifetimes and loss mechanisms of particles were studied.

In order to study these microparticles more thoroughly, an acoustic particle trap was constructed. This devise consisted of a piezoelectric driver and reflector system contained in a vacuum chamber.

After considerable effort, it was concluded that an optical spectrometer with broadband scanning capability and much higher sensitivity than those available was required. Such a system is now under construction (Cavity Ringdown Laser Absorption Spectrometer). Future research on microparticles will proceed after the system is tested.

Publications

Journals and Proceedings

H.H. Hooper, J.P. Baker, H.W. Blanch, and J.M. Prausnitz, "Swelling Equilibria for Positively Ionized Polyacrylamide Hydrogels," *Macromolecules* 23, 1096 (1990); LBL-27284.

H.H. Hooper, H.W. Blanch, and J.M. Prausnitz, "Configurational Properties of Partially Ionized Polyelectrolytes from Monte Carlo Simulation," *Macromolecules* 23, 4820 (1990); LBL-28665.

H.H. Hooper, S. Beltran, A.P. Sassi, H.W. Blanch, and J.M. Prausnitz, "Monte Carlo Simulations of Hydrophobic Polyelectrolytes. Evidence for a Structural Transition in Response to Increasing Chain Ionization," *J. of Chem. Phys.* 93 (4), 2715 (1990); LBL-28677.

S. Beltran, H.H. Hooper, H.W. Blanch, and J.M. Prausnitz, "Swelling Equilibria for Ionized Temperature-Sensitive Gels in Water and in Aqueous Salt Solutions," *J. Chem. Phys.* 92 (3), 2061 (1990); LBL-29053.

H.H. Hooper, H.W. Blanch, and J.M. Prausnitz, "Molecular Thermodynamics of Aqueous Polymers and Gels," *Studies in Polymer Science*, Vol. 8, edited by L. Brannon-Peppas and R. Harland, Elsevier (1990); LBL-28666.

S. Beltran, H.H. Hooper, H.W. Blanch, and J.M. Prausnitz, "A Monte Carlo Study of Polyelectrolyte Adsorption on a Planar Charged Surface," submitted to *Macromolecules*; LBL-29238.

Presentations and Seminars

H.H. Hooper, "Swelling of Thermally-Sensitive Hydrogels," Annual Meeting, AIChE Annual Meeting, San Francisco, California, November 1989.

J.M. Prausnitz, "Applications of Molecular Thermodynamics," Polymer section, Marshall Laboratory, DuPont, Philadelphia, PA, April 1990.

J.M. Prausnitz, "Molecular Thermodynamics for Chemical Process Design," BASF 125th Birthday Symposium, Ludwigshafen, Germany, September 1990.

Laboratory Demonstration of Aqueous Foam for Mobility Control in Surfactant Washing for Aquifer Remediation

Principal Investigator: Peter Persoff

Funding: $50,800

Project Description

A commonly used method for removing immobile nonaqueous phase liquid (NAPL) from the subsurface is to flush the contaminated region with air or other fluid. Such treatments are often inefficient because of aquifer heterogeneity: the flushing fluid cleans the permeable zones but does not flow through the less-permeable zones. As a result, contaminant removal is incomplete. This problem is analogous to the problem of achieving efficient sweep in enhanced oil recovery. Aqueous foams have been used to block permeable zones in enhanced oil recovery operations.

Several technical issues must be resolved if foam is to become a useful tool for assisting subsurface remediation. First, the technical feasibility of forming and propagating foam in the subsurface must be demonstrated, while keeping injection pressures low enough to avoid uplifting of soil or creating fractures to the surface. Foam has a very large viscosity in porous media, and a minimum gas injection velocity is necessary to form foam, both of which tend to require large injection pressures. The effectiveness of foam as a blocking agent must also be demonstrated. Another potential application of foam (aside from its use as a blocking agent to improve sweep efficiency) would make use of its large viscosity to displace NAPL at residual saturation. Finally, any application of foam in environmental applications would require that surfactants be biodegradable with no significant long-term residue.

Accomplishments

To investigate some of these technical issues, experiments were conducted in 2-ft-long laboratory sandpacks using pure alkanes as surrogates for NAPL contaminants such as diesel fuel. Foam was formed by injecting a 1% solution of biodegradable surfactant into the sandpack, followed by gas injection at 1.5 psi; the pressure gradient was therefore limited to 0.75 psi/ft. Two experiments were conducted to demonstrate foam formation at low injection pressure and to demonstrate the use of foam as a blocking agent to improve the efficiency of NAPL removal by *in-situ* surfactant washing. We also conducted a third experiment in which we attempted to use foam to displace NAPL at residual saturation.

Foam formation was demonstrated by saturating a sandpack with surfactant solution and then injecting gas at 1.5 psi. This showed that foam could be formed at low injection pressure. The foam completely blocked the flow of gas for two months. Following this, we demonstrated the use of foam as a blocking fluid to improve the sweep efficiency of NAPL removal by *in-situ* surfactant washing. Results of this experiment are shown in Fig. 1. Two sandpacks (A and B, with permeabilities of 76 and 8 darcy, respectively) were flushed in parallel with a 1% surfactant solution. The effluents from the two sandpacks were

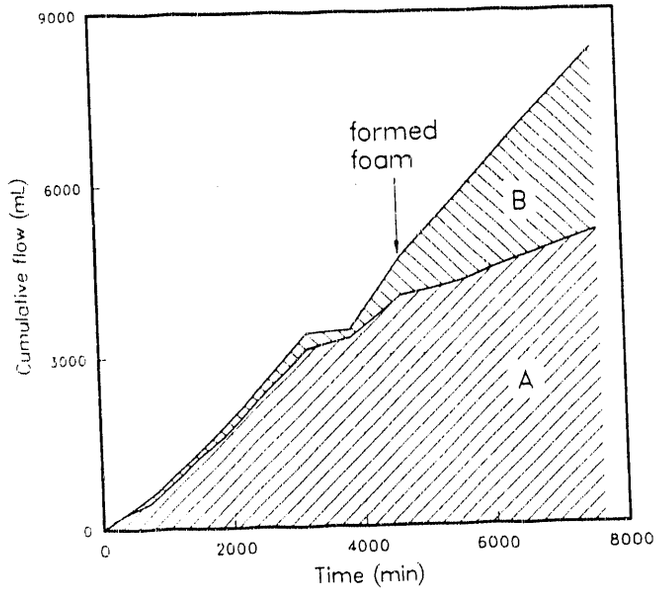

Figure 1. Division of flow between sandpacks A (76 darcy) and B (8 darcy) during surfactant flushing. Both sandpacks were spiked with NAPL, and flushed in parallel at 1 mL/min. From 4600 to 4700 min, gas was injected into sandpack A, causing foam formation and blockage. When flow was resumed, most of the flow went through sandpack B. This technique can be used to ensure that low-permeability zones in a contaminated aquifer are swept.

collected and analyzed separately. Most of the flow went through sandpack A, bypassing B. When sandpack A was completely cleaned of NAPL, further flushing would be wasteful and would not clean sandpack B. Then gas was injected into A at 1.5 psi, forming foam and blocking it. When surfactant flow was resumed, most of the flow went through B, so that it, too, was swept.

A "foam drive" experiment was conducted to determine whether the large apparent viscosity of foam in porous media would make it an effective fluid for displacing NAPL at residual saturation. Beadpacks were initially brought to residual saturation of both water and NAPL. Then slugs of surfactant solution alternating with gas were injected in an attempt to drive a foam bank through the beadpack, that might drive a bank of NAPL ahead of itself to the outlet. Several programs of gas and liquid injection rates were tried. In all cases, gas permeability was very small, indicating that most of the pores normally available to gas flow were occupied by trapped gas bubbles, i.e., foam was formed. However, the flowing gas was never effective in displacing NAPL. It is interesting to note that the presence of oil in the beadpack changed the foam from a "blocking" foam (gas flow reduced to zero) to a "non-blocking" foam (gas permeability reduced but not to zero).

This work has indicated the need for further work to develop foam as a useful tool for aquifer remediation. One important issue remaining is propagation of foam at low injection pressure. The observation that gas flow became blocked by foam in a two-foot sandpack suggests that propagation of a foam plume to substantial distances, as would be required in most field applications, could be difficult. Injection strategies for long-distance propagation of foam, such as varying injection rates and surfactant concentrations, need to be investigated. One technique for distant penetration of foam that merits investigation is foam formation by delayed release of gas by chemical reactions.

Publications

Other Publications

P. Persoff, S.M. Benson, I. Javandel, "Laboratory Demonstration of Aqueous Foam for Mobility Control in Surfactant Washing for Aquifer Remediation," LBID-1706 (1991).

Diamond Hexagonal Silicon

Principal Investigators: Ulrich Dahmen and Kenneth H. Westmacott

Funding: $91,900

Project Description

In research performed in the Soviet Union almost twenty years ago, it was reported that ribbons of hexagonal materials were produced when silicon is indented in the range 400–650 C. Using electron diffraction, the ribbons were identified as diamond-hexagonal (dh) silicon with lattice parameters, a = 0.386 nm and c = 0.631 nm. Of particular interest was the fact that the habit plane between the two phases was {511} diamond cubic (dc) and the orientation relationship (011)dc~3.5° from (0001)dh with [011 dc ∥ $\bar{1}\bar{2}10$]dh. In recent work, researchers from Case Western Reserve University have completely verified the earlier results. The purpose of the present project was the exploration and control of conditions that lead to the formation of diamond hexagonal silicon.

Silicon wafers were treated by a number of thermomechanical techniques designed to induce the formation of the hexagonal phase. Thin foil samples were examined by high resolution electron microscopy.

Accomplishments

A crystallographic model was developed that explained the observed phenomena as a stress-induced martensitic transformation. {511}dh ribbons are a consequence of multiple twinning under the high shear stresses existing in the regions near the indent. During extensive deformation by twinning, secondary twins propagating into the matrix lead to formation of the diamond-hexagonal phase.

Direct confirmation of this model was obtained by high resolution electron microscopy, and it was shown that a {511} habit plane is a coherent interface between cubic and hexagonal Si, made up of five- and seven-fold rings with no dangling bonds. These findings formed the basis for our attempt to bias and enhance the transformation. Various possibilities have been explored.

1) Stress-induced transformation. According to our model, it is not the hydrostatic component but the shear component of the stress that induces the transformation. We have attempted to manipulate the state of stress in the temperature range near 550 C to bias the transformation. A nonuniform stress similar to that prevailing during hot-indentation was produced by abrasion while a uniform stress was produced by mechanical bending.

2) Ion implantation. Rendering the top layer of the crystal amorphous by ion implantation establishes clean conditions for regrowth of epitaxial Si. It is known that under these conditions different low index surfaces regrow with different twin and stacking fault densities. We expected to find that regrowth of an amorphized {511} surface under some conditions could grow large areas of hexagonal phase.

3) Faulted Homoepitaxy. We used cubic Si substrates cut in {511} orientation as a substrate for the regrowth of Si. As our model has shown that this crystallographic orientation is the coherent interface between cubic and hexagonal Si, accidental twinned growth could result in a continuous surface layer of hexagonal Si.

All of the three approaches outlined above resulted in the normal epitaxial growth of cubic Si in preference to the faulted hexagonal form. This means that the range of conditions employed did not produce high enough shear stresses on the correct crystallographic shear system to induce formation of the hexagonal phase. It is concluded that, while the model is an accurate description of the origin of diamond hexagonal silicon, the conditions required for formation of the phase in significant amounts have not yet been optimized.

The most interesting observation was a {110} texture that developed during the regrowth of {115}-oriented wafers after amorphization by ion-implantation at liquid nitrogen temperature. This procedure is known to lead to a high density of twins in other substrate orientations. It was expected that the {115} orientation as the coherent interface between cubic and hexagonal Si would lead some coherent growth of hexagonal material as another form of growth accident. It was found that regrowth was indeed heavily twinned, not however, on the {115} substrate surface but on all four {111} planes inclined to the surface. The same {110} texture, though less pronounced, was observed in

samples treated by hot-abrasion at 600 C. Under these conditions of deformation, twinning on the inclined twin planes is an expected deformation mode, entirely consistent with the observed grain orientations.

Further, recent reports have shown that small regions of hexagonal phase form during low pressure chemical vapor deposition of silicon. Silicon formed under these conditions experiences high stress due to conical growth of individual grains. However, at present, the hot indentation technique still produces the largest amounts of hexagonal phase.

Use of Scanning Tunneling Microscopy for In-Situ Studies of Metal-Solution Interfaces

Principal Investigators: Thomas M. Devine and Miquel Salmeron

Funding: $48,000

Project Description

The objectives of this research were twofold: (1) to construct a scanning tunneling microscopy (STM) that is capable of obtaining atomic-level resolution (in the direction perpendicular to the surface) of metals immersed in aqueous solutions and (2) to use the STM to examine the reconstruction of silver surfaces following an oxidation-reduction treatment in aqueous 1 M KCl.

Accomplishments

When a silver electrode is alternately oxidized and reduced in 1 M KCl, its surface is roughened and capable of enhancing the Raman scattered radiation from species located close to the silver surface, a phenomenon known as SERS (surface enhanced Raman scattering). The anomalous ~10^6-fold increase in the Raman scattering cross section of species adsorbed on a roughened surface of silver is thought to result from either or both of two effects. The first is the chemical enhancement mechanism of SERS which, according to several models, requires atomic-scale roughness of the silver surface. The second is the electromagnetic enhancement mechanism of SERS which, according to models, requires sub-micron-scale roughness of the silver surface. Features with sub-micron size dimensions (50–100 nm) on surfaces that were freshly oxidized and reduced, were thought to be stable while the atomic-scale roughness features were thought to be unstable. As a result, time-dependent changes in the intensity of SERS were ascribed to changes in the atomic-scale roughness features. Consequently, researchers have sought to distinguish between the chemical enhancement and electromagnetic enhancement mechanisms by measuring the intensity of SERS as a function of time. Time-dependent changes were associated with the chemical enhancement mechanism. In particular, immediately after the completion of a roughening treatment (i.e., an oxidation-reduction cycle (ORC) in 1 M KCl), the intensity of SERS abruptly decreased with time for 1–2 minutes and then slowly decreased with time for the next ~5 minutes. These changes were ascribed to changes in the atomic-scale roughness.

Our results show that <u>both</u> the atomic-scale roughness and the sub-micron-scale roughness change markedly with time following an ORC. Specifically, clusters of silver atoms that were 3 nm in diameter were observed to coalesce into large, single-atom-high plateaus on the silver surface. In addition, ellipsoidal mounds that initially had cross-sectional diameters of ~50 nm, and major axes that were oriented perpendicular to the surface (z-direction) and equal to ~70 nm, were shrunk in the z-direction to ~15 nm within 5 minutes. Consequently, these results indicate that changes with time in the intensity of SERS following an ORC must be attributed to changes in <u>both</u> the electromagnetic enhancement mechanism as well as the chemical enhancement mechanism. This finding necessitates a reinterpretation of previously published investigations of the mechanism of ERS.

The above work has demonstrated the ability of STM to rapidly image corroded surfaces *in situ*. This technique will be exploited in proposals that are being written to the National Science Foundation and the Gas Research Institute to determine if stress corrosion cracking is the result of the rapid failure of 20 nm wide surface regions that contain ~5 nm voids that are formed by the coalescence of vacancies that are produced by the preferential dissolution of less-noble constituents in multi-component alloys.

Synthesis of Composite Ceramics by Microwave-Assisted Chemical Vapor Infiltration

Principal Investigators: Lutgard C. De Jonghe and James W. Evans

Funding: $55,000

Project Description

Ceramic-ceramic composites are materials with resistance to creep and corrosion at high temperatures and toughness superior to that of monolithic ceramics. They are already being used in applications where cost is a secondary consideration to performance (e.g., aerospace applications). One route for producing these materials is by chemical vapor infiltration (CVI) of a preform made up of ceramic fibers. CVI results in partial or complete filling of the interstices between fibers by solid generated by reaction of gaseous species (e.g., the thermal decomposition of trichloromethyl silane). As presently carried out CVI suffers from the disadvantage of unusually long processing times, resulting in high cost materials, or in materials with considerable residual porosity. This is a consequence of reaction occurring preferentially near the preform exterior, sealing the outside and preventing further infiltration. The tendency is aggravated if the preform is heated conventionally, e.g., in a furnace, and the exterior is hotter and therefore the preferential locale for reaction. The objective of the investigation described below was to determine whether superior materials (of lower porosity) could be produced in shorter processing times by employing microwave heating and external cooling of the preform. This has the effect of inverting the normal temperature profile in the preform, making the center hotter and therefore the preferential site for reaction. The approach has been a combination of mathematical modeling and experimental studies.

Accomplishments

A mathematical model for microwave assisted CVI has been developed. The model computes the local rate of heat generation by microwaves within the preform and then solves the heat conduction equation, with a convective boundary condition, to determine the temperature distribution in the preform. The equations for diffusion and reaction of the gaseous reactant within the preform are then solved and finally the evolution of the pore structure computed. When parameters for the infiltration of SiC preforms by trichloromethyl silane pyrolysis are used in the model, then substantial advantages for microwave processing over conventional processing are predicted. The computed final porosities are much lower than those achievable under isothermal processing, and processing times are approximately one half of isothermal processing times.

The experimental program used a modified domestic microwave oven to demonstrate that SiC preforms could be brought to temperatures necessary for reaction.

Atomic Structure of Catalyst Surfaces under High Pressure Reaction Conditions

Principal Investigators: Gabor Somorjai and Miquel Salmeron

Funding: $88,000

Project Description

The purpose of this project was to develop a special version of the Scanning Tunneling Microscope (STM) that will operate under real conditions of high pressure and temperature on catalyst surfaces. The goal is to be able to ascertain the atomic scale structure of the catalyst surface during a chemical reaction. This is not possible today with any of the existing microscopy tools.

To reach that goal we proposed to construct a specially designed STM and enclose it in a controlled atmosphere reaction cell.

Accomplishments

The small reaction cell with capability to house a special STM has been constructed. It can be pumped to Ultra High Vacuum (UHV) and then pressurized with reactant gases to several atmospheres. It allows sample transfer to a standard UHV chamber without air exposure. It allows sample heating *in situ* for cleaning.

The special version of the STM has also been constructed. It is compact and of a reentrant design that minimizes space. Thermal drift is also minimized by the concentric tube arrangement of the piezoelectric

ceramics. A resistive heating coil surrounds the STM head. This provides uniform heating over the head and results in a sufficiently small drift for imaging operation.

The first tests on graphite demonstrated that the instrument is working according to expectations. Images with atomic resolution were obtained first in high vacuum and subsequently after pressurizing the cell up to one atmosphere. Imaging was being performed at the intermediate pressures. Heating of the system was also successfully tried with images taken up to temperatures of 340 K.

At present the instrument is used to image platinum crystals that are covered with one monolayer of iodine at one atmospheric pressure. Atomic steps are clearly resolved. We plan to study the stability of this surface when exposed to hydrogen and hydrocarbon environments and at temperatures of up to 500 K. The stability of the step structure when exposed to this environment is an important question in catalysis research.

Stimulated Desorption of Halogens from Semiconductor Surfaces

Principal Investigator: Jory A. Yarmoff

Funding: $31,100

Project Description

Photon-stimulated desorption (PSD) and electron-stimulated desorption (ESD) are useful techniques for the determination of the local electronic and geometric structures of adsorbates on surfaces. Collectively, these processes are known as desorption induced by electronic transitions, or DIET processes. DIET studies are of particular utility in studies of halogen-semiconductor bonding. Because the bonding is rather ionic, desorption can be easily induced via core-hole excitation, thereby allowing the PSD spectra to be used as a measure of the local electronic structure associated with the bonding atom. Due to the high DIET yield of halogen ions, measurements of both the excitation energy dependence and the resulting ion kinetic energies can be easily obtained. In addition, measurements of the ESD ion angular distributions (ESDIAD) provide information as to the geometrical structure of the adsorbates.

DIET studies of halogen-semiconductor interactions were begun with the fluorine-silicon system employing XeF_2 as a source of atomic fluorine. This system provides a good model for displaying the various factors important in chemically selective stimulated desorption processes, since it is possible to prepare a single silicon surface with a variety of surface fluoride species. In addition, information obtained from surfaces which have been etched by XeF_2 are useful to industrial researchers who are interested in gaining an understanding of the mechanisms involved in the plasma etching of silicon.

The data for the PSD experiments performed during FY 1990 was obtained on beamline UV-8b at the NSLS. The beamtime was obtained through the NSLS general user program.

Accomplishments

In previous work, it was shown that the PSD of F^+ from a silicon surface is a chemically selective process, i.e., the thresholds for PSD observed at the substrate core level edge coincide with the oxidation state of the bonding surface atom. Work continued with the fluorine-silicon system in order to answer some important questions which remain. Efforts also began to extend this work to other halogen-semiconductor systems.

The bulk of the new research has concentrated on surfaces which had been etched by XeF_2. These surfaces are covered by a reaction layer composed of SiF, SiF_2, SiF_3 and trapped SiF_4 moieties, as determined by previous soft x-ray photoemission spectroscopy (SXPS) studies (Fig. 1). SXPS was unable, however, to be used for determining the detailed structure of this reaction layer. The difference in the probe depths of

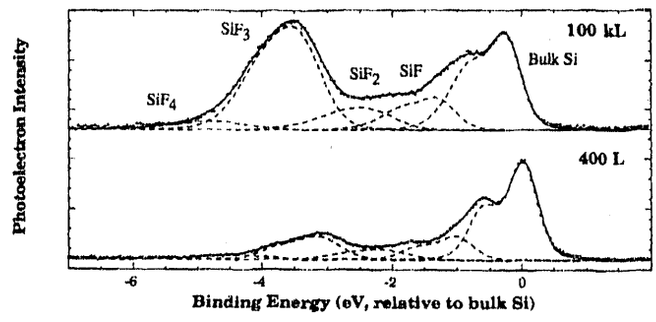

Fig. 1. Soft x-ray photoemission (SXPS) spectra of Si(111) after reaction with XeF_2. The raw data has been numerically fit with Gaussian-broadened Lorentzian lineshapes in order to determine the relative abundance of the fluorosilyl species in the near-surface region.

SXPS and PSD was exploited to ascertain that the reaction layer has a structure in which the lower fluorides are positioned at the interface between the reaction layer and the underlying substrate, and that the SiF_3 groups are located at the surface of the reaction layer. It was also shown that the trapped SiF_4 is located at sites which are visible to the surface, and that the trapping of the SiF_4 is facilitated by metallic contaminants which deposit on the sample surfaces after being removed from the walls of the reaction chamber, thereby demonstrating that trapped SiF_4 is *not* an integral part of the basic fluorine-silicon reaction. More recently, we have begun to measure the distribution and structure of reaction layers obtained by exposing silicon to XeF_2 at elevated temperatures (Fig. 2).

Efforts to study halogen reactions on III-V semiconductor surfaces were also begun. We have already collected SXPS data from GaAs(110) and GaAs(100) surfaces after reaction with chlorine. Solid-state electrochemical cells were constructed for the production of molecular halogens in UHV. We have found that Cl etching of GaAs does occur spontaneously at room temperature, although the rate is fairly small. This etching is non-isotropic, as we observe the preferential removal of Ga atoms. We will soon be collecting PSD data from these surfaces, and thereafter plan on studying the reaction as a function of sample temperature with both SXPS and PSD, since it is known that the etch rate increases dramatically at elevated temperatures. Additionally, we will be studying Br, I and F chemisorption on the III-V surfaces.

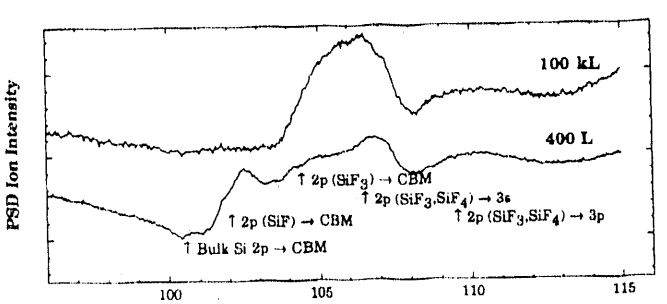

Fig. 2. Photon stimulated desorption (PSD) spectra of Si(111) after reaction with XeF_2. Some of the transitions have been indicated in the figure. Edges corresponding to SiF and SiF_3 are observed after a 400 L exposure, but only an edge due to surface SiF_3 remains after a 100 kL exposure. Because the SXPS from this surface shows an abundance of SiF species, it can be concluded that the SiF is buried below the surface of the reaction layer.

Publications

Journals and Proceedings

C.J.D. Hetherington, "HREM of Defects in Silicon at Twin Intersections," *MRS Proc.* vol 183, R. Sinclair, D.J. Smith and U. Dahmen, eds, p. 123 (1990) (LBL-28118).

C.W. Lo, D.K. Shuh and J.A. Yarmoff, "The Structure and Buildup of the XeF_2/Si(111) Etching Reaction Layer," *Phys. Rev. B*, in preparation.

C.W. Lo, D.K. Shuh, V. Chakarian, K.A. German, and J.A. Yarmoff, "Synchrotron Radiation Studies of the XeF_2 Etching of Silicon," in *Proceedings of the Conference on Dry Processing*, Tokyo, Japan, November, 1990.

D.K. Shuh and J.A. Yarmoff, "The Interaction of Cl_2 with GaAs Surfaces," in preparation.

L.C. De Jonghe, J.W. Evans, and D. Gupta, "A Mathematical Model for Microwave-Assisted Chemical Vapor Infiltration with Microwave Heating and External Cooling," LBL-29320, submitted to *J. of Mat. Res.*

L.C. De Jonghe, J.W. Evans, and D. Gupta, "Mathematical Modeling of the Production of Composites by Chemical Vapor Infiltration," to appear in *Proc. Symp. Materials Processing in the Computer Age*, TMS, New Orleans, 1991.

N. Thangaraj, K. H. Westmacott and U. Dahmen, "HVEM Studies of the Sintering of MgO Nanocrystals prepared by $Mg(OH)_2$ Decomposition," *Ultramicroscopy*, in press (LBL-28653).

P. Pirouz, R. Chaim, U. Dahmen and K.H. Westmacott, "The Martensitic Transformation in Silicon I. Experimental Observations," *Acta Met.* 38, 313 (1990) (LBL-27071).

P. Pirouz, R. Chaim, U. Dahmen and K.H. Westmacott, "The Martensitic Transformation in Silicon III. Comparison with Other Work," *Acta Met.* 38, 329 (1990) (LBL-27073).

S.A. Joyce, C. Clark, V. Chakarian, D.K. Shuh, J.A. Yarmoff, T.E. Madey, P. Nordlander, B. Maschoff and H.-S. Tao, "The Influence of Coadsorbed Potassium on the Electron Stimulated Desorption of Fluorine from PF_3 on Ru (0001)," *J. Chem. Phys.*, in preparation.

T.M. Devine and M. Salmeron, "*In-Situ* Electrochemical Scanning Tunneling Microscopy Study of the Structural Changes of Silver Surfaces Following an

Oxidation-Reduction Cycle in 1 M KCl," submitted to *Surf. Sci.*, April 1991.

U. Dahmen, C.J. Hetherington, P. Pirouz and K.H. Westmacott, "The Formation of Hexagonal Silicon at Twin Intersections," *Scr. Met.*, 23, 269 (1989) (LBL-26233).

U. Dahmen, K.H. Westmacott, P. Pirouz and R. Chaim, "The Martensitic Transformation in Silicon II. Crystallographic Analysis," *Acta Met.* 38, 323 (1990) (LBL-27072).

V. Chakarian, D.K. Shuh, J.A. Yarmoff, B. Maschoff, T. Hui-Shu and T.E. Madey, "Coadsorption of PF_3 and Potassium on Ru(0001) Studied by High-Resolution Photoelectron Spectroscopy," *J. Chem. Phys.*, in preparation.

Presentations and Seminars

C.W. Lo, D.K. Shuh, V. Chakarian, K.A. German and J.A. Yarmoff, "Synchrotron Radiation Studies of the XeF_2 Etching of Silicon," Dry Processing Symposium, November 1-2, 1990, Tokyo, Japan.

F.R. McFeely, E. Cartier, L.J. Terminello, A. Santoni and J.A. Yarmoff, "Low Energy Photoelectron Transport and Escape in Thin Overlayers of SiO_2 on Si(111)," American Physical Society, Anaheim, California, March 12-16, 1990.

J.A. Yarmoff, "Synchrotron Radiation Studies of the Fluorine-Silicon Interaction," RIKEN (The Institute of Physical and Chemical Research), Saitama, Japan, October 30, 1990.

J.A. Yarmoff, C.W. Lo and D.K. Shuh, "Photon Stimulated Desorption from XeF_2-Etched Silicon," American Vacuum Society, October 8-12, 1990, Toronto, Canada.

J.A. Yarmoff, D.K. Shuh, J. Song, C.W. Lo, K.A. German, V. Chakarian, L.J. Whitman, L.J. Terminello and F.R. McFeely, "Chemisorption of Chlorosilanes on Semiconductor Surfaces," American Physical Society, Anaheim, California, March 12-16, 1990.

J.A. Yarmoff, D.K. Shuh, K.A. German, V. Chakarian, J. Song, C.W. Lo, S.A. Joyce, B. Maschoff and T.E. Madey."The Chemisorption of PF_3 on Ru(0001) Studied with Soft X-Ray Photoemission and Photon Stimulated Desorption," American Physical Society, Anaheim, California, March 12-16, 1990.

J.A. Yarmoff, W. Lo, K.A. German, D.K. Shuh, V. Chakarian and F.R. McFeely, "Photon Stimulated Desorption Studies of XeF_2 Etching of Silicon," Gordon Conference on the Chemistry of Electronic Materials, February 26-March 2, 1990, Ventura, California.

J.R. Lince, S.V. Didziulis and J.A. Yarmoff, "Initial Oxidation of the $Fe_{.85}Cr_{.15}$(100) Surface Studied by Photoelectron Spectroscopy," American Vacuum Society, October 8-12, 1990, Toronto, Canada.

J.R. Lince, S.V. Didziulis and J.A. Yarmoff, "Resonant Photoemission Study of the Mo 4p-4d Absorption in MoS_2," American Vacuum Society, October 8-12, 1990, Toronto, Canada.

L.C. De Jonghe, J.W. Evans, and D. Gupta, "A Mathematical Model for Microwave-Assisted Chemical Vapor Infiltration," Materials Research Society Spring Meeting, San Francisco (1990).

L.C. De Jonghe, J.W. Evans, and D. Gupta, "Mathematical Modeling of Microwave-Assisted Chemical Vapor Infiltration for the Production of Ceramic-Ceramic Composites," *Proc. Intl. Conf. Computer Applications to Materials Science and Engineering*, Tokyo, August 1990.

T.M. Devine and M. Salmeron, "Use of STM for *in-situ* Studies of Silver Oxidized in 1 M KCl," Spring Meeting 1990, National Association of Corrosion Engineers, Las Vegas.

Other Publications

C.J.D. Hetherington, "High-Resolution Image Simulation of a Tilted Crystal," *Proc. XII ICEM*, p. 68, (1990) San Francisco Press (LBL-29359a).

C.J.D. Hetherington, U. Dahmen, P. Pirouz, and K.H. Westmacott, "HREM of Twin Intersections in Silicon," *47th EMSA Proc.*, G.W. Bailey, ed., p.132 (1989) (LBL-26929a).

Nuclear Science Division

Transition from Order to Chaos in Nuclei

Principal Investigators: William D. Myers and Wladyslaw J. Swiatecki

Funding: $67,100 (third year of funding)

Project Description

The purpose of this project is to establish and exploit points of contact between nuclear studies and closely related developments in order-to-chaos research. The expression "order-to-chaos transition" is a short-hand phrase referring to a huge gap, now being filled, between relatively simple, integrable systems (used almost exclusively as examples in all but the most recent textbooks on mechanics) and the insoluble, non-integrable systems that one attempts to treat by statistical mechanics and thermodynamics by introducing the hypothesis of chaos. One of the most fundamental discoveries in dynamics, ranking with the advances made by Hamilton and Boltzmann, is the realization that the intermediate regime between order and chaos has an incredibly rich structure, compared to which the structures of Hamiltonian mechanics of integrable systems and Boltzmann's statistical mechanics appear as lifeless skeletons.

This field of research owes its explosive growth in large measure to computer studies of relatively simple non-linear, non-integrable systems, such as the Henon-Heiles two-dimensional anharmonic oscillator or the stadium potential (an oval two-dimensional cavity with impenetrable walls). Even such simple systems exhibit many of the fractal subtleties of the generic order-to-chaos transition, but despite the great efforts expended on them in the past decade, unexpected new discoveries continue to be made and many questions remain unanswered, especially as regards the quantal version of the order-to-chaos problem.

The relevance of these studies to nuclear physics, and the relevance of nuclear physics to order-to-chaos research, is becoming obvious. A good starting point for nuclear theory is the mean-field approximation, in which nearly independent nucleons move in a common potential, which for light nuclei resembles a three-dimensional anharmonic oscillator and for heavy nuclei a three-dimensional cavity. Thus, much of nuclear theory done in the past has been unwittingly exploring aspects of the order-to-chaos problem. Conversely, the insights gained into the nuclear problem have, almost without exception, not been incorporated into order-to-chaos research. The two points of contact that are being established currently concern, first, the statistics of nuclear level spacings (which are Poisson-like in the integrable regime and Wigner-like in the regime of chaotic nucleonic motions). Second (and this has been a special concern of the Nuclear Theory Group), there is a very close connection between the nature of the dynamics of nuclear shape evolutions (in fission or nucleus-nucleus collisions) and the ordered or chaotic nature of the nucleonic motions in the nuclear mean field. (In the regime of ordered motions the nucleus should behave as an elastic solid, in the regime of chaotic motions as a fluid with an exotic viscosity, and in the intermediate regime as a viscoelastic substance.)

Accomplishments

Short visits and seminars of a number of scientists, including F. Izrailev from the U.S.S.R. and W.M. Zhang from the University of Washington, were supported. Most of our effort, however, went into longer visits and collaborations. Two extended stays were made by M. Wilkinson from the United Kingdom. We were fortunate to be able to host S.J. Wang (from the Center of Theoretical Physics, Chinese Center of advanced Science and Technology Beijing and the Department of Modern Physics, Lauzhou University). His six month stay was most productive. Joint seminars with the group of R. Littlejohn of UC Physics Department and AFRD have continued throughout the year. DOE has provided about $100 K in support of Chaos Studies in FY 1991.

The accomplishments of the past three years may be summarized under four headings. First, our own understanding of classical and quantal aspects of Chaos has been greatly expanded and we can view the nuclear problem from a much better perspective than three years ago. Second, a number of specific research projects were carried out in collaboration with visitors, ranging from studies of the properties of random matrices as representations of nuclear spectra, to dissipative effects in independent particle models of nuclei, to aspects of Berry's phase in spinning nuclei

and optical fibers. Third, through a number of conference talks, the awareness of the relevance of chaos studies to nuclear physics has been spread to workers outside the nuclear community. The most notable contacts established in this way were with M. Wilkinson in Glasgow, M. Berry and his group in Bristol, and O. Bohigas in Paris. Locally, R. Littlejohn's group at UCB and AFRD has been exposed to a number of nuclear physics problems that they had not been aware of previously. Fourth, extra funds to continue this work have been secured, with the possibility of further support from NSF.

Publications

Journals and Proceedings

H. Frisk, "Scars and the Order to Chaos Transition," *Proceedings of the 7th International Symposium on Capture Gamma-Ray Spectroscopy*, Asilomar, California, 14-19 Oct. 1990.

M. Feingold, D.M. Leitner, and O. Piro, "Semiclassical Structure of Hamiltonians," *Phys. Rev.* A39, 6507 (1990).

M. Feingold, R.G. Littlejohn, S.B. Solina, S. Pehling, and O. Piro, "Scars in Billiards: The Phase Space Approach," *Phys. Lett. A146*, 199 (1990).

P. Leboeuf, J. Kurchan, M. Feingold, and D.P. Arovas, "Phase-Space Localization: Topological Aspects of Quantum Chaos," *Phys. Rev. Lett.*, *65*, 3076 (1990).

S.-J. Wang, "Nonadiabatic Berry's Phase for a Quantum System With a Dynamical Semi-simple Lie Group," *Phys. Rev. A42*, 5103 (1990).

S.-J. Wang, "Nonadiabatic Berry's Phase for a Spin Particle in a Rotating Magnetic Field," *Phys. Rev. A42*, 5107 (1990).

W.J. Swiatecki, "Order, Chaos and Nuclear Dynamics: An Introduction," *Proceedings of the XXI Summer School on Nuclear Physics*, Mikolajki, Poland, August 26–September 5, 1990.

Other Publications

M. Feingold, D.L. Gonzalez, M.O. Magnasco, and O. Piro, "On the Universality Class Dependence of Period Doubling Indices," LBL-28256 (1990).

M. Feingold, D.M. Leitner, and M. Wilkinson, "Scaling in Semiclassical Random Matrix Ensembles," LBL-29302 (1990).

M. Wilkinson, M. Feingold, and D.M. Leitner, "Localisation and Spectral Statistics in a Banded Random Matrix Ensemble," LBL-29329 (1990).

S.-J. Wang, "New Algebraic Representations of Quantum Mechanics," LBL-29467 (1990).

S.-J. Wang, "Non-Adiabatic Effect on Berry's Phase for Light Propagating in an Optical Fibre," LBL-29253 (1990).

S.-J. Wang, "Spin Alignment Quantization, Berry" Phase Quantization, Stationary Condition and Twinned Superdeformed Bands," LBL-29543 (1990).

Physics Division

Pulsar Studies

Principal Investigators: Richard A. Muller and Carlton R. Pennypacker

Funding: $60,000

Project Description

There was strong evidence of a pulsar in the heart of supernova 1987a, the supernova that exploded in the Large Magellanic Cloud. The pulsar has a higher frequency than any previously detected, 1968 Hz; it was so high, in fact, that the pulsar caused great theoretical difficulties. The principal problem is that there was no plausible nuclear equation that allows sufficient mass in the pulsar to hold it together against the tremendous centrifugal forces of the spin. The pulsar had not been seen since the initial discovery run on January 18, and additional searches were supported in order to confirm or deny this pulsar and to explore its consequences.

Accomplishments

We were able to demonstrate that the reported observation of the pulsar was spurious, although not until the theorists had discovered ways to amend their theories to make the high reported frequency possible.

In data obtained in February, 1990, a signal similar to the originally reported one was seen not only in data from the supernova, but also in comparison data taken on the Crab pulsar at the same time. From this, it was clear that the signal did not originate in the supernova. We believe that the observed signal was electrical noise from a closed circuit television camera used for acquisition and guiding at the Cassegrain focus of the 4-meter telescope at Cerro Tololo Interamerican Observatory (CTIO), where both sets of data were taken. The observed frequency of 1968.627 Hz is close to the 16th subharmonic of the nominal horizontal sync pulse of the camera (1968.75 Hz); the coincidence seems too close to be accidental.

We do not know how the signal coupled into the detector, nor have we been able to totally reconstruct events during the observations. However, there are plausible explanations for some of those things that made the original observation appear real. The most important of these are:

(1) The signal disappeared when the telescope was pointed at a different object immediately after the run on the supernova. It is likely that the offending guider camera was turned off between the two sets of observations in order to prevent it being damaged by the increasing light of twilight.

(2) The signal was not observed with the same equipment on the same telescope either before or after the detection run, until the run in February 1990. It is impossible after the fact to determine why this is so, but a number of plausible explanations come to mind, any one or more of which might have occurred; for example, there may have been subtle differences in the mounting of the detector system, or changes in the adjustment of components, or a different guider camera (one without the 1968 Hz problem) may have been used (there are two such cameras at the telescope, which are used interchangeably), etc. It should be noted in this context that the system is extremely sensitive, and the detected signal was very small by normal standards: the equivalent interference current was of order 10–15 amps.

(3) Several highly suggestive properties of the observed frequency were totally fortuitous. The stability of the frequency over the 7 hour run was quite high (10^{-6}), which indicated a good timekeeping mechanism. This is about a factor of 100 better than the stability specification for the time base of the camera. Furthermore, the observed small frequency change was quite smooth, and when the data were corrected for the earth's motion, they were well fit by a sine wave, which suggested an external orgin. (When a sine wave was subtracted from the data, the frequency residuals decreased by an order of magnitude.

This was the basis for considerable speculation: for example, that the pulsar might be in a binary orbit.) Likewise, the fact that the first two higher harmonics were in the same proportions as those seen in the Crab pulsar was a coincidence. All of this was undoubtedly a combination of bad luck, misplaced pattern-finding skills, and the common human tendency to overinterpret a limited amount of data.

We have received support from the Institute for Geophysics and Planetary Physics to continue our search for an optical pulsars in supernova 1987A, and in other objects, in collaboration with physicists at the Los Alamos National Laboratory.

Publications

Journals and Proceedings

J. Kristian, Pennypacker, J. Middleditch, M.A. Hamuy, S. Heathcote, J.N. Imamura, W.E. Kunkel, R. Lucinio, D.E. Morris, R.A. Muller, S. Perlmutter, S.J. Rawlings, T.P. Sasseen, I.K. Shelton, T.Y. Steiman-Cameron, and I.R. Touhy, "There is no Optical Pulsar in Supernova 1987A," submitted to *Nature* (1990).

Research Medicine and Radiation Biophysics Division

Mechanisms of Heavy Atom Scintillators

Principal Investigator: William W. Moses

Funding: $60,500

Project Description

The purpose of this study is to understand scintillation mechanisms in order to develop denser, faster, and more luminous scintillators for medical imaging and nuclear radiation detection instrumentation. Ultraviolet photoelectron emission spectroscopy (UPS) is used to identify the electron energy levels, then fluorescence emission spectroscopy (FES) is used to identify the energy level transitions that cause the scintillation. In a separate study, a large variety of compounds were tested for scintillation, and several new scintillating compounds were discovered. With this study we hope to determine the scintillation mechanisms of these compounds, and in addition determine the scintillation mechanisms of several known scintillators in order to make theoretical predictions for new scintillating compounds.

Accomplishments

The positions of the outermost molecular energy levels (typically 5 eV to 25 eV) must be measured in order to predict scintillation via this crossover transition mechanism. Compounds that satisfy the energy inequality $\Delta E_2 < \Delta E_1$ should be fast scintillators, but measurements of the molecular energy levels of inorganic heavy atom compounds are only available for a few compounds.[1] Ultraviolet photoelectron emission spectroscopy (UPS) provides an ideal tool for measuring these energy levels. Monochromatic ultraviolet photons from a synchrotron vacuum ultraviolet (VUV) source impinge upon the scintillator, liberating photoelectrons whose kinetic energy is measured with a commercial spherical mirror analyzer (Fig. 1). Each photoelectron has a kinetic energy equal

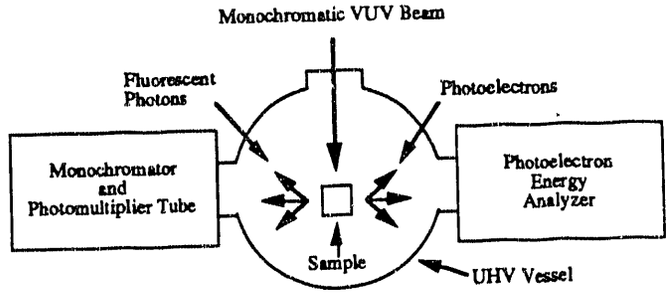

Fig. 1. Diagram of the experimental apparatus.

to the (constant) energy of the incident photon minus the electron's binding energy, so measuring the photoelectron kinetic energy is equivalent to measuring the energy of the molecular level that the photoelectron came from. The electron population density is then determined by measuring the energies of all liberated photoelectrons.

Once the energies of the populated molecular energy levels are known, we wish to determine which levels participate in the fluorescent decay using fluorescence emission spectroscopy (FES).[2] The emission wavelength spectrum of the scintillator is measured by exciting the compound with high energy (>50 eV) photons from the VUV source and analyzing the wavelength of its fluorescent emissions with a monochromator and a photomultiplier tube (Fig. 1). The analyzing monochromator is then set at the peak of the emission spectrum and the energy of the VUV beam is scanned. The scintillation intensity is plotted as a function of VUV beam energy, and the location of thresholds helps identify participating energy levels. For example, the fast scintillation in BaF_2 is caused by a transition from the $2pF^-$ band to the $5pBa^{2+}$ band. Therefore, the scintillation light output should be low when the VUV beam energy is less than 18.3 eV (the energy of the $5pBa^{2+}$ band) and become much higher when the VUV beam energy is greater than the 18.3 eV threshold.

During this fiscal year we have had two three-week experimental runs at SRC. The data acquired during

these runs has been partially analyzed, and results are extremely encouraging. We partially understand the scintillation mechanism of CeF_3, which is slightly more complicated than the ultra-fast mechanism described above. This understanding has led us to postulate that the scintillation properties of CeF_3 could be enhanced by doping it with LaF_3, effectively "designing" a new scintillator. Further tests confirmed this theory, and we are in the process of publishing these results and patenting the resulting material.

We are also refining the UPS and FES techniques described above for use with scintillator crystals. In particular, scintillator crystals tend to have high surface resistivity, and so accumulate an electrical charge when exposed to the VUV beam. This charge alters the photoelectron kinetic energy spectrum, and so gives an inaccurate measurement of the electron population density. We have developed several schemes to neutralize this surface charge and so obtain more accurate measurements of the electron population density.

References

1. R. T. Poole, J. G. Jenkin, J. Liesegang, and R. C. G. Leckey, "Electronic Band Structure of the Alkali Halides. 1. Experimental Parameters," *Phys. Rev.* **B11**, 5179 (1975).

2. S. Kubota, M. Itoh, J. Ruan, S. Sakuragi, and S. Hashimoto, "Observation of Interatomic Radiative Transition of Valence Electrons to Outermost-Core-Hole States in Alkali Halides," *Phys. Rev. Lett.* **60**, 2319 (1988).

Publications

Journals and Proceedings

W.W. Moses and S. E. Derenzo, "The Scintillation Properties of Cerium-Doped Lanthanum Fluoride," *Nucl. Instr. Meth. A*, in press (1991).

Acronyms and Abbreviations

AES	Auger electron microscopy
AFM	Atomic Force Microscope
APS	Advanced Photon Source
BEHS	Biomedical Environmental Health Sciences
CAT	Chloramphenicol acetyl transferase
CCD	charged coupled device
CPM	colliding-pulse mode-locked (dye laser)
CTIO	Cerro Tololo Interamerican Observatory
CVD	chemical vapor disposition
CVI	chemical vapor infiltration
CW	continuous wave
ERF	Exploratory R&D Fund
ESD	electron-simulated desorption
ESDIAD	ESD ion angular distribution
EXAPS	X-ray absorption spectroscopy
FACV	formal average copper valency
FEL	Free Electron Laser
FES	fluorescence emission spectroscopy
GEMS	Generalized Equilibrium Modeling System
HMEC	Human Mammary Epithelial Cell
HMEC	human mammary epithelial cells
HSPG	heparan sulfate proteoglycan
IEP	Indoor Environment Program
IRFEL	infrared free electron laser
ISOL	Isotope Separator on Line
LACI	lipoprotein associated coagulation inhibitor
LLNL	Lawrence Livermore National Laboratory
MCD	magnetic circular dichroism
MEL	mouse erythroleukemia
MMEC	murine mammary epithelial cell
NAPL	nonaqueous phase liquid
NEP	noise equivalent power
NIH	National Institutes of Health

NSD	Nuclear Science Division
NSLS	National Synchrotron Light Source
PBPK	physiologically-based pharmacokinetic
PCVD	photochemical vapor disposition
PSD	photon-stimulated desorption
PSZ	partially stabilized zirconia
R&D	research and development
RSV	Rous sarcoma virus
SEM	scanning electron microscopy
SERS	surface enhanced Raman scattering
SIPNs	simultaneous interpenetrating networks
SQUIDs	Superconducting Quantum Interference Devices
SRC	Synchrotron Radiation Center
SSC	Superconducting Super Collider
STM	scanning tunneling microscopy
SXPS	soft x-ray photoemission spectroscopy
TLS	thermal lens spectroscopy
UCLA	University of California at Los Angeles
UHV	ultra high vacuum
UPS	ultraviolet photoelectron emission spectroscopy
UV	ultraviolet
VUV	vacuum ultraviolet
XRD	x-ray powder diffraction
YACS	yeast artificial chromosomes

END

DATE FILMED

8/24/92